



# HHS Public Access

Author manuscript

*Pharmacol Ther.* Author manuscript; available in PMC 2023 October 01.

Published in final edited form as:

*Pharmacol Ther.* 2022 October ; 238: 108177. doi:10.1016/j.pharmthera.2022.108177.

## Anti-cancer Activity of Sustained Release Capsaicin Formulations

Justin C. Merritt<sup>1,§</sup>, Stephen D. Richbart<sup>1,§</sup>, Emily G. Moles<sup>1</sup>, Ashley J. Cox<sup>1</sup>, Kathleen C. Brown<sup>1</sup>, Sarah L. Miles<sup>1</sup>, Paul T. Finch<sup>2</sup>, Joshua A. Hess<sup>2</sup>, Maria T. Tirona<sup>3</sup>, Monica A. Valentovic<sup>1</sup>, Piyali Dasgupta<sup>1,\*</sup>

<sup>1</sup>Department of Biomedical Sciences, Joan C. Edwards School of Medicine, Marshall University, Huntington, WV, 25755

<sup>2</sup>Department of Oncology, Edwards Cancer Center, Joan C. Edwards School of Medicine, Marshall University, 1400 Hal Greer Boulevard, Huntington, West Virginia, WV 25755

<sup>3</sup>Department of Hematology-Oncology, Edwards Cancer Center, Joan C. Edwards School of Medicine, Marshall University, 1400 Hal Greer Boulevard, Huntington, West Virginia, WV 25755

### Abstract

Capsaicin (trans-8-methyl-N-vanillyl-6-noneamide) is a hydrophobic, lipophilic vanilloid phytochemical abundantly found in chili peppers and pepper extracts. Several convergent studies show that capsaicin displays robust cancer activity, suppressing the growth, angiogenesis and metastasis of several human cancers. Despite its potent cancer-suppressing activity, the clinical applications of capsaicin as a viable anti-cancer drug have remained problematic due to its poor bioavailability and aqueous solubility properties. In addition, the administration of capsaicin is associated with adverse side effects like gastrointestinal cramps, stomach pain, nausea and diarrhea and vomiting. All these hurdles may be circumvented by encapsulation of capsaicin in sustained release drug delivery systems. Most of the capsaicin-based the sustained release drugs have been tested for their pain-relieving activity. Only a few of these formulations have been investigated as anti-cancer agents. The present review describes the physicochemical properties, bioavailability, and anti-cancer activity of capsaicin-sustained release agents. The asset of such continuous release capsaicin formulations is that they display better solubility, stability, bioavailability, and growth-suppressive activity than the free drug. The encapsulation of capsaicin in sustained release carriers minimizes the adverse side effects of capsaicin. In summary, these capsaicin-based sustained release drug delivery systems have the potential to function as novel chemotherapies, unique diagnostic imaging probes and innovative chemosensitization agents in human cancers.

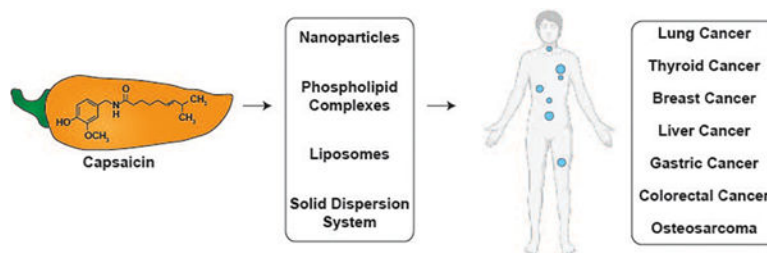
### Graphical Abstract

\*Correspondence to: Piyali Dasgupta, Department of Biomedical Sciences, Joan C. Edwards School of Medicine, Marshall University, 1700 3rd Avenue, Huntington, WV, 25755. dasgupta@marshall.edu.

§These authors contributed equally to the work presented here and should therefore be regarded as equivalent first authors.

<sup>5</sup>Conflict of Interest Statement

The authors declare that they have no conflict of interest



## Keywords

Capsaicin; cancer; solid dispersion; liposomes; nanoparticles; signaling

## 1. Introduction

Capsaicin is the spicy pungent ingredient of chili peppers. It is a potent analgesic agent and a common ingredient in over-the-counter pain-relieving lotions and creams (Bannerjee & McCormack, 2020; Basith, Cui, Hong, & Choi, 2016; Evangelista, 2015). The analgesic activity of capsaicin is mediated by the transient receptor potential vanilloid (TRPV1) receptor. Capsaicin is a high affinity agonist of the TRPV1 receptor (Andresen, 2019; L. Li, et al., 2021). However, several lines of evidence show that the biological functions of capsaicin may be mediated by TRPV1-dependent or TRPV1-independent pathways (Arul & Ramalingam, 2020; S. Zhang, Wang, Huang, Hu, & Xu, 2020).

Early studies showed that capsaicin displayed robust chemopreventive activity in a several types of human cancers including lung, prostate, pancreatic, and skin cancer. Subsequent research demonstrated that capsaicin suppressed the growth and progression of human breast, lung, prostate, gastric, renal, oral cholangiocarcinoma and hepatocellular carcinoma (Arul & Ramalingam, 2020; Basith, et al., 2016; Chapa-Oliver & Mejía-Teniente, 2016; Clark & Lee, 2016; Srinivasan, 2016; S. Zhang, et al., 2020) in cell culture and animal models. Although, an overwhelming majority of research papers show that capsaicin displays growth-inhibitory effects in human cancer cells (Arul & Ramalingam, 2020; Basith, et al., 2016; Chapa-Oliver & Mejía-Teniente, 2016; Clark & Lee, 2016; Srinivasan, 2016; S. Zhang, et al., 2020), a few studies have suggested that capsaicin promotes the survival and growth of breast, colon and skin cancers (Bode & Dong, 2011; Toth & Gannett, 1992). Erin et al., (2004 and 2006) showed that the administration of capsaicin at high doses (125 mg capsaicin/kg body weight) increased breast cancer aggressiveness and promoted mammary tumor metastasis to the lung and heart (Erin, Boyer, Bonneau, Clawson, & Welch, 2004; Erin, Zhao, Bylander, Chase, & Clawson, 2006). An important point to note here is that the authors used extremely high doses of capsaicin (125mg/kg bodyweight) for their experiments. The aim of their studies was to demonstrate that capsaicin caused denervation of sensory neurons in breast carcinomas and such denervation promoted breast cancer metastasis (Erin, et al., 2004; Erin, et al., 2006). In fact, several publications have demonstrated the growth-suppressive activity of have shown that the capsaicin in breast cancer using cell culture and orthotopic mouse models. Similarly studies by Yang et al., (2013) have shown that the capsaicin promoted the metastasis of colon cancers

in CT-26 syngenic mouse models (Yang, et al., 2013). However, they used an atypical protocol to measure the effect of capsaicin on metastasis of colon tumors in syngenic mice. Conventionally, the protocol to perform such experiments is to first establish the metastatic tumors in the mice (Guerin, Finisguerra, Van den Eynde, Bercovici, & Trautmann, 2020). Subsequently, the mice should be randomized into control and treatment groups. The treatment group should be administered capsaicin (via diet, or oral gavage or osmotic pumps or intraperitoneal injections) for a period of 3–4 weeks. After the treatment period the mice should be euthanized and the effect of capsaicin on the number of metastatic foci should be determined. However, Yang et al., (2013) treated CT-26 cells *in vitro* with a high dose of capsaicin (100  $\mu$ M) for 48 hours and then injected these cells intravenously (via the tail vein) of BALB/C mice. The fact that they used a different protocol to perform the mice experiments may explain the aberrant results obtained in their studies. This is clearly exemplified by the data of Caetano et al., (2021) who demonstrated that capsaicin did not possess any tumor-promoting activity on colon carcinogenesis (Caetano, et al., 2021). In fact, several publications show capsaicin inhibits the growth of colon cancers in cell culture and mouse models (Jin, et al., 2014; Lee & Clark, 2016).

A few published reports suggested that the administration of capsaicin in Swiss albino mice induced duodenal adenocarcinomas (Hwang, et al., 2010; Toth & Gannett, 1992; Toth, Rogan, & Walker, 1984). However, a close survey of their data show that the appearance of such tumors were not related to the administration of capsaicin. Studies by the research group of Bode et al. showed that the co-administration of capsaicin with 7,12-dimethylbenz(a)anthracene (DMBA) and tetradecanoylphorbol-13-acetate (TPA) increased the incidence of skin tumors in TRPV1 knockout mice. The study did not include a group of mice treated exclusively with capsaicin. Bley et al., (2012) have rigorously analyzed the data published in these papers and inferred that the capsaicin could be increasing the number of TPA-induced skin tumors by enhancing the delivery and bioavailability of TPA in the skin of these mice (Bley, Boorman, Mohammad, McKenzie, & Babbar, 2012).

Chanda et al., (2007) explored the direct effect of capsaicin on skin tumorigenesis was in female hemizygous Tg.AC mice (Chanda, et al., 2007). They administered varying doses of capsaicin (via topical application) on the dorsal skin of female Tg.AC mice for 26 weeks. Specifically, the doses of capsaicin used in this study ranged from 0.64mg capsaicin/ mouse/ week-2.56mg capsaicin/mouse/week. The volume of capsaicin solution applied on the skin was 0.1ml. It must be noted that the concentration of capsaicin applied to the treated skin areas was quite high, as the lowest capsaicin dose level in the present study (0.64 mg/0.1 ml) corresponds to a concentration of 20.9 mM. After 26 weeks, the authors observed no increased dermal masses or preneoplastic and neoplastic lesions in skin (exposed to very high concentrations of capsaicin). Based on their data, they concluded that capsaicin did not display any oncogenic activity on the skin of mice. In summary, all these studies did not provide any concrete evidence that capsaicin promoted the growth of colon, breast and skin cancers.

Apart from its direct growth-suppressive activity, capsaicin sensitizes human cancer cells to the cytotoxic effects of standard-of-care chemotherapeutic agents. These include radiation-therapy, synthetic small molecules, conventional chemotherapeutic drugs, as well as targeted

signal-transduction inhibitors (Friedman, Richbart, Merritt, Perry, et al., 2019; S. Zhang, et al., 2020). It is well established that prolonged treatment with cancer chemotherapy drugs (or radiation) leads to the acquisition of drug-resistance in human cancers (Alfarouk, et al., 2015; Vasan, Baselga, & Hyman, 2019). Such resistance is one of the reasons contributing to the dismal survival rates of many cancers. We believe that the ability of capsaicin to sensitize tumors to the effects of chemotherapy drugs may have important clinical applications in cancer therapy. The addition of capsaicin to existing anti-cancer drug regimens may improve the therapeutic index of such combination therapies and improve health outcomes of cancer patients. Since capsaicin is already used in the clinic for its pain-relieving effect, the idea of repurposing this drug for cancer therapies has generated considerable enthusiasm amongst cancer researchers (Efferth & Oesch, 2021; Kale, Amin, & Pandey, 2015). Taken together, such facts emphasize the translational potential of capsaicin-based therapy in patients.

The chemosensitization and anti-tumor activity of capsaicin involves multiple molecular pathways including, inhibition of cell proliferation (Ali Al-Samydai, 2019; Chan, Azlan, Ismail, & Shafie, 2020), induction of apoptosis (Clark & Lee, 2016; S. Zhang, et al., 2020), regulation of autophagic pathways (Chang, Islam, Liu, Zhan, & Chueh, 2020; C. H. Choi, Jung, & Oh, 2010; Lin, et al., 2017; Ramos-Torres, Bort, Morell, Rodríguez-Henche, & Díaz-Laviada, 2016) and alteration of the pharmacokinetics of conventional chemotherapeutic drugs (Wang, Zhu, Zhang, Zhai, & Lu, 2018) (Figure 1). In addition, an important mechanism underlying the growth-suppressive activity of capsaicin is its ability to inhibit tumor angiogenesis and metastasis (Chakraborty, et al., 2014; Friedman, Richbart, Merritt, Brown, et al., 2019; Min, et al., 2004; Pyun, et al., 2008). All these facts emphasize the therapeutic potential of capsaicin as a useful anti-cancer drug, both as a single agent or in combination with existing chemotherapeutic drug regimens.

The clinical development of capsaicin as a viable anti-cancer drug is hampered by three factors, 1) the low solubility of capsaicin in aqueous environments, 2) the short biological half-life and bioavailability of capsaicin in vivo, 3) the adverse side effects of oral administration of capsaicin. The solubility of capsaicin in water is extremely low (0.0013 g/100 mL water). Therefore, all cell culture studies exploring the use of capsaicin as an anti-cancer drug have used solutions of capsaicin in water mixed with low concentrations of organic solvents such as DMSO or ethanol (Costanzo, Yost, & Davenport, 2014; Turgut, Zhang Newby, & Cutright, 2004). Secondly, capsaicin has a short biological half-life in plasma and is rapidly eliminated from the (O'Neill, et al., 2012; Reyes-Escogido Mde, Gonzalez-Mondragon, & Vazquez-Tzompantzi, 2011; Rollyson, et al., 2014) (Figure 2). Kawada et al., (1985) analyzed the metabolism of capsaicin after intraperitoneal (i.p) injection in anesthetized male Wistar rats. They observed that capsaicin was rapidly metabolized after injection. The maximal amount of capsaicin was detected in the thigh venous blood 16 minutes after the intraperitoneal injection. Furthermore, the amount of capsaicin in the blood decreased rapidly within 40 minutes after injection. The half-life of capsaicin was found to be approximately 12 minutes in the blood (Teruo Kawada & Iwai, 1985; T. Kawada, Suzuki, Takahashi, & Iwai, 1984). The third disadvantage with capsaicin is that it causes skin redness, hyperalgesia, nausea, intense tearing in the eyes, conjunctivitis, blepharospasm (sustained, forced, involuntary closing of the eyelids), vomiting, abdominal pain, stomach cramps, bronchospasm, and burning diarrhea in patients (Drewes, et al., 2003;

Evangelista, 2015; Hammer, 2006). Clinical trials exploring the pain-relieving activity of capsaicin have shown that such side effects have resulted in patients discontinuing use of the drug.

A strategy to overcome all these hurdles is to entrap capsaicin within polymeric drug carriers to generate sustained release formulations. The encapsulation of capsaicin in sustained release systems ensures that the drug is uniformly dispersed within the polymeric matrix (Chittepu-Reddy, Kalhotra, Revilla, & Gallardo-Velazquez, 2018; Rollyson, et al., 2014). The capsaicin is released from the polymer in a slow, steady and prolonged manner which improves its solubility properties. Some forms of sustained release drugs contain chaotropic salts, surfactants and co-surfactants which enhance the ability of capsaicin to disperse uniformly in the aqueous microenvironment (Chittepu-Reddy, et al., 2018; Rollyson, et al., 2014). The capsaicin is homogeneously entrapped within the polymeric matrix scaffold and so it is not available to intracellular enzymes for degradation. Drug release studies and biodistribution experiments have shown that sustained release platforms considerably increase the amount of capsaicin being delivered to the blood (and specific organs) in mouse and rat model systems. Finally, the gradual release of capsaicin ensures that only a small amount of the drug is present in the blood which reduces the incidence of gastrointestinal and skin irritation in patients.

Clinical studies reveal that extended release capsaicin formulations are used to combat neuropathic pain in patients. The long acting formulation of capsaicin (the transdermal patch Qutenza) is used in the clinic to relieve neuropathic pain (associated with postherpetic neuralgia) and diabetic nerve pain (Burness & McCormack, 2016; Uceyler & Sommer, 2014). The clinical application of QUETENZA raises the possibility that sustained release capsaicin formulations may have applications in the treatment of other diseases like cancer. A plethora of published papers have provided evidence that slow-release capsaicin formulations display potent anti-tumor activity in cell culture systems and mouse models (S. Zhang, et al., 2020). Most importantly, these long-acting capsaicin formulations selectively kill cancer cells and have minimal growth-suppressive activity on normal cells.

An exciting development has been the discovery of sustained release formulations which are capable of releasing capsaicin and chemotherapeutic drugs simultaneously. Polymeric drugs capable of releasing paclitaxel, gefitinib and irinotecan with capsaicin have shown robust anti-cancer activity in multiple in vivo model models of human cancer (Lan, et al., 2019; P. Parashar, et al., 2019; L. Wang, et al., 2017). A cutting edge application of capsaicin-based sustained release formulations has been as imaging probes for the early detection and diagnosis of cancers. It is well established that one of the challenges in the treatment of lung cancer, hepatocellular carcinoma and pancreatic cancer is the lack of methods for early detection of these tumors in patients (Cassim, et al., 2019; Gheorghe, et al., 2020; Midthun, 2016; Parikh, et al., 2020; X. R. Wang, et al., 2017). Taken together, we believe that capsaicin-based sustained release formulations may have multiple clinical applications in the detection and treatment management of cancers. In particular, the chemosensitization ability of slow-release capsaicin drugs and their ability to function as imaging agents (for early diagnosis of cancers) has the potential to improve the health outcomes of cancer patients in the clinic. The primary objective of this manuscript is to describe the pharmacological

and biological properties of capsaicin-based sustained release formulations which have been explored for the treatment of human cancers. An asset of these long-acting capsaicin formulations is that they selectively kill cancer cells and have minimal growth-suppressive activity on normal cells.

Several review articles describing the analgesic activity of capsaicin-sustained release formulations can be found in literature (Arora, Campbell, & Chung, 2021; Fattori, Hohmann, Rossaneis, Pinho-Ribeiro, & Verri, 2016). However, none of them have provided a comprehensive overview about the anti-cancer activity of capsaicin-based sustained release drug delivery systems. Our manuscript fills this void of knowledge. We believe that this review article is timely, relevant and will provide novel insights (involving the pharmacology of capsaicin formulations) to a wide spectrum of researchers working in the field of cancer biology.

## 2. Sustained Release Capsaicin Drugs for Cancer Therapy

Many research publications have described the anti-neoplastic activity of capsaicin-containing sustained release drug delivery systems such as solid dispersion systems (Oliveira, et al., 2020; Tran, et al., 2019), phospholipid complexes (J. Li, et al., 2014), liposomes (Pawar, Bhosale, & Derle, 2021), polymeric micelles (Ghezzi, et al., 2021) and nanoparticles (Beltrán-Gracia, López-Camacho, Higuera-Ciapara, Velázquez-Fernández, & Vallejo-Cardona, 2019) (Figure 3). The main objective of all these sustained release drugs is to improve the stability, bioavailability and pharmacokinetics of capsaicin. Many capsaicin-containing sustained release formulations have been functionalized with biological ligands which enable them to deliver the capsaicin drug cargo to specific types of tumors/organs. A novel application of these long-acting capsaicin formulations is as imaging agents capable of providing deep penetration images within solid tumors (P. Nigam, et al., 2014). We will be discussing the physiochemical characteristics, pharmacokinetic profiles and biological applications of these sustained release capsaicin in human cancers.

### 2.1 Capsaicin containing Solid Dispersion (SD) Drug Delivery Systems

A solid dispersion (SD) system is a sustained release drug delivery platform where the pharmacologically active drug is uniformly dispersed within a polymeric solid-state carrier. A majority of SD drug-polymers are two component systems which facilitate drug dispersion and its stabilization within a three-dimensional matrix (Oliveira, et al., 2020; Tran, et al., 2019). SD systems have proved to be very useful for improving the dissolution properties of hydrophobic drugs in aqueous milieu (Alshehri, et al., 2020). While the exact mechanisms by which SD systems improve the solubility index of the drug are yet to be fully understood, it is generally recognized that the polymer's role is to facilitate gradual drug release from the amorphous matrix and to delay subsequent aggregation of the drug. The drug is released from the solid-state matrix at a slow steady manner which enhances its bioavailability and retention properties of the drug *in vivo* (Alshehri, et al., 2020). Currently, more than twenty solid dispersion anti-cancer drug formulations are being used in the clinic. Such findings confirm that the solid-state dispersion drug delivery system is an efficient

technique to improve dissolution of poorly water-soluble anti-cancer drugs to enhance their bioavailability and growth-suppressive activity *in vivo*.

**2.1.1 Physiochemical Properties of Capsaicin SDDD Systems**—The poor solubility of drug molecules (in aqueous environment) is a major challenge in cancer drug discovery (Gala, Miller, & Williams, 2020). Although, capsaicin displays potent growth-suppressive activity in several human cancers, the poor water solubility (0.0013 g/100 mL) of capsaicin is a major hindrance in its development as a clinically useful anti-cancer drug. Bera et al., (2020) observed that urea enhanced the solubility of capsaicin in aqueous solvents. Specifically, they discovered that the presence of urea (as a carrier) increased the aqueous solubility of capsaicin by 3.6-fold compared to pure capsaicin (Bera, Maity, Ghosh, Ghosh, & Giri, 2020). Based on these results, they synthesized a SDDDS where capsaicin was dispersed in a hydrophilic urea matrix by using the solvent evaporation method. The SDDDS were characterized by X-ray Diffraction and Differential Scanning Calorimetry (DSC) techniques. The capsaicin-urea SDDDS (CAP-UREA-SDDDS) was an amorphous powder in which capsaicin and urea were distributed as a 1:3 molar ratio (Table 1). DSC thermograms revealed that the melting point of the CAP-UREA-SDDDS was lower than pure capsaicin which reflected the formation of a stable capsaicin-urea complex. Solubility studies confirmed that the dissolution efficiency and mean dissolution rate of CAP-UREA-SDDDS in aqueous buffer (at pH=7.4) was about 6-times higher than pure capsaicin. This can be explained by the fact that urea reduces the interfacial tension between the capsaicin molecules and enables them to be uniformly distributed within the solid dispersion system (Bera, et al., 2020). Also, urea disrupts the hydrogen bonding within the water molecules which allows hydrophobic solutes to become solvated in water.

**2.1.2 Drug Release Kinetics of Capsaicin SDDD Systems**—The *in vitro* drug release pattern of CAP-UREA-SDDDS revealed that the drug cargo (capsaicin) was released from the CAP-UREA-SDDDS at a steady constant rate. A noteworthy observation was that there was no initial spike in the release of the drug. This implied that the drug was stably entrapped within the solid matrix and not adsorbed passively on the surface of the urea polymer (Bera, et al., 2020). Almost 38% of the drug cargo (capsaicin) was released from the SDDDS within the first hour (Table 2). In contrast, only 7% of pure capsaicin was released into the aqueous microenvironment in one hour. Such observations provide the “proof of concept” that the SDDDS enhanced the release rate and the steady state concentration of capsaicin compared to the pure drug. Essentially, 100% of the capsaicin was released from the CAP-UREA-SDDDS over 8 days (Bera, et al., 2020). Such enhancement of drug release could be attributed to the decrease in the particle size of the solute (due to loss of crystallinity of capsaicin) and to the ability of urea to solubilize and disperse the capsaicin uniformly within the solvent matrix.

**2.1.3 Anti-Cancer Activity of Capsaicin SDDD systems**—The growth suppressive activity of CAP-UREA-SDDDS was investigated in the two human breast cancer cell lines MCF-7 and MDA-MB-231. The blank SDDDS did not have any impact on the viability of either of these human breast cancer cell lines (Bera, et al., 2020). Both free capsaicin and CAP-UREA-SDDDS decreased the viability of MCF-7 cells at concentrations ranging

from 100–300 $\mu$ M at 24 hours. The growth-suppressive activity of CAP-UREA-SDDDS was almost identical to free capsaicin (Bera, et al., 2020). These experiments were repeated in triple negative MDA-MB-231 human breast cancer cells and similar results were obtained (Table 3). The fact that CAP-UREA-SDDDS does not display higher growth inhibitory activity than free capsaicin is indeed surprising. The drug release kinetics of CAP-UREA-SDDDS show that the release of capsaicin is sluggish over the first 2 days and then increases substantially over the next 7 days (Bera, et al., 2020). If the MTT assay was done over longer time points (instead of 24 hours), then perhaps CAP-UREA-SDDDS would have displayed higher growth suppressive activity (in MCF-7 and MDA-MB-231 human breast cancer cell lines) than free capsaicin.

## 2.2 Capsaicin Phospholipid Complexes and Liposomes

Phospholipids are unique, amphiphilic versatile molecules which have been extensively used to fabricate drug delivery systems. The structure of phospholipids comprises of a hydrophilic head group (containing phosphorous and a polar group) and a hydrophobic tail (a fatty acyl group). Phospholipids play a vital role in structuring and stabilizing biological interfaces. Such interactions between these phospholipids and the aqueous microenvironment have formed the basis of a wide variety of drug delivery systems like phospholipid-drug complexes (phytosomes), lipid emulsions, micelles and liposomes (Drescher & van Hoogevest, 2020; A. Gao, et al., 2019; J. Li, et al., 2014; Mirzavi, et al., 2021). Several anti-cancer drugs doxorubicin, daunorubicin, cytoarabine and cyclophosphamide are administered to patients as liposomal formulations in the clinic (A. Gao, et al., 2019; Mirzavi, et al., 2021; Pandey, Rani, & Aggarwal, 2016) Saheli et al., 2019, 2020).

### 2.2.1 Physicochemical Properties of Capsaicin Phospholipid Complexes and Liposomes

—Published data show that nutritional agents have a high affinity for phospholipids, and they can form stable drug-phospholipid complexes (called phytosomes) which display improved pharmacological activities compared to the parent drug (Drescher & van Hoogevest, 2020; J. Li, et al., 2014). The amphiphilicity of these phytosomes increases their solubility (and absorption) in the gastrointestinal tract. Furthermore, these drug-phospholipid complexes display improved bioavailability, duration of action and stability of the drug *in vivo* (Drescher & van Hoogevest, 2020; J. Li, et al., 2014). Mondal et al., (2019) formulated a drug delivery system whereby capsaicin was complexed in soyabean phospholipids in the molar ratio of 1:2. The capsaicin-soyabean phospholipid complex (CAP-SOY-PL) was synthesized by the solvent evaporation method (Table 1). CAP-SOY-PL was stable as a dry lyophilized powder at room temperature (Mondal, Bobde, Ghosh, & Giri, 2019). The capsaicin phospholipid complex drug was characterized by Fourier Transform infra-red spectroscopy (FT-IR), DSC and X-ray diffraction studies. FT-IR and DSC studies revealed that the spectra of the CAP-SOY-PL was different from a physical mixture of capsaicin and the soyabean phospholipid (Mondal, et al., 2019). The fatty acid chains in CAP-SOY-PL rotate freely and envelop the capsaicin molecule to enable its efficient dispersion into the phospholipid milieu. The X-ray diffraction spectra of CAP-SOY-PL suggested that the complexation of capsaicin (by phospholipids) reduced its crystalline properties. It also confirmed the fact that most of the capsaicin in CAP-SOY-PL was present in the amorphous form (Mondal, et al., 2019). This agrees with previous studies which show

that the drug-phospholipid complexes interact with the aqueous environment to generate self-assembled supramolecular structures which have better stability and bioavailability properties than the parent compound (Semalty, 2014; Semalty, Semalty, Singh, & Rawat, 2010; Telange, et al., 2017).

The solubility of CAP-SOY-PL in water was 2.6-fold higher than free capsaicin. Notably, the physical mixture of capsaicin and soybean phospholipids did not improve the aqueous solubility of capsaicin. This may be explained by the fact that the formulation of CAP-SOY-PL induced amorphization of capsaicin which resulted in the formation of a stable micelle with phospholipids (Mondal, et al., 2019). Phospholipids are surface-active wetting agents which can coat the surface of crystalline drugs to enhance the dissolution efficiency of hydrophobic drugs. The amphiphilic stable CAP-SOY-PL micelles trigger the “wetting” of capsaicin, thereby increasing its solubility in water (Drescher & van Hoogevest, 2020; J. Li, et al., 2014). In summary, the improved stability and solubility properties of CAP-SOY-PL suggest that it may be an efficient drug delivery system for the treatment of human cancers.

Qi et al., (2021) formulated a liposome drug delivery system which could deliver two nutritional anti-cancer drugs namely curcumin and capsaicin. These liposomes were functionalized with glycyrrhetic acid (GA) and galactose (GAL) to specifically target them to hepatocellular carcinoma cells (Qi, et al., 2021). The ligand for the GA and GAL molecules is the asialoglycoprotein receptor (ASGP-R) which is highly expressed in hepatocellular carcinoma cells (Roggenbuck, Mytilinaiou, Lapin, Reinhold, & Conrad, 2012; Shi, Abrams, & Sepp-Lorenzino, 2013). The ASGP-R has been explored as an attractive drug target for the diagnosis and treatment of human hepatocellular carcinoma in patients (Harris, van den Berg, & Bowen, 2012; D. Peng, et al., 2007; X. Song, et al., 2019). Normal hepatocytes contain very meagre amounts of the ASGP receptor (Harris, et al., 2012). The ASGP-R protein is a unique protein biomarker that is almost exclusively localized to liver tissues. ASGP receptors are not expressed in most organs but have been detected in blood monocytes and dendritic cells (Harris, et al., 2012; Roggenbuck, et al., 2012; Shi, et al., 2013). Therefore, these GLY-and GAL-functionalized liposomes should be only internalized by liver tissue. The loading of capsaicin and curcumin on these GLY-GAL-functionalized liposomes (CAP-CUR-GLY-GAL-LIPO) was accomplished by the thin film evaporation method (Qi, et al., 2021). In addition to CAP-CUR-GLY-GAL-LIPO, three other types of liposomes were synthesized as the controls for the pharmacological and biological assays. These were :1) Capsaicin and curcumin containing polyethylene glycol (PEG) liposomes (CAP-CUR-LIPO), 2) Capsaicin and curcumin containing galactose functionalized liposomes (CAP-CUR-GAL-LIPO), 3) Capsaicin and curcumin containing glycyrrhetic acid functionalized liposomes (CAP-CUR-GLY-LIPO). All of these capsaicin-curcumin containing liposomes were characterized by Dynamic light scattering technology (DLS) and Transmission electron microscopy (TEM).

The size of the liposomes is an important parameter that impacts passive targeting of these drugs to tumor tissue. The accumulation of liposomes in the tumor strongly depends on the size of the endothelial gaps in the capillary vasculature for a particular cancer (Golombek, et al., 2018; Maruyama, 2011). Liposomes smaller than 400 nm diameter utilize the enhanced permeability and retention (EPR) effect to preferentially extravasate into tumors. The EPR

effect is a mechanism by which high-molecular drug delivery systems (typically prodrugs, liposomes, nanoparticles, and macromolecular drugs) tend to accumulate in tumor tissue much more than they do in normal tissues (Golombek, et al., 2018; Maruyama, 2011). Such preferential accumulation in tumor tissues can be explained by the fact that these sustained release drugs leak into the tumor tissue (due to increased vascular permeability of the tumor tissue) and then are retained in the tumor bed due to reduced lymphatic drainage in tumors (Golombek, et al., 2018; Maruyama, 2011). The efficiency of such extravasation is maximum when the size of the liposomes less than 200 nm. The CAP-CUR-GLY-GAL-LIPO were spherical in shape with a narrow range of size distribution ranging from 135–155nm (Table 1). The size range of the CAP-CUR-GLY-GAL-LIPO (< 200nm) implies that these liposomes will display a greater retention in solid tumors as compared to normal organs in the body.

The polydispersity index is used to estimate the average uniformity of the size of liposome. The numerical value of polydispersity index ranges from zero (for a perfectly uniform sample with respect to the particle size) to 1.0 (for a highly polydisperse sample with multiple particle size populations) (Danaei, et al., 2018; Verma, Verma, Blume, & Fahr, 2003). The polydispersity index of these capsaicin-curcumin-loaded liposomes (CAP-CUR-LIPO) were below the threshold value of 0.7, which indicated a good dispersion homogeneity. The particle size and polydispersity index of these CAP-CUR-GLY-GAL-LIPO was unaffected by their dissolution in saline or in DMEM cell culture media, indicating that these dual function liposomes were stable at physiological conditions. The zeta potential provides a measure of the stability, circulation time, protein interaction, particle cell permeability, and biocompatibility of liposomes *in vivo* (Rasmussen, Pedersen, & Marie, 2020; Smith, Crist, Clogston, & McNeil, 2017). Normally, particle suspensions with zeta potentials greater than +30 mV or less than –30 mV are considered stable (Rasmussen, et al., 2020). As Table 1 indicates, all the capsaicin-curcumin loaded liposomes had a zeta-potential lower than –30mV, which means that these particles formed a stable dispersion in aqueous environments, without undergoing aggregation.

The drug entrapment efficiency (DEE) reflects the percentage of the free drug that is successfully entrapped/adsorbed into the sustained release drug delivery system. The DEE of liposomal drugs provides a measure of *the in vivo* performance of these drug delivery platforms and determines the amount of the drug that is released (and redirected) from the carrier to the cancer tissues (Ong, Ming, Lee, & Yuen, 2016; Ullmann, Lenewit, & Nirschl, 2021). All the CAP-CUR liposomes had excellent drug encapsulation efficiency (>85%). The small liposome size (135–155 nm) and high DEE predicted that all the CAP-CUR-liposomal drugs will have excellent the bioavailability and penetration properties in tumor tissue.

**2.2.2 Drug Release, Pharmacokinetics and Biodistribution of Capsaicin Phospholipid Complexes and Liposomes**—The *in vitro* drug release experiments revealed that most of the capsaicin was released from CAP-SOY-PL at pH=7.4 (pH of the intestine). In contrast, a very small amount of capsaicin was released at pH=1.2 (pH of the stomach). The fact that the drug cargo is preferentially released at pH=7.4 suggests that CAP-SOY-PL may be a good drug for oral administration in patients (Mondal, et al.,

2019). No initial spike in drug concentration was observed, which suggested that the entire drug was complexed within the interior regions of the phospholipid complex. At 10 hours, CAP-SOY-PL released 60% of capsaicin whereas only 20% of the drug was released from pure capsaicin (Table 2). The physical mixture of capsaicin and the phospholipids released capsaicin at approximately the same rate as the pure compound. Nearly, the entire capsaicin was released from CAP-SOY-PL at 30 hours, whereas only 60% of the drug cargo was released from the physical mixture on pure capsaicin at this time point (Mondal, et al., 2019). The enhanced drug release efficiency of CAP-SOY-PL may be attributed to the enhanced wettability and solubility of capsaicin when it is complexed with phospholipids (Drescher & van Hoogevest, 2020; J. Li, et al., 2014).

The CAP-CUR-GLY-GAL-LIPO targeted liposome was a distinctive drug delivery system, designed to release capsaicin and curcumin to human hepatocellular carcinoma cells. A modified dialysis bag method was used to measure the *in vitro* drug release properties CAP-CUR-GLY-GAL-LIPO (Qi, et al., 2021). The drug release medium was modified by adding 20% ethanol and 1.5% Tween-80, to enable better solubility of the hydrophobic drugs as well as to satisfy the sink condition. The pH of the buffer was maintained at 7.4, which resembled the pH of the small intestine. Both the drugs were released at a steady and uniform rate over 48 hours (Table 2). There was no early burst of the release of capsaicin and curcumin, which indicated that both the drugs were securely entrapped inside the liposome, and neither were non-specifically bound on the surface (Qi, et al., 2021). At all the time points, the release rate of capsaicin was higher than curcumin. The drug was released at a faster rate over the first 15 hours (approximately 60% of both the drugs being released) and then the release rate plateaued from 24–48 hours (Qi, et al., 2021). The majority of the drug cargo (~95% capsaicin, ~85% curcumin) was released at 48 hours. The authors did not compare the drug release rates of CAP-CUR-GLY-GAL-LIPO and CAP-CUR-LIPO. Therefore, it would be difficult to speculate if the addition of the GLY and GA targeting moieties had any effect on the drug release properties of these liposomes.

The cellular uptake of these dual function targeting liposome was measured in HepG2 human hepatocellular carcinoma cells. The blank liposomes (BLANK-LIPO), Glycyrrhetic acid functionalized PEG liposomes (GLY-LIPO), Galactose functionalized PEG liposomes (GAL-LIPO) and Glycyrrhetic acid and galactose functionalized PEG liposomes (GAL-GLY-LIPO) were labeled with the fluorescent tag fluorescein isothiocyanate (FITC) and their uptake in HepG2 cells was measured by confocal microscopy (Qi, et al., 2021). The FITC-labeled BLANK-LIPO showed moderate uptake in HepG2 cells at 4 hours. In contrast, FITC-labeled GA-LIPO and GLY-LIPO were internalized by HepG2 cells as early as 15 minutes (Table 2). At 4 hours, the amount of FITC-labeled GA-LIPO and GLY-LIPO internalized by HepG2 cells was substantially higher than FITC-labeled BLANK-LIPO. The dual targeted liposome GAL-GLY-LIPO showed the highest uptake (relative to GAL-LIPO, GLY-LIPO and BLANK-LIPO) in HepG2 cells. All the liposomes were predominantly localized in the cytosol of HepG2 cells (Qi, et al., 2021). The presence of the GAL and GLY targeting groups enabled the cells to internalize higher amounts of GLY-GAL-LIPO, GA-LIPO and GLY-LIPO. In summary, the pattern of internalization of the liposomes was FITC-GAL-GLY-LIPO > FITC-GLY-LIPO = FITC-GAL-LIPO > CAP-LIPO in HepG2 hepatocellular carcinoma cells.

The tumor microenvironment of hepatocellular carcinoma comprises of activated hepatic stellate cells (HSC), endothelial cells, tumor-associated macrophages, and immune cells. The crosstalk between the primary tumor and the HSCs plays a vital role in promoting the growth, angiogenesis, and distant metastasis of hepatocellular carcinoma (Barry, et al., 2020; Dapito & Schwabe, 2015; Y. Song, et al., 2016; Wu, Miao, Fu, Zhang, & Zheng, 2020). Qi et al., (2019) designed a co-culture system of HepG2 hepatocellular carcinoma cells and LX2 human stellate cells to mimic the interactions between the primary tumor and its stroma (Qi, et al., 2021). The capsaicin-loaded liposomes (CAP-LIPO), capsaicin-loaded-glycyrrhetic acid-galactose-functionalized liposomes (CAP-GAL-GLY-LIPO) and capsaicin-loaded-galactose-functionalized liposomes (CAP-GA-LIPO) were labeled with the fluorescent dye coumarin-6 and the uptake of these coumarin-labeled liposomes (in the HepG2/LX2 co-culture model) was measured by confocal microscopy. All of the liposomes were exclusively localized in the cytoplasm of HepG2/LX2 co-cultured cells (Qi, et al., 2021). The uptake of coumarin-labeled free capsaicin and CAP-LIPO steadily increased over time and was highest at 12 hours and then decreased again to baseline levels by 24 hours (Table 2). The presence of two targeting ligands GAL- and GLY- triggered the maximal uptake of the liposomal drug. At 12 hours, the amount of coumarin-labeled CAP-GAL-GLY-LIPO localized in HepG2/LX2 co-cultured cells was about 6-fold higher than free capsaicin or CAP-LIPO. Although, the uptake of CAP-GAL-GLY-LIPO declined at 24 hours, it remained about 4-fold higher than capsaicin or CAP-LIPO (Qi, et al., 2021). The targeting efficiency of the liposomal drug containing only one targeting ligand (namely GAL) was intermediate between CAP-GAL-GLY-LIPO and the non-functionalized liposome (Qi, et al., 2021). The levels of CAP-GAL-LIPO internalized by HepG2/LX2 co-cultured cells was intermediate between free capsaicin, CAP-LIPO and CAP-GLY-GAL-LIPO. At all the time points tested, the pattern of uptake of the liposomes in HepG2/LX2 co-cultured cells was CAP-GAL-GLY-LIPO > CAP-GAL-LIPO > CAP-LIPO = free capsaicin in HepG2/LX2 co-cultured cells.

Near infrared fluorescence imaging experiments revealed that CAP-GAL-GLY-LIPO and CAP-GAL-LIPO displayed better retention properties in HepG2/LX2 co-cultured cells than free capsaicin and CAP-LIPO at 24 hours (Qi, et al., 2021). The elimination rate of CAP-GAL-GLY-LIPO was the lowest followed by CAP-GAL-LIPO, which was higher CAP-LIPO and free capsaicin at 24 hours. Conversely, the retention rate of the CAP-GAL-GLY liposomes > CAP-GAL liposomes > CAP-LIPO > free capsaicin or in in HepG2/LX2 co-cultured cells. In summary, the presence of two targeting ligands (GAL and GLY) on the capsaicin-loaded liposomes facilitated better uptake, internalization, and retention of the CAP-GAL-GLY-LIPO in HepG2/LX2 co-cultured cells.

The biodistribution of the GAL- and GLY-functionalized liposomes was investigated in Balb/c mice bearing two types of tumors known as B16 murine melanoma tumors and H22 murine liver cancer tumors (Qi, et al., 2021). The B16 tumor served as the non-specific controls for the uptake and biodistribution experiment. Melanoma do not express the ASGP receptor, so they should not bind to GLY- and GAL-labeled liposomes. The GAL- and GLY-functionalized liposomes were labeled with near infrared (NIR) fluorescent dye 1,1'-dioctadecyl-3,3',3'-tetramethylindotricarbocyanine iodide (DiR) (Gangadaran, Hong, & Ahn, 2018; Liu & Wu, 2016). Female Balb/c mice were subcutaneously injected with H22

liver cancer cells (on the right flank) and B16 melanoma cells (on the left flank). The tumors were allowed to grow to a threshold volume of 200mm<sup>3</sup> after which they were injected with Free DiR (40µg/ml) or DiR-LIPO or DiR-GAL-GLY-LIPO via the tail vein. The drug distribution was monitored at time points ranging from 2–48 hours by NIR fluorescence microscopy (Table 2). The H22 liver cancer tumors showed robust uptake of the DiR-GAL-GLY-LIPO as early as 2 hours and the uptake of these liposomes steadily increased and was maximum at 8 hours (Qi, et al., 2021). In contrast, no DiR-GAL-GLY-LIPO was detected in the melanoma tumor. These findings confirm that the DiR-GAL-GLY-LIPO are being specifically targeted to the liver cancer tumor via the ASGP-R pathway. The uptake of DiR-GAL-GLY-LIPO by the H22 hepatocellular carcinoma tumor was approximately 27 times higher than free DiR or DiR-LIPO (Qi, et al., 2021). At 48 hours, the DiR-GAL-GLY-LIPO was seen to specifically localize in the liver of the tumor-bearing mice. Very meagre amounts of DiR-GAL-GLY-LIPO were observed in the heart, spleen, kidneys or the lungs of these tumor bearing mice (Qi, et al., 2021). The amount of DiR-GAL-GLY-LIPO present in the liver of these tumor-bearing mice was significantly higher than the free DiR dye or the DiR-labelled no-functionalized liposomes ( $P<0.05$ ). These observations confirm the liver-targeting abilities of glycyrrhetic acid and galactose functionalized liposomes.

The ability of these GAL-GLY-LIPO to penetrate deep inside the tumor tissue was measured by the DiD-labeling technique (Gangadaran, et al., 2018; Liu & Wu, 2016). DiD (1,1'-dioctadecyl-3,3',3'- tetramethylindodicarbocyanine, 4-chlorobenzenesulfonate) is a lipophilic fluorescent dye with longer excitation and emission wavelengths relative to DiR. The lipophilic properties of DiD and its prolonged retention abilities in cells make it suitable for deep penetration imaging inside solid tumors and organs (Gangadaran, et al., 2018; Liu & Wu, 2016). The authors generated DiD labeled glycyrrhetic acid and galactose functionalized liposomes (DiD-GAL-GLY-LIPO) and injected them (via the tail vein) into H22 tumor bearing Balb/c mice. After 48 hours, the tumors were harvested and cryosectioned. These tumor sections were visualized by NIR fluorescence microscopy (Table 2). The free DiD dye showed staining in the outer peripheral regions of the tumor (Qi, et al., 2021). In contrast, the DiD-GLY-GAL-LIPO showed strong uniform staining in all the regions within the solid liver tumor, indicating that these glycyrrhetic acid and galactose functionalized liposomes displayed excellent targeting, penetration, and retention abilities in hepatocellular carcinoma tumors *in vivo*.

**2.2.3 Anti-cancer Activity of Capsaicin Phospholipid Complexes and Liposomes**—The growth-suppressive activity of CAP-SOY-PL in MCF-7 and MDA-MB-231 human breast cancer cell lines was analyzed by the tetrazolium bromide-based viability assay. The CAP-SOY-PL (at a concentration of 100µM) decreased the viability of MDA-MB-231 cells better than capsaicin at 24 hours (Mondal, et al., 2019). However, there was no statistically significant differences between the growth-inhibitory activity of CAP-SOY-PL and free capsaicin at higher concentrations namely 150µM, 225µM and 300µM ( $P<0.05$ ) (Table 3). On the other hand, both CAP-SOY-PL and free capsaicin did not significantly decrease the viability of MCF-7 cells (between 15–25%) at concentrations ranging from 100–300 µM (Mondal, et al., 2019). This observation conflicts with the findings of Chen et al., (2021) who observed that capsaicin (at concentrations 100–300 µM)

decreases the viability of MCF-7 cells by 30–60% (compared to untreated control) after 24 hours (M. Chen, et al., 2021). The fact that CAP-SOY-PL and free capsaicin did not impact the viability of MCF-7 cells is a puzzling result. This may be due to differences in the methodology of the two studies. Whereas Chen et al., (2021) cultured MCF-7 cells in DMEM supplemented with 10% FBS, the authors used RPMI medium containing 5% FBS to culture their cells (M. Chen, et al., 2021; Mondal, et al., 2019). Published data show that culturing MCF-7 cells in 5% FBS elevate the levels of cancer stem cells by approximately 20% (Tavaluc, Hart, Dicker, & El-Deiry, 2007). These cancer stem cells are responsible for accelerated growth and increased heterogeneity of MCF-7 cells. The exposure of MCF-7 cells to 5% FBS may have resulted in subtle variations in the growth pattern and subpopulations in these cells which could be responsible for the aberrant results in the MTT assay.

Qi et al., (2021) created the multifunctional liposomal drug CAP-CUR-GLY-GAL-LIPO to simultaneously release capsaicin and curcumin to human liver cancer cells (Qi, et al., 2021). The unique feature of the CAP-CUR-GLY-GAL-LIPO liposomal drug delivery system was the presence of glycyrrhetic acid and galactose to specifically target these liposomes to human hepatocellular carcinoma cells. The glycyrrhetic acid and galactose moiety bind to the ASGP receptor on human hepatocellular carcinoma cells. Several congruent studies show that ASGP-R is overexpressed on human hepatocellular cancer tumors in patients (Roggenbuck, et al., 2012; Shi, et al., 2013). The ASGP-R has proved to be a clinically relevant molecular target for diagnosis and therapy of human hepatocellular carcinoma (D. Peng, et al., 2007). With this background, Qi et al., (2021) tested the cytotoxic activity of CAP-CUR-GLY-GAL-LIPO in HepG2 cells. The blank liposomes, GA-LIPO and GLY-LIPO had no impact on the viability of HepG2 cells (Qi, et al., 2021). A 24-hour incubation of CAP-CUR-GLY-GAL-LIPO decreased the viability HepG2 cells by 60% at a concentration of 13.6 $\mu$ M, which increased to 85% at and a concentration of 27.2 $\mu$ M (Table 3, 4). The growth-inhibitory activity of CAP-CUR-GLY-GAL-LIPO was higher CAP-CUR-GAL-LIPO and CAP-CUR-GLY-LIPO in HepG2 cells. Such findings suggest that the co-presence of two targeting ligands improves the growth-suppressive activity of the CAP-CUR-GLY-GAL-LIPO in human hepatocellular carcinoma cells (Qi, et al., 2021). Similarly, CAP-CUR-GLY-GAL-LIPO decreased the viability of cells better than the non-targeted liposome CAP-CUR-LIPO. At 24 hours, the growth-suppressive activity of CAP-CUR-GAL-GLY-LIPO > CAP-CUR-GAL-LIPO = CAP-CUR-GLY-LIPO > CAP-CUR-LIPO > mixture of capsaicin and curcumin = free curcumin > free capsaicin in HepG2 human hepatocellular carcinoma cells (Table 4).

The anti-tumor activity of CAP-CUR-GLY-GAL-LIPO was investigated *in vivo* in syngenic mouse models of liver cancer. Female Balb/C mice were subcutaneously injected (in the right flank) with H22 murine hepatocellular cancer cells (Qi, et al., 2021). After the tumor attained a threshold volume of 200mm<sup>3</sup>, the mice were treated with 5mg/kg body weight of CAP-CUR-GLY-GAL-LIPO or CAP-CUR-GAL-LIPO or CAP-CUR-LIPO. The controls in this experiment included tumor bearing mice were treated with free capsaicin (5mg/kg body weight) or free curcumin (5mg/kg body weight) or a physical mixture of capsaicin and curcumin. The drugs were intravenously injected every two days and the study was terminated at 2 weeks. None of the drugs had any effect on the body weights of the

mice (Qi, et al., 2021). Histological analysis showed that none of the drugs caused any off-target toxicity to the heart, liver, kidney, spleen or the lungs. The administration of CAP-CUR-GLY-GAL-LIPO caused robust decrease in the growth rates of the H22 tumors; the volume of the tumor was decreased by approximately 94% relative to the untreated control tumors (Table 3, 4). The anti-tumor activity of CAP-CUR-GLY-GAL-LIPO was higher than CAP-CUR-GAL-LIPO, indicating that the presence of two targeting molecules enhanced the anti-tumor activity of these liposomal drugs (Qi, et al., 2021). The anti-neoplastic activity of CAP-CUR-GLY-GAL-LIPO was also greater than the non-targeted liposomes (CAP-CUR-LIPO) or the physical mixture of capsaicin and curcumin. In conclusion, the anti-neoplastic activity of CAP-CUR-GAL-GLY-LIPO > CAP-CUR-GAL-LIPO > CAP-CUR-LIPO > mixture of capsaicin and curcumin = free curcumin > free capsaicin in H22 hepatocellular carcinoma bearing Balb/c mice (Table 4).

The activation of HSCs contributes to accelerated growth and progression of human hepatocellular carcinoma. The activated HSCs secrete many cytokines and growth factors which promote tumor growth, angiogenesis, epithelial-to-mesenchymal transition (EMT) and distant metastasis of the primary tumor (Barry, et al., 2020; Dapito & Schwabe, 2015; Geng, Li, Li, Zheng, & Shah, 2014; X. Liao, et al., 2019; Ma, et al., 2018; Wu, et al., 2020; Z.-C. Xu, et al., 2018). Activated HSCs possess a cancer-associated fibroblast like morphology which is responsible for the elevated production of extracellular matrix (ECM) proteins, ECM remodeling and acquisition of drug resistance of human hepatocellular carcinoma tumors in patients (Barry, et al., 2020; Dapito & Schwabe, 2015; X. Liao, et al., 2019; Ma, et al., 2018; Y. Song, et al., 2016). The co-culture of HepG2 human hepatocellular carcinoma cells with LX2 human hepatic stellate cells is an excellent preclinical model to investigate the problem of drug resistance in human liver cancer. Qi et al., (2021) grew HepG2 cells with LX2 cells at a ratio of 5:1 to generate a HepG2/LX2 co-culture system. The drug sensitivity properties of HepG2/LX2 co-cultured cells were compared with parent HepG2 cells (Qi, et al., 2021). MTT assays revealed that the amount of curcumin required to achieve 50% reduction in cell viability was 3-fold higher in HepG2/LX2 co-cultured cells, relative to parent HepG2 cells. In addition, the level of the multidrug resistance protein P-glycoprotein was elevated in HepG2/LX2 co-cultured cells by 1.3-fold as compared to the parent HepG2 cells. Taken together, these data suggest that HepG2/LX2 co-cultured cells showed greater drug resistant traits as compared to parent HepG2 cells.

An important objective of the experiments of Qi et al., (2021) was to determine whether CAP-CUR-GLY-GAL-LIPO could abrogate the growth of HepG2/LX2 co-cultured cells. The impact of CAP-CUR-GLY-GAL-LIPO on the viability of HepG2/LX2 co-cultured cells was examined by using the MTT and the Calcein-AM/PI assay. Both the MTT and the Calcein-AM/PI assays gave similar results (Qi, et al., 2021). The blank liposomes, GA-LIPO and GLY-LIPO did not display any cytotoxic activity in HepG2/LX2 co-cultured cells. The CAP-CUR-GLY-GAL-LIPO displayed the greatest growth-suppressive activity in the HepG2/LX2 co-cultured cell system, decreasing the viability of HepG2/LX2 cells by 60% (at a concentration of 13.6 $\mu$ M), which increased to 85% (at and a concentration of 27.2 $\mu$ M) at 24 hours. The ability of CAP-CUR-GLY-LIPO and CAP-CUR-GAL-LIPO to inhibit the growth of HepG2/LX2 co-cultured cells was lower than the dual targeting CAP-CUR-GLY-

GAL-LIPO (Qi, et al., 2021). Predictably, both CAP-CUR-GLY-LIPO and CAP-CUR-GAL-LIPO decreased the viability of HepG2/LX2 co-cultured cells to a similar extent, in 24 hours (Table 3, 4). At all the time points tested, the growth-inhibitory activity of CAP-CUR-GAL-GLY-LIPO > CAP-CUR--GAL-LIPO = CAP-CUR-GLY-LIPO > CAP-CUR-LIPO > mixture of capsaicin and curcumin > free curcumin = free capsaicin in HepG2/LX2 co-cultured cells (Table 4). A noteworthy observation is that CAP-CUR-LIPO displayed better growth-inhibitory activity than a physical mixture of capsaicin and curcumin or free curcumin or free capsaicin (Qi, et al., 2021). Presumably, the slow prolonged release of capsaicin and curcumin (from the CAP-CUR-LIPO liposomal drug delivery system), achieved a “depot effect” led to higher accumulation of these drugs (Nisini, Poerio, Mariotti, De Santis, & Fraziano, 2018) within the cellular milieu which in turn resulted in greater decrease in the viability of HepG2/LX2 co-cultured cells, compared to the capsaicin-curcumin mixture.

The treatment of HepG2/LX2 co-cultured cells with CAP-CUR-GLY-GAL-LIPO correlated triggered a greater magnitude of decrease of P-glycoprotein expression than CAP-CUR-LIPO, capsaicin-curcumin mixture, free curcumin, and free capsaicin (Qi, et al., 2021). Such findings prove that the CAP-CUR-GLY-GAL-LIPO drug delivery system circumvented the classic attributes of drug resistance in human hepatocellular carcinoma cells. Wang et al., (2019) extended these investigations in HepG2/LX2 cell culture systems in mice models. Balb/c mice were co-injected with H22 murine hepatocellular carcinoma cells and LX2 hepatic stellate cells (Qi, et al., 2021). After the H22/LX2 cells formed palpable tumors (~200mm<sup>3</sup> in volume) the mice were administered of CAP-CUR-GLY-GAL-LIPO (5mg/kg body weight) or CAP-CUR-GLY-LIPO (5mg/kg body weight) or CAP-CUR-GAL-LIPO (5mg/kg body weight) or CAP-CUR-LIPO (5mg/kg body weight) intravenously every two days for a total period of two weeks. Tumor bearing mice treated with free capsaicin (5mg/kg body weight), free curcumin (5mg/kg body weight) and a physical mixture of capsaicin and curcumin (dose of each drug at=5mg/kg body weight) served as the controls for the experiment. The intravenous injection of CAP-CUR-GLY-GAL-LIPO caused a considerable reduction in the volume of the H22/LX2 tumors; the tumor size was decreased by 90% (over two weeks) as compared to the vehicle-treated control tumors (Table 3, 4). The anti-neoplastic activity of CAP-CUR-GLY-GAL-LIPO was higher than CAP-CUR-GAL-LIPO, indicating that the presence of two targeting molecules conferred these drugs with increased growth-inhibitory activity, relative to a single targeting moiety in the liposome (Qi, et al., 2021). The anti-cancer activity of CAP-CUR-GLY-GAL-LIPO was also greater than the non-targeted liposomes (CAP-CUR-LIPO) or a physical mixture of capsaicin and curcumin. In summary, the anti-tumor activity of CAP-CUR-GAL-GLY-LIPO > CAP-CUR--GAL-LIPO > CAP-CUR-LIPO > mixture of capsaicin and curcumin > free curcumin = free capsaicin in H22/LX2 tumors cells xenografted in Balb/c mice (Table 4).

Copious evidence indicates that the HSCs secrete ECM proteins and induce ECM remodeling events, to confer drug resistance on human hepatocellular carcinoma cells (Barry, et al., 2020; Dapito & Schwabe, 2015; X. Liao, et al., 2019; Ma, et al., 2018; Y. Song, et al., 2016). Immunohistochemistry experiments revealed that CAP-CUR-GLY-GAL-LIPO abrogated the activation of HSC's as evidenced by decreased expression of alpha-smooth muscle actin in H22/LX2 tumors. Amongst all the liposomal drug formulations studied, CAP-CUR-GLY-GAL-LIPO induced the maximal decrease in ECM deposition

and ECM remodeling. CAP-CUR-GLY-GAL-LIPO also decreased the expression of CD31 (in murine H22/LX2 tumors) suggesting that CAP-CUR-GLY-GAL-LIPO suppressed angiogenesis of H22/LX2 tumors (Qi, et al., 2021). A major drawback of this research paper is the lack of experimental details regarding the co-culture models used in the study (Qi, et al., 2021). For example, were the HepG2 cells co-cultured with LX2 cells as spheroids, or were they grown on three-dimensional scaffolds or were they co-cultured using a transwell assay system. A similar ambiguity exists in the H22/LX2 mice models used in this research paper (Qi, et al., 2021). The HepG2/LX2 co-culture model in athymic mice is a well-established system to study the interactions between the primary liver tumor and its microenvironment (Bárcena, et al., 2015; Z.-C. Xu, et al., 2018). Notably, no publications have described the H22/LX2 model system in Balb/c mice. The authors likely substituted the murine H22 cells (instead of HepG2 cells) to create the syngenic H22/LX2 model in Balb/c mice. However, there is no evidence that the H22 cells behave identically to HepG2 cells and that the biochemical characteristics of the H22/LX2 system are identical to the HepG2/LX2 co-culture model (Qi, et al., 2021). The fact that the authors did not characterize the Balb/c-H22/LX2 tumor models make it difficult to critically interpret the data obtained from the *in vivo* experiments described in this paper.

The anti-angiogenic activity of CAP-CUR-GLY-GAL-LIPO and its ability to inhibit the activation of HSC's strongly suggested that this drug would possess anti-metastatic activity in human hepatocellular carcinoma. The processes of migration and invasion of tumor cells contributes to their eventual distant metastasis to secondary organs (Meirson, Gil-Henn, & Samson, 2020; Wittekind & Neid, 2005). Wound healing migration assays showed that CAP-CUR-GLY-GAL-LIPO strongly inhibited the migration of HepG2 cells. The anti-migratory activity was classified as CAP-CUR-GLY-GAL-LIPO > CAP-CUR-GLY-LIPO = CAP-CUR-GAL-LIPO > CAP-CUR-LIPO > physical mixture of capsaicin and curcumin > free capsaicin = in human HepG2 cells (Table 3, 4). These wound healing assays with repeated with HepG2/LX2 co-cultured cells and analogous outcomes were obtained (Qi, et al., 2021). A noteworthy difference was the finding that the anti-migratory activity of CAP-CUR-GLY-GAL-LIPO, CAP-CUR-GLY-LIPO and CAP-CUR-GAL-LIPO were equivalent to each other in HepG2/LX2 cells.

The anti-migratory activity of CAP-CUR-GLY-GAL-LIPO correlated to its ability to suppress EMT of HepG2/LX2 co-cultured cells. CAP-CUR-GLY-GAL-LIPO increased the levels of the epithelial biomarker E-cadherin and decreased the expression of the mesenchymal protein vimentin. The EMT-inhibitory activity of CAP-CUR-GLY-GAL-LIPO > CAP-CUR-LIPO > physical mixture of capsaicin and curcumin > free capsaicin in human HepG2 cells. It is unclear why the authors did not investigate the anti-invasive activity of CAP-CUR-GLY-GAL-LIPO in HepG2 cells (Qi, et al., 2021). The Boyden Chamber invasion assay involves measuring the movement of cancer cells across a Matrigel-coated polycarbonate membrane. The cancer cells secrete proteases to degrade the basement membrane proteins (present in Matrigel), then penetrate the pores of the membrane (diameter of the pore=8µm) and stick on the basolateral side of the membrane (Hurley, et al., 2017). A similar process occurs during the metastasis of cancer cells. The metastatic cancer cells degrade the basement membrane to launch themselves into circulation in the adjoining blood vessel/lymph nodes (Meirson, et al., 2020; Wittekind & Neid, 2005). Therefore,

the measurement of the anti-invasive activity of CAP-CUR-GLY-GAL-LIPO along with its anti-migratory activity would have been a better predictor of its anti-metastatic activity *in vivo*.

Qi et al., (2021) measured the anti-metastatic activity of CAP-CUR-GLY-GAL-LIPO by two independent mouse models. The first was a lung colonization assay where H22 murine hepatocellular carcinoma cells were injected in the tail vein of Balb/C mice (Qi, et al., 2021). This was designated as Day zero of the study. The tumor cells travel through the blood vessels to produce metastatic nodules in the lungs of the mice. The mice were injected intravenously with 5mg CAP-CUR-GLY-GAL-LIPO /kg body weight on Day 1 of the study. Subsequently, the CAP-CUR-GLY-GAL-LIPO was injected once every two days and the study was terminated at 14 days (Qi, et al., 2021). Other treatment groups in the study included mice injected with free capsaicin, free curcumin, capsaicin-curcumin mixture, CAP-CUR-LIPO and CAP-CUR-GLY-LIPO. All the drugs were administered once every 2 days at a dose of 5mg/kg body weight. At Day 14, the mice were euthanized, and the metastatic nodules present on the lung were photographed and counted (Qi, et al., 2021). The administration of CAP-CUR-GLY-GAL-LIPO produced a 15-fold decrease in the number of metastatic lung nodules, relative to saline-treated mice (Table 3, 4). The number of metastatic lung nodules observed in CAP-CUR-GLY-GAL-LIPO-treated mice were < CAP-CUR-GLY-LIPO-treated mice < CAP-CUR-LIPO-treated mice < capsaicin/curcumin mixture-treated mice < free capsaicin--treated mice = free curcumin--treated mice. Hematoxylin-Eosin-staining of the lungs of the mice (treated with the indicated drugs) confirmed the results of obtained by counting the metastatic foci on the lung.

The findings obtained from the lung colonization assay were verified using the H22 orthotopic model of metastasis (Qi, et al., 2021). In this model, H22 murine hepatocellular carcinoma cells were implanted in the liver of Balb/c mice. Subsequently, the mice were injected intravenously with 5mg CAP-CUR-GLY-GAL-LIPO /kg body weight or 5mg CAP-CUR-GLYLIPO /kg body weight or 5mg CAP-CUR- LIPO /kg body weight once every two days. Other treatment groups in the study included mice injected with free capsaicin (5mg/kg body weight), free curcumin (5mg/kg body weight) and the physical mixture of capsaicin and curcumin mixture (5mg/kg body weight of each drug), All drugs were administered once every 2 days at a dose of 5mg/kg body weight and the study was ended after 24 days (Qi, et al., 2021). After 24 days, the mice were sacrificed and the metastatic tumors in livers of the mice were analyzed by phase-contrast microscopy. The treatment of the mice with CAP-CUR-GLY-GAL-LIPO produced fewer liver metastases compared to CAP-CUR-LIPO-treated mice (Table 3, 4). Mice administered with free curcumin and curcumin/capsaicin mixture showed higher number of metastatic foci in the liver than CAP-CUR-GLY-GAL-LIPO- or CAP-CUR-GLY- LIPO-treated mice. In summary, the number of liver metastatic tumors present in the CAP-CUR-GAL-GLY-LIPO-treated mice < CAP-CUR-LIPO- treated mice < mice treated with a mixture of capsaicin and curcumin < free curcumin-treated orthotopic tumor-bearing mice. The administration of CAP-CUR-GLY-GAL-LIPO decreased the activation of HSCs as shown by reduced alpha-smooth muscle actin staining of tumor tissues (Qi, et al., 2021). Furthermore, CAP-CUR-GLY-GAL-LIPO inhibited angiogenesis and deposition of ECM proteins (particularly collagen fibers) inside the tumor. The presence of GLY- and GAL-groups on the CAP-CUR-GLY-GAL-liposome

facilitated the improved delivery, penetration, and retention of the drug in the tumor (Qi, et al., 2021). All these factors resulted in improving the anti-tumor, anti-migratory and anti-metastatic activity of CAP-CUR-GLY-GAL-LIPO in human hepatocellular carcinoma.

The molecular target of the capsaicin and curcumin containing glycyrrhetic acid and galactose functionalized liposomes (CAP-CUR-GLY-GAL-LIPO) is the ASGP-R glycoprotein receptor expressed on the surface of human hepatocellular carcinoma cells. Apart from liver cancer cells, normal hepatocytes robustly express the ASGP-R on the sinusoidal and basolateral surface of the plasma membrane (Harris, et al., 2012; Roggenbuck, et al., 2012; Shi, et al., 2013; X. Song, et al., 2019). An important question is whether CAP-CUR-GLY-GAL-LIPO exert any off-target adverse effects on normal liver tissues. The studies of Qi et al., (2021) do not include any direct experiments aimed at exploring the biological effects of CAP-CUR-GLY-GAL-LIPO on normal hepatocytes. However, the authors have studied the biodistribution and anti-cancer activity of CAP-CUR-GLY-GAL-LIPO in multiple mouse models (Qi, et al., 2021). During these experiments they have conducted histological examination of the liver, lung, heart, kidney, and spleen. The authors have not reported any injury or damage to these organs. Another noteworthy observation was that the administration of CAP-CUR-GLY-GAL-LIPO did not have any impact on the body weights of the mice (Qi, et al., 2021). The ASPG-R receptor has been shown to be expressed on blood monocytes and dendritic cells (Harris, et al., 2012). No hemolysis or abnormal immune reaction was observed in the mice treated with CAP-CUR-GLY-GAL-LIPO (Qi, et al., 2021). Such findings allow us to speculate that the CAP-CUR-GLY-GAL-LIPO is a safe drug delivery system which has a high probability to be well tolerated by liver cancer patients in the clinic.

### 2.3 Capsaicin-Nanoparticle Drug Delivery Systems

The term “Nanoparticle” refers to a diverse class of particulate materials which have one dimension less than 100 nm (Khan, Saeed, & Khan, 2019; Laurent, et al., 2010). Depending on the nature of these materials, the ultrastructure of nanoparticles can be one-dimensional, two dimensional or three-dimensional. The general structure of nanoparticles is comprised of multiple layers. The outer or surface layer (also called the external layer), which may be functionalized using biomolecules, dyes, metal ions, surfactants and polymers. The shell layer is chemically distinct layer (from the surface or the core of the nanoparticle) and may incorporate drugs, radionuclide for radiotherapy, proteins/nucleotides for bioactivity, or contrast agents for detection (Anselmo & Mitragotri, 2019; Beltrán-Gracia, et al., 2019; Khan, et al., 2019; Mudshinge, Deore, Patil, & Bhalgat, 2011). Depending on the nature of the nanoparticles, the shell layer may be one layer or a combination of multiple layers. The core layer is the central portion of the nanoparticle. It must be remembered that this is a simplified description of nanoparticles; there are many kinds of nanomaterials of varying structures and composition (Anselmo & Mitragotri, 2019; Beltrán-Gracia, et al., 2019; Khan, et al., 2019; Mudshinge, et al., 2011). Although, many capsaicin nanoparticles have been described in literature only a small fraction of these drugs have been investigated for their anti-cancer activity. We will discuss the physiochemical properties, drug release patterns, biodistribution and the anti-neoplastic activity of these capsaicin-nanomaterials.

Finally, we will provide an overview of the signaling pathways underlying the anti-cancer activity of these capsaicin-nanoparticle drug delivery systems.

**2.3.1 Physiochemical Properties of Capsaicin Nanoparticles**—Capsaicin has been encapsulated in a diverse array of nanomaterials to improve its growth-suppressive activity in human cancer (Chittepu-Reddy, et al., 2018; Rollyson, et al., 2014). These include capsaicin-containing nanocapsules, nanocomposites (magnetic nanoparticles), polymeric nano-micelles, nano-liposomes, nanodots, solid lipid nanoparticles and nano-dendrosomes (Figure 3). Table 5 describes the physiochemical characteristics of these drug delivery systems. Almost all the nanoparticles have an integrated dense structure and are spherical in shape. A unique property of the capsaicin loaded methoxy polyethylene glycol-poly caprolactone nanoparticles (CAP-mPEG-PCL-NPs) is that the spherical nanoparticles have a hollow inner structure (W. Peng, et al., 2015). The capsaicin-containing nanospheres usually have a homogenous composition. An exception to this finding is the near infra-red light sensitive capsaicin loaded mesoporous silica nanoparticles capped gold nanodots (NIR-CAP-Gold-NR-MSN-NPs) where the gold nanorods are embedded within the spherical mesoporous silica nanoparticle scaffold (Yu, et al., 2019). Similarly, capsaicin loaded hydroxyapatite-polyxylitol sebacate nanoparticles (CAP-HAP-PXS) nanoparticles are comprised of rod-shaped HAP nanocrystals (Rajan, et al., 2017). The PXS polymer wraps around the HAP scaffold to produce agglomerated clusters of elongated rod-shaped nanocomposites. The incorporation of PXS polymers reduce the crystalline character of the HAP nanorods. The loading of capsaicin on the HAP-PXS polymer does not alter its three-dimensional shape (Rajan, et al., 2017). The presence of targeting ligands (like hyaluronic acid, folic acid, and biotin) did not alter the spherical morphology (or the diameter), drug loading efficiency and encapsulation efficiency of the nanoparticles (L. Li, et al., 2021; Lv, et al., 2017; Poonam Parashar, et al., 2019). The diameter of these nanospheres ranged from 20–220nm. It has been reported that nanospheres ranging from 50–200nm diameter preferentially accumulate in tumor cells, do not readily travel to healthy cells and show excellent retention in the cytoplasm of cancer cells (M. Zhang, et al., 2021; Y. R. Zhang, et al., 2019; Z. Zhang, et al., 2018).

TEM and DLS experiments showed that all nanoemulsions were comprised of spherical droplets with smooth surfaces. The spherical shape of these nanoemulsion droplets results in enhanced EPR effects which facilitate the uniform release of the drug cargo (in this case capsaicin) into human cancer cells (Golombek, et al., 2018; Homan Kang, et al., 2020; Maruyama, 2011; Yhee, Son, Son, Joo, & Kwon, 2013). Similarly, the smooth surface of these lipid nanoemulsions contribute to release of capsaicin in a sustained manner (Mehanna & Mneimneh, 2021; Puri, et al., 2009). The nanoemulsions namely capsaicin loaded solid lipid nanoparticles (CAP-SLNs), CAP-SNEDDS and 1-SEDDES showed uniform particle sizes ranging from 20–80nm (Bhagwat, et al., 2021; Kunjiappan, et al., 2021; L. Wang, et al., 2017). The emulsion particle size is a very important characteristic of the nanoemulsions because it influences bioavailability, drug release pattern and absorption rate of the drug cargo (A. J. Choi, Kim, Cho, Hwang, & Kim, 2009; Sutradhar & Amin, 2013). Several convergent studies show that droplet sizes below 100nm showed optimal drug bioavailability *in vivo* (L. Wang, et al., 2017) The droplet size of CAP-SLNs, CAP-SNEDDS and

1-SEDDS are below 100nm, so it may be anticipated that these nanoformulations will demonstrate excellent bioavailability in cell culture as well as animal models.

Nanoliposomes are nanoscale bilayer lipid vesicles which represent a new generation of “smart” drug delivery platforms for the encapsulation and delivery of pharmaceuticals, cosmetics and nutraceuticals. Al-Samydai et al., (2021) generated three types of nanoliposomes by varying the percentage of their constituent lipids namely DPPC (1,2-dipalmitoyl-sn-glycero-3-phosphocholine), cholesterol and DSPE-PEG2000 [1,2-distearoyl-sn-glycero-3-phosphoethanolamine-N- {amino (polyethyleneglycol)-2000}]. The authors created three types of nanoliposomes (called F1, F2 and F3 liposomes in the paper) by varying the ratio of DPPC, Cholesterol and DSPE-PEG2000. TEM experiments revealed the capsaicin loaded nanoliposomes were a homogenous population of spherical particles with smooth surfaces. The TEM images also confirmed that capsaicin was stably encapsulated in the bilayer of liposomes (Table 5). The diameter of the F1 nanoliposomes (99.5nm) were the least followed by F2 (118.5nm) and F3 nanoliposome had the maximal size (123.7nm). The polydispersity index and zeta potential of F1, F2 and F3 was almost same. However, the encapsulation efficiency was greatest for F2 nanoliposome followed by F3 and F1. Due to the maximal drug encapsulation efficiency of F2 liposome, the authors performed all biodistribution and biological studies with the F2 nanoliposome.

A unique versatile class of nanoparticle drug delivery systems are polymeric micelles. Polymeric micelles are self-assembling supramolecular nanomaterials comprising of hydrophilic and hydrophobic polymeric structures in an aqueous environment (Jhaveri & Torchilin, 2014; Majumder, et al., 2020). Lan et al., (2019) synthesized a polyethylene glycol-derivatized prodrug micelle which could release two drugs capsaicin and paclitaxel in a sustained release manner (Lan, et al., 2019). NMR spectroscopy confirmed the correct assembly and folding of the polymeric micelle. The paclitaxel (PTX) was found to be loaded in the hydrophobic core of the PTX-CAP-Fmoc-PEG micelle. The PTX-CAP-Fmoc-PEG-NMs were structurally homogenous and spherical in shape (Table 5) The loading of the paclitaxel on the CAP-Fmoc-PEG micelle produced three distinct subtypes of micelles where the loading ratio of paclitaxel to the carrier was 1:1, 2.5:1 and 5:1 (Lan, et al., 2019). Furthermore, the encapsulation of paclitaxel on CAP-Fmoc-PEG micelle decreased the particle size of the micelle from 262.4 nm to 218.3 nm indicating that the physical encapsulation of paclitaxel induced the micelle to become denser and compact. All pharmacological and biological assays were performed with the 1:1 PTX-CAP-Fmoc-PEG-NMs.

Table 5 shows that the zeta potential of most of the nanoparticles range from 19–50mV. Early studies suggested that particles having a zeta potential above 30mV are usually resistant to aggregation (Rasmussen, et al., 2020; Smith, et al., 2017). However, recent studies have found exceptions to this rule and stable nanospheres having all ranges of zeta potential have been reported (Rasmussen, et al., 2020). The polydispersity index of a nanoparticle is a measure of the average uniformity of particle size within the bulk of the nanomatrix. Large values of polydispersity index correspond to greater variability in particle sizes within the nanoparticle sample (Danaei, et al., 2018; Verma, et al., 2003). The polydispersity index also indicates the extent of nanoparticle aggregation along with

the consistency and efficiency of particle surface modifications throughout the particle sample. Values of 0.2 and below are most deemed acceptable in practice for polymer-based nanoparticle materials (Danaei, et al., 2018; Verma, et al., 2003). The polydispersity index of most of the capsaicin-loaded nanoparticles is ~0.2. Furthermore, the polydispersity index is also an accurate reflection of nanoparticle aggregation along with the consistency and efficiency of particle surface modifications throughout the nanoparticle sample (Danaei, et al., 2018; Verma, et al., 2003).

Almost all the nanoparticles had a DEE of 80–95% except for HA-PCL-CAP-NPs (hyaluronic acid functionalized poly- $\epsilon$ -caprolactone nanoparticles) which had a DEE of approximately 52%. It must be remembered that HA-PCL-CAP-NPs are targeted nanoparticles containing a hyaluronic acid moiety which targets them to bind to the CD44 protein on the membrane of human cancer cells (C. Chen, Zhao, Karnad, & Freeman, 2018; Sahin & Klostergaard, 2015). It is known that functionalization of the nanoparticles (with a targeting ligand) improves their drug delivery properties. Therefore, even if the drug entrapment efficiency of HA-PCL-CAP-NPs is lower than the other nanoparticles (described in Table 5), the presence of hyaluronic acid ensures an efficient prolonged release of the capsaicin to human tumor tissues (Poonam Parashar, et al., 2019).

The drug loading efficiency (DLE) and DEE of the polymeric nanomicelle drug PTX-CAP-Fmoc-PEG depended on the molar ratio of the paclitaxel to the inert carrier (Lan, et al., 2019). The DLE of the 1:1 PTX-CAP-Fmoc-PEG-NM was 12.06% which was higher than the 2.5:1 PTX-CAP-Fmoc-PEG-NM (DLE=5.53%) and 5:1 PTX-CAP-Fmoc-PEG-NM (DLE=2.81%). In contrast, the DEE of 2.5:1 PTX-CAP-Fmoc-PEG-NM was 99.4% which was greater than the 5:1 PTX-CAP-Fmoc-PEG-NM (DEE=98.3%) and 1:1 PTX-CAP-Fmoc-PEG-NM (DEE=94.2%).

The bioavailability and biological half-life of capsaicin is low and is independent of the route of administration. In most cases, capsaicin is eliminated from the body within twelve hours of administration (Figure 2). Table 5 shows that almost all the capsaicin nanoparticles are stable for days to months. Such findings predict that these capsaicin nanoformulations will have the ability to release the active drug for long periods of time *in vivo*.

### 2.3.2 Drug Release, Pharmacokinetics and Biodistribution of Capsaicin Nanoparticles

—A survey of literature show that capsaicin-nanoparticle drugs show enhanced bioavailability and biodistribution compared to capsaicin. The *in vitro* drug release profile of nanoparticles drugs is measured by resuspending them in a buffer containing PBS and Tween-80, pH=7.4 at 37 °C (D'Souza, 2014; Weng, Tong, & Chow, 2020). At various time points, an aliquot of eluted drug medium is removed for quantification. The *in vitro* drug release profile of most capsaicin nanoparticle drugs demonstrate that the drug cargo is released within 5 hours and reaches a peak at 24 hours and is maintained at the peak levels for 3–6 days (Table 6). No initial burst of release (of the drug cargo) was observed meaning that the capsaicin was stably entrapped at the core of the nanoparticles and none at the surface. Roughly, 30–60% of the capsaicin is released from the nanoparticles within 24 hours. An exception to this trend were the CAP-HAP-PXS nanoparticles which released the drug cargo in an unusually slow and steady pattern as approximately 60% of the capsaicin

was released from these CAP-HAP-PXS nanoparticles in ten days (Rajan, et al., 2017). In contrast, free capsaicin was quickly degraded (with only 20% of capsaicin remaining unchanged at 15 minutes) and then eliminated from the system within 12 hours.

CAP-SLNs were formulated using stearic acid (as a lipid matrix) and a mixture of surfactants (namely Tween-80 and sodium deoxycholate). These CAP-SLNs comprise of a solid lipid (in this case stearic acid) as the outer layer of the matrix which is stabilized in an aqueous layer using surfactants and co-surfactants (Kunjiappan, et al., 2021). Dialysis bag drug release experiments revealed that the CAP-SLNs released the drug at a slow steady rate. Within 4 hours, 12% of the loaded capsaicin was released and the amount increased to 31.2% at 18 hours and peaked at 50% at 30 hours (Table 6). The pH of the buffer significantly impacted the kinetics of capsaicin release. At 31 hours, the amount of capsaicin released from the CAP-SLNs was approximately 44% at pH=1.2 (pH of the stomach); 77% at pH 5.4 (pH of the duodenum) and 52% at pH =7.4 (the pH of the small intestine). The biodistribution of CAP-SLNs *in vivo* was studied in male adult rat models (Kunjiappan, et al., 2021). CAP-SLNs were labeled with the far-red sensitive fluorescent dye FITC and injected intravenously (via the tail vein) every 24 hours for a cumulative period of 3 days. The uptake of these FITC-CAP-SLNs in the liver, kidneys, spleen, lungs and heart was detected as early as 6 hours, reached a peak at 48 hours and then declined at 72 hours. It was observed that most of the FITC-labeled CAP-SLNs were localized to the liver (~15%), followed by the heart (~3.76%), then the kidneys (~3.05%), lungs (1.31%) and spleen (~1.01%) at 48 hours (Table 6). The FITC-labeled CAP-SLNs were not detected in the brain at any time point.

Jiang et al., (2015) devised a capsaicin-based nanoemulsion drug delivery system which could deliver the drug cargo inside the brain. They encapsulated capsaicin in a methoxy polyethylene glycol-poly caprolactone (mPEG-PCL) amphiphilic block nano-copolymer matrix (Z. Jiang, et al., 2015). These CAP-mPEG-PCL-NPs displayed a uniform drug release rate over a week. Confocal microscopy experiments revealed that the CAP-mPEG-PCL-NPs were robustly internalized by U251 human glioma cells and were predominantly located in the cytoplasm of U251 cells. The ability of these CAP-mPEG-PCL-NPs to cross the blood brain barrier was measured in syngeneic C57BL6 mouse models of glioma (Z. Jiang, et al., 2015). The fluorescent probe NIR-797 isothiocyanate was loaded onto CAP-mPEG-PCL-NPs and subsequently injected intravenously (via the tail vein) in these tumor-bearing mice. The animals were imaged using a near-infrared *in vivo* animal imaging system (Z. Jiang, et al., 2015). The NIR-797-CAP-mPEG-PCL-NPs robustly localized in the brain at 3 hours and remained (at steady state levels) in the brain until 24 hours (Table 6). The efficient transport of CAP-mPEG-PCL-NPs across the blood brain barrier fosters the hope of developing capsaicin-based anti-cancer drugs capable of penetrating the blood brain barrier to suppress the growth of CNS tumors.

The pharmacokinetics of the capsaicin nanoemulsion drug CAP-SNEDDS was measured in male Wistar albino rats (Bhagwat, et al., 2021). The rats were administered orally with free capsaicin (as a solution in carboxymethyl cellulose) or CAP-SNEDDS. The plasma concentration of capsaicin upon administration of CAP-SNEDDS was significantly higher than free capsaicin at all-time points studied. Free capsaicin reached its peak plasma

concentration within 30 minutes and rapidly declined to undetectable levels at 24 hours. In contrast, the capsaicin encapsulated in nanoparticles was slowly released and reached its peak plasma levels at 4 hours (Bhagwat, et al., 2021). The rate of metabolism of capsaicin-nanoparticles was much slower than free capsaicin; approximately 60% of the peak plasma concentration of capsaicin was detected at 24 hours (Table 6). The bioavailability of capsaicin-loaded SNEDDS was observed to be 3.6-fold higher than free capsaicin. The elimination half-life of CAP-SNEDDS was four-fold higher than free capsaicin (Bhagwat, et al., 2021). The mean residence time (MRT, also called mean transit time) of a drug is a very important measure of its bioavailability *in vivo*. The MRT time is the average time the drug molecules spend in the body before being eliminated (Chenthamara, et al., 2019; D'Souza, 2014). The MRT for capsaicin loaded on SNEDDS nanoparticles was approximately 4-fold higher than free capsaicin. In summary, the capsaicin nanoparticle drugs had better bioavailability and drug delivery properties relative to free capsaicin drugs.

Wang et al., (2017) synthesized a chemical conjugate of capsaicin and SN38 (the active metabolite of irinotecan) and then encapsulated this drug conjugate in a self-emulsifying nanoparticle formulation called 1-SEDDS (L. Wang, et al., 2017). The authors hypothesized that this prodrug conjugate will be hydrolyzed in a pH-dependent manner *in vivo* to generate capsaicin and SN38. The *in vitro* drug release profiles of 1-SEDDS reveal that the hydrolysis of the prodrug SN38-capsaicin conjugate is maximal at pH=7.4 (pH of small intestine). The rate of hydrolysis of 1-SEDDS (at a pH=7.4) is maximal within 6 hours when 80% of the active drugs SN38 and capsaicin are released out of the nanoparticle formulations (Table 6) (L. Wang, et al., 2017). No hydrolysis was observed at pH=1.2 (pH of the stomach) or at pH=5.4 (pH of the duodenum). The 1-SEDDS was stable in acidic environments (like the stomach and duodenum) and only delivered its drug cargo at the intestinal pH (approximately 7.4). It must be remembered that the small intestine is the primary absorption site for drugs administered orally (L. Wang, et al., 2017). Therefore, the 1-SEDDS drug delivery platform facilitates the simultaneous release of two anti-cancer drugs SN38 and capsaicin at the desirable site of action.

The drug release profile of CAP-NANO-LIPO showed a biphasic trend over 48 hours. Initially, the drug (capsaicin) was released rapidly with 8.5% of the capsaicin being released within 15 minutes (Table 6). After 2 hours, the capsaicin was released in a slow, steady manner with about 24% of the drug being released over 48 hours. The initial rapid release of capsaicin may be explained by the release of capsaicin trapped near the outer membranes of the nanoliposomes. The presence of cholesterol stabilized the lipid bilayer and allowed the capsaicin to be slowly released over a long period of time. In addition, cholesterol intercalates between the phospholipid molecules conferring higher stability and better membrane permeability to these nanoliposomes. Polymeric nanomicelles have been extensively investigated as for drug delivery platforms for anti-cancer drugs. Most anti-cancer drugs have poor aqueous solubility properties. The unique ultrastructure of these micelles enables non-polar hydrophobic molecules to be solubilized within the core of micelles. Apart from solubilizing hydrophobic drugs, polymeric micelles also protect them from inactivation, degradation and metabolism in the biological milieu thereby increasing their bioavailability (Ghezzi, et al., 2021; Jhaveri & Torchilin, 2014; Kapse, et al., 2020; Majumder, N, & Das, 2020). The dual function polymeric nanomicelle drug PTX-CAP-

Fmoc-PEG-NM released both paclitaxel and capsaicin into the aqueous microenvironment (Lan, et al., 2019). The *in vitro* release kinetics experiments revealed that free paclitaxel was released as an “initial burst” with 80% of the drug being released within 24 hours. Free capsaicin showed a slightly slower drug release profile with about 60% of the drug being released in 24 hours. The PTX-CAP-Fmoc-PEG-NMs released both the drugs at a much slower steady rate with approximately 30% of paclitaxel being released in the first 24 hours (Table 6). Similarly, only 20% of capsaicin was released from the PTX-CAP-Fmoc-PEG-NMs in 24 hours (Lan, et al., 2019). An important observation was that both paclitaxel and capsaicin were released from these PTX-CAP-Fmoc-PEG-NMs at very similar rates which would facilitate efficient co-delivery of these two drugs to the tumor.

The critical micelle concentration (CMC) is the minimum concentration of amphiphilic polymers required to self-assemble into micelles in solution (Jhaveri & Torchilin, 2014; Lu, Zhang, Yang, & Cao, 2018). The CMC is determined by the inherent properties of the micelle and is a vital indicator of micellar stability: the lower the CMC value, the more stable the micelles will be (Jhaveri & Torchilin, 2014; Lu, et al., 2018). The CMC of PTX-CAP-Fmoc-PEG-NMs was approximately 3.8 $\mu$ M in aqueous solution (Table 6). Such low value of CMC suggested that the PTX-CAP-Fmoc-PEG-NMs would probably maintain micellar stability in plasma after intravenous administration. The stability of the PTX-CAP-Fmoc-PEG-NMs *in vitro* depended on the composition of the polymeric micelle (Lan, et al., 2019). The stability of the 5:1 PTX-CAP-Fmoc-PEG-NMs was the greatest (at 8 days) followed by 2.5:1 PTX-CAP-Fmoc-PEG-NMs (at 7 days) and 1:1 PTX-CAP-Fmoc-PEG-NMs (at 5 days). Such findings imply that the increase in paclitaxel/CAP-PEG-Fmoc carrier ratio improves the colloidal stability of the micelles (Lan, et al., 2019). The hydrophilic PEG domain in the CAP-Fmoc-PEG prodrug carrier may form a “protective stealth shell” which prolongs the stability of the micelles and prevent their degradation in the aqueous environment.

The uptake and release of capsaicin from the CAP-Fmoc-PEG carrier was studied in 4T1 mouse metastatic breast cancer cells. Initially the release of capsaicin from the CAP-Fmoc-PEG carrier was more sluggish than free capsaicin (Lan, et al., 2019). This trend was maintained until 12 hours, after which there was a reversal in the release pattern. From 12–48 hours, the amount of capsaicin released from the CAP-Fmoc-PEG carrier was greater than free capsaicin. The pharmacokinetics of PTX-CAP-Fmoc-PEG-NMs were studied in the ICR mouse model. Female ICR mice were injected intravenously with 10mg/kg body weight of paclitaxel or PTX-CAP-Fmoc-PEG-NMs (Lan, et al., 2019). Blood samples were drawn at varying time points (1, 2, 4, 6, 8, 12 and 24 hours) and the concentration of paclitaxel in the plasma was measured by HPLC coupled to mass spectrometry (HPLC-MS) analysis. The levels of free paclitaxel declined rapidly by approximately 4-fold within one hour of injection (Lan, et al., 2019). After 3 hours, concentration of paclitaxel decreased by 40-fold in the blood (Table 6). In contrast, paclitaxel was released slowly (at a uniform rate) from the PTX-CAP-Fmoc-PEG-NMs. The bioavailability of PTX-CAP-Fmoc-PEG-NMs was 3-fold higher than free paclitaxel. The elimination half like of PTX-CAP-Fmoc-PEG-NMs was 3.6-fold higher than free paclitaxel. Similarly, the clearance time of the PTX-CAP-Fmoc-PEG-NMs from the blood was approximately 5-fold lower than free paclitaxel (Lan, et al., 2019). These results argue for an improved pharmacokinetic profile for PTX-CAP-

Fmoc-PEG-NMs relative to free paclitaxel. Unfortunately, the authors did not compare the release kinetics of capsaicin from the PTX-CAP-Fmoc-PEG-NMs with free capsaicin treated groups.

The biodistribution of PTX-CAP-Fmoc-PEG-NMs was investigated in breast tumor-bearing Balb/c mice. Female Balb/C mice were injected subcutaneously with 4T1 mouse metastatic breast cancer cells. After the volume of the 4T1 tumors reached a threshold value of 300–400mm<sup>3</sup>, the mice were randomized into two groups (Lan, et al., 2019). The tumor-bearing mice in Group 1 were injected intravenously with 10mg paclitaxel/kg body weight. Mice in Group 2 were injected intravenously with 10mg PTX-CAP-Fmoc-PEG-NMs/kg body weight. After 24 hours, the mice were sacrificed, and the concentration of paclitaxel was analyzed in the tumor tissue, liver, kidney, heart, lung, and spleen by HPLC-MS method. The PTX-CAP-Fmoc-PEG-NMs-treated mice showed 3-fold higher levels of paclitaxel in the tumor tissue relative to the free drug (Lan, et al., 2019). In contrast, the levels of paclitaxel in the heart and kidney were lower in the PTX-CAP-Fmoc-PEG-NMs-treated mice compared to the paclitaxel treated mice (Table 6). One of the side effects of paclitaxel in patients is cardiotoxicity (Albini, et al., 2010; Arbuck, et al., 1993) and nephrotoxicity (Jagięła, Bartnicki, & Rysz, 2021; Merouani, Davidson, & Schrier, 1997; Rabah, 2010). The fact that lower amounts of paclitaxel were accumulated in the heart and kidney (after PTX-CAP-Fmoc-PEG-NMs administration) suggests that this dual function PTX-CAP-Fmoc-PEG-NMs nanomicelle drug will display a better side effect profile in patients compared to free paclitaxel.

Targeted nanoparticles refer to nanoparticle drug platforms that contain specific ligands (like folic acid, biotin, chitosan and hyaluronic acid) which target these nanoparticles specifically to human cancer cells (Anselmo & Mitragotri, 2019; Beltrán-Gracia, et al., 2019; Khan, et al., 2019; Mudshinge, et al., 2011). Furthermore, capsaicin nanoparticles may be functionalized by specific tumor biomarkers (such as heparin and folic acid) which facilitate the delivery of these nanoparticles to specific type of tumors that overexpress the cognate ligand of these biomarkers. It has been observed that such functionalization of capsaicin-nanoparticles improves their drug release profile and delivery properties. For example, studies by Heng et al., (2021) compared the drug release profiles of free capsaicin, free biotin, biotin-nanoparticles (BT-NP), capsaicin nanoparticles (CAP-NP) and biotin-labelled capsaicin nanoparticles (CAP-BT-PNPP-NP) (Heng, 2021). The biotin moiety enables these nanoparticles to be specifically targeted towards human tumor cells (which have a higher consumption rate of vitamins like biotin) and minimally affect normal tissue. The *in vitro* drug release kinetics of CAP-BT-PPNP, CAP-NP, BT-NP, free biotin, and free capsaicin were studied at pH=5.0 (pH of the duodenum) and pH=7.4 (pH of the small intestine). Free capsaicin and free biotin were rapidly released within 10 hours and then quickly degraded within 30 hours at both of these pH conditions (Heng, 2021). Also, a higher percentage of the drug cargo (from all nanoparticle drugs) was released at pH=7.4 as compared to pH=5.0 (Table 6). All nanoparticle drugs released their drug cargo in a slow, prolonged manner. The initial release of drugs (from all nanoparticles) was observed at 5 hours, followed by a sluggish release rate of the drug over the next 6 days and attained its peak value in 7 days (Heng, 2021). Approximately 10–15% of the drug cargo (from capsaicin nanoparticles and BT-NP) was released at 24 hours, which then slowly reached a value of 45–55% at the end

of one week. At all the time points tested, the biotinylated capsaicin nanoparticles released higher amounts of the drug relative to unmodified capsaicin nanoparticles or free capsaicin (Heng, 2021). Such differences in the drug release profiles of capsaicin-biotin nanoparticles versus unmodified capsaicin-nanoparticles may be due to differences in the ultrastructure of these two types of nanoparticle drugs.

Several convergent studies show that the folate receptor is highly expressed on many human ovarian cancer cells and minimally expressed on normal ovarian epithelial cells (Birrer, Betella, Martin, & Moore, 2019; Scaranti, Cojocar, Banerjee, & Banerji, 2020; Zwicke, Mansoori, & Jeffery, 2012). Such observations led Lv et al., (2017) to fabricate capsaicin-loaded-folate-lipid nanoparticles (CFLN) (Lv, et al., 2017) Confocal microscopy and flow cytometry experiments revealed that CFLNs showed higher intracellular uptake efficiency in SKOV-3 human ovarian cancer cells relative to capsaicin-lipid nanoparticles (CLN). Such observations suggest that the presence of folic acid (in the nanoparticles) facilitates the increased cellular uptake of CFLN via the receptor mediated endocytosis pathway (Lv, et al., 2017). The *in vitro* drug release experiments revealed that capsaicin-loaded folic acid functionalized nanoparticles showed a biphasic pattern of drug release. Initially, the drug was released at a fast rate with about 30% of the capsaicin being released at 4 hours. After 4 hours, the drug was released at a slow and steady manner. Almost the entire drug (~80%) of the drug was released at 72 hours. The metabolism of CFLNs *in vivo* was examined in male Sprague Dawley rats [Li et al., (2017)]. The free capsaicin was rapidly eliminated from the blood of these rats within 5 hours. In contrast, CLN and CFLN both released capsaicin in an efficient manner and this capsaicin could be detected in the blood for nearly 20 hours (Table 5). At long time periods (~100 hours), the CFLN displayed better release properties than CLN (Lv, et al., 2017). However, the authors did not perform any statistical analysis to determine whether such differences in drug release profiles were statistically significant.

Parasher et al., (2019) invented a novel a capsaicin-based drug delivery platform in which capsaicin was loaded on hyaluronic acid functionalized poly- $\epsilon$ -caprolactone nanoparticles (HA-PCL-CAP-NP). These HA-PCL-CAP-NPs released capsaicin in a biphasic manner by diffusion-controlled processes (Poonam Parashar, et al., 2019). The percentage of capsaicin released from HA-PCL-CAP-NPs varied linearly over time until approximately 30 hours after which a plateau was observed. The capsaicin was released more slowly in the first six hours from HA-PCL-CAP-NP than capsaicin containing poly- $\epsilon$ -caprolactone nanoparticles (CAP-PCL-NP). At 36 hours, the release profiles of HA-PCL-CAP-NP was almost equal to CAP-PCL-NPs. Approximately 61% of the capsaicin drug cargo was released from HA-PCL-CAP-NPs over 24 hours (Table 5). The slower drug release kinetics of HA-PCL-CAP-NP could be attributed to the presence of a chitosan coating in HA-PCL-CAP-NP. This chitosan coating slowed down the erosion of the nanoparticles and led to slower and prolonged release of the drug (Poonam Parashar, et al., 2019). The drug release profiles of HA-PCL-CAP-NP and chitosan coated CAP-PCL-NPs was almost identical suggesting that the presence of hyaluronic acid did not impact the release pattern of the two nanoparticle drugs. Subsequently, the authors went on to test the anti-neoplastic activity of (HA-PCL-CAP-NPs) using a urethane-induced lung carcinogenesis rat models (for detailed description see 2.3.3). They investigated the biodistribution of these HA-PCL-CAP-NPs in these tumor-bearing rats (Poonam Parashar, et al., 2019). They observed that when the tumor bearing rats

were administered free capsaicin, the capsaicin was rapidly metabolized and the maximal levels of the drug (~50%) was observed at 4 hours post administration. The capsaicin was predominantly present in the liver with lower levels measured in the heart, spleen, and renal tissue. Notably, a very meagre fraction of the drug was detected in the lung of tumor-bearing rats. The biodistribution of CAP-PCL-NPs was remarkably different from free capsaicin. HPLC analysis showed that the capsaicin drug cargo was primarily detected in the lungs and liver of tumor-bearing rats (Table 5). Unlike free capsaicin, the administration of CAP-PCL-NPs resulted in the capsaicin being released in a steady prolonged manner from 4–24 hours (Poonam Parashar, et al., 2019). This trend was maintained in the HA-PCL-CAP-NP-treated tumor bearing rats. The administration of HA-PCL-CAP-NPs resulted in most of the capsaicin (~50%) being retained in the lung. The lung was the major site for accumulation of the drug from 4–48 hours. The objective of the study of Parasher et al., (2019) was to determine the anti-tumor activity of HA-PCL-CAP-NPs and CAP-PCL-NPs in lung cancer (Poonam Parashar, et al., 2019). The fact that both HA-PCL-CAP-NPs and CAP-PCL-NPs were predominantly localized to the lung implied that such PCL nanoparticles may be promising drug carrier to specifically delivering anti-cancer drugs to human lung tumors *in vivo*.

In summary, the administration of targeted capsaicin nanoparticles prolonged the bioavailability and retention properties of the drug *in vivo*, which allowed the folic acid or hyaluronic acid to be targeted to specific tumor tissues which overexpress these proteins.

**2.3.3 Anti-Cancer Activity of Capsaicin Nanoparticles**—Polymeric dendrimers are an important class of nanoparticulate carriers which have been used to deliver anti-cancer drugs such as doxorubicin, cisplatin, and 5-fluorouracil to tumor tissues (Ambekar, Choudhary, & Kandasubramanian, 2020; L. Jiang, Zhou, Zhang, Wu, & Jiang, 2018). Dendrimers are a unique class of repeatedly branched polymeric macromolecules with tree-like branches built around a central core molecule (Najafi, Salami-Kalajahi, & Roghani-Mamaqani, 2021; Nikzamir, Hanifehpour, Akbarzadeh, & Panahi, 2021). Malar et al., (2015) described the growth-suppressive activity of capsaicin-containing nanoparticle dendrimers in human breast cancer and hepatocellular carcinoma cell lines (Malar & Bavanilathamuthiah, 2015). They observed that capsaicin-nanodendrimers (CND) potentially decreased the viability of MCF-7 human breast cancers cells and HepG2 human liver cancer cells. Most importantly, these dendrosomal capsaicin nanoformulations were selective for human cancer cells over normal cells. MTT assays showed that the IC<sub>50</sub> value for CNDs in Vero normal monkey kidney cells (IC<sub>50</sub>~1.25ug/ml) was double of its IC<sub>50</sub> value in in MCF-7 and HepG2 cells (IC<sub>50</sub>~0.62μg/ml). A caveat of this study was the fact that the authors did not compare the growth-suppressive activity of CNDs with blank nanodendrimers or with free capsaicin (Table 6) (Malar & Bavanilathamuthiah, 2015).

An important class of nanoparticles investigated for oral delivery of drugs are lipid based self-assembling nanoemulsifying drug delivery systems (SNEDDS) (Cherniakov, Domb, & Hoffman, 2015; Kazi, et al., 2019). The administration of SNEDDS into the gastrointestinal (GI) tract induces their self-assemble into ultrafine droplet oil/water nanoemulsions. The large surface area of these SNEDDS help the drug to remain in solution and improve the bioavailability of poorly soluble drugs (Cherniakov, et al., 2015; Kazi, et al., 2019). All

these facts suggest that capsaicin-loaded SNEDDS (CAP-SNEDDS) could be promising strategy for oral delivery of capsaicin for the treatment of gastrointestinal cancers. Bhagwat et al., (2021) experimented with different varieties of oils, surfactants, and co-surfactants to fabricate CAP-SNEDDS. They selected isopropyl myristate (IPM) as the oil phase due to its high potential to solubilize capsaicin (Bhagwat, et al., 2021). Tween-80 and ethanol were used as the surfactants and co-surfactants to stabilize the oil/water CAP-SNEDDS nanoemulsions. CAP-SNEDDS were synthesized using the adsorption technique and characterized by FT-IR, DSC, and TEM methodology (Table 5). The cytotoxic activity of CAP-SNEDDS on HT-29 human colorectal carcinoma cells was evaluated by the tetrazolium salt-based cell viability assay. At a concentration of 100 $\mu$ g/ml, CAP-SNEDDS decreased the viability of HT-29 cells by 67.7% whereas free capsaicin decreased the viability of HT-29 cells by 43.3%. Similarly, the IC<sub>50</sub> of CAP-SNEDDS was lower (64.45 $\mu$ g/ml) than free capsaicin (119.48 $\mu$ g/ml) in HT-29 cells (Bhagwat, et al., 2021). These observations confirm that CAP-SNEDDS displayed greater growth-suppressive activity in HT-29 cells than free capsaicin (Bhagwat, et al., 2021). Annexin-FITC assays revealed that that CAP-SNEDDS triggered a greater magnitude of apoptosis (~35.7%) and necrosis (~20.9%) compared to free capsaicin (magnitude of apoptosis ~12.2%; amount of necrosis ~ 2.6%). The higher growth-inhibitory activity of CAP-SNEDDS (relative to free capsaicin) was attributed to its higher uptake by HT-29 cells (Table 7). A drawback of these studies is that the pro-apoptotic activity free SNEDDS was not determined in HT-29 cells (Bhagwat, et al., 2021).

Nanoliposomes are nanosized liposomal carriers which have superior drug-delivery properties compared to conventional liposomes. Nanoliposomes have prolonged half-life in the blood and this helps them to deliver increased amounts of anti-cancer drugs to the site of the tumor (Aguilar-Pérez, Avilés-Castrillo, Medina, Parra-Saldivar, & Iqbal, 2020; Nomani & Govinda, 2016). Al-Samyai et al., (2020) generated capsaicin loaded nanoliposomes (CAP-NANO-LIPO) and tested them for their growth-inhibitory properties in a panel of five human cancer cell lines namely A375 (melanoma), MCF-7 (breast cancer), PANC1 (pancreatic cancer), K562 (leukemia) and MDA-MB-231 (triple negative breast cancer). These nanoliposomes contained a mixture of DPPC, cholesterol and DSPE-PEG2000 in the ratio of 75:20:5 (A. Al-Samydai, Alshaer, Al-Dujaili, Azzam, & Aburjai, 2021). The growth-suppressive activity of CAP-NANO-LIPO was compared to free capsaicin in all the above mentioned cell lines (Table 7). A survey of the IC<sub>50</sub> values for CAP-NANO-LIPO and free capsaicin reveals that CAP-NANO-LIPO decreased the viability of these cell lines at a 15–40-fold lower concentrations, compared to free capsaicin (A. Al-Samydai, et al., 2021). A drawback of these experiments was that all the experiments were performed in cell culture models. It is hoped that future studies from this research group will determine the anti-tumor activity of CAP-NANO-LIPO in mouse models.

Gliomas are a category of brain tumors arising from glial or glial precursor cells. Gliomas account for about 32% of primary CNS cancers and over 75% of all malignant primary brain tumors (Molinaro, Taylor, Wiencke, & Wrensch, 2019; Weller, et al., 2015). The incapability of most drugs to penetrate the blood brain barrier (BBB) constitutes major challenge in the treatment of gliomas (Arvanitis, Ferraro, & Jain, 2020; Luo & Shusta, 2020). Conventional approaches that use the drug molecules in their free form have demonstrated poor BBB

penetration due to the presence of efflux pumps on the endothelial cells that block the delivery of the drug molecules to the target cells in the brain (Blanco, Shen, & Ferrari, 2015). A strategy to circumvent this challenge is to encapsulate the drugs in specifically engineered nanoparticles which can travel across the BBB and deliver the drug cargo to specific sites within the central nervous system. Jiang et al., (2015) fabricated an amphiphilic mPEG-PCL block nano-polymer matrix aimed to deliver capsaicin across the BBB (Z. Jiang, et al., 2015). The mPEG-PCL block nano copolymer was synthesized by the ring opening polymerization method. Confocal fluorescence microscopy demonstrated that the CAP-mPEG-PCL-NPs were efficiently internalized by U251 cells by endocytosis. The intravenous injection of CAP-mPEG-PCL-NPs (in the tail vein) in glioma tumor-bearing C57BL6 mice showed that these capsaicin nanopolymers permeated efficiently across the BBB (Z. Jiang, et al., 2015). These findings suggest that capsaicin mPEG-PCL nanoparticle drugs may have applications in the chemotherapy of human gliomas. Studies in cell culture systems revealed that CAP-mPEG-PCL-NPs decreased the viability of U251 human glioma cells in a concentration-dependent- and time dependent manner. The  $IC_{50}$  value for CAP-mPEG-PCL-NPs in U251 human glioma cells was approximately 20 $\mu$ M at 48 hours. In contrast, the  $IC_{50}$  value for free capsaicin was 1.5-fold higher (approximately 30 $\mu$ M) in U251 cells (Table 7). At concentrations below 30 $\mu$ M, the CAP-mPEG-PCL-NPs showed greater growth-inhibitory activity (in U251 human glioma cells) than free capsaicin (Z. Jiang, et al., 2015). At concentration higher than 40 $\mu$ M, CAP-mPEG-PCL-NPs and free capsaicin showed equivalent growth-suppressive activity in U251 cells. The cytotoxic activity of CAP-mPEG-PCL-NPs was also dependent on the time of drug treatment (Z. Jiang, et al., 2015). Whereas 40 $\mu$ M CAP-mPEG-PCL-NPs decreased the viability of U251 cells by about 55% (relative to untreated cells) at 24 hours, the same concentration of CAP-mPEG-PCL-NPs decreased the viability of U251 cells by approximately 80% at 48 hours. Unfortunately, the authors did not perform any statistical analysis of their data, so it is impossible to compare the growth suppressive activity of CAP-mPEG-PCL-NPs in U251 cells at 48 hours versus at 24 hours.

Elkholi et al. (2014) synthesized capsaicin-loaded trimethyl chitosan nanoparticles (CAP-TMC-NP) and investigated their growth suppressive activity in HepG2 human hepatocellular carcinoma cells at 24 and 48 hours (Elkholi, et al., 2014). As a control, the cells were also treated with equivalent amounts of free capsaicin, blank trimethyl chitosan nanoparticles (BLANK-TMC-NP). MTT assays revealed that 100  $\mu$ M of CAP-TMC-NPs decreased the viability of HepG2 cells by greater than 10-fold at 48 hours. However, free capsaicin and the blank loaded trimethyl chitosan nanoparticles also decreased the viability of HepG2 cells to the same magnitude as CAP-TMCS-NPs (Elkholi, et al., 2014). Subsequently, the authors examined the apoptotic activity of CAP-TMCS-NPs in HepG2 cells using the Annexin-FITC assay. They found that that the treatment of HepG2 cells with 50  $\mu$ M CAP-TMC-NPs induced robust apoptosis (~74%) at 24 hours (Table 7). In contrast, free capsaicin and BLANK-TMC-NP triggered very little programmed cell death (less than 3%) in HepG2 cells. A similar trend was observed at 75- and 100  $\mu$ M of CAP-TMC-NPs. At 48 hours, CAP-TMC-NPs, BLANK-TMC-NPs, and free capsaicin triggered a similar magnitude of apoptosis (~60–80%) in HepG2 cells. These observations raise the possibility that the pro-apoptotic activity of CAP-TMC-NPs is due to the trimethyl chitosan polymeric matrix;

the loading of capsaicin does not seem to have any additional growth-suppressive effects on this nanodrug (Elkholi, et al., 2014). Another point to note is that CAP-TMCS-NPs (at concentrations ranging from 50  $\mu$ M-100  $\mu$ M) trigger the same magnitude of programmed cell death at 24 hours and 48 hours. These authors verified their findings using the DNA fragmentation apoptosis assays and similar results were obtained. The loading of capsaicin in these trimethyl chitosan nanoparticles does not improve their anti-cancer activity or selectivity (over free capsaicin and blank nanoparticles) in human hepatocellular carcinoma cells (Elkholi, et al., 2014). Based on these observations we infer that trimethyl chitosan nanoparticles are not an ideal drug-delivery system for capsaicin in human liver cancers. A similar study by Dhamodaran et al., (2021) investigated the anti-tumor activity of capsaicin-chitosan nanoparticles (CAP-CS-NP) in DMBA-rat model of mammary carcinogenesis. Swiss albino mice were injected with 25mg DMBA/kg bodyweight to induce mammary gland carcinogenesis. After 7 weeks, the tumor-bearing rats were treated with 4mg CAP-CS-NP/kg bodyweight thrice a week via oral administration (Dhamodharan, Vengaimaran, & Sankaran, 2021). Tumor bearing mice treated with blank nanoparticles (at a dose of 5mg/kg bodyweight) and free capsaicin (at a dose of 8mg/kg bodyweight) serves as the control groups for the experiment. The entire experiment was performed for 14 weeks. The administration of CAP-CS-NP decreased the tumor volume by about 5-fold as compared to the DMBA-treated control group (Table 7). Free capsaicin also exerted robust antitumor activity decreasing the tumor volume by about 50% relative to the control group (Dhamodharan, et al., 2021). Therefore, the anti-cancer activity of CAP-CS-NP was substantially higher than free capsaicin. The authors excised the tumors and analyzed them for oxidative stress markers, detoxification enzymes and cell cycle proteins. They found that the treatment of rats with DMBA elevated the levels of oxidative stress markers (SOD, GSH, catalase, GPx, vitamin C and E and TBARS) in the mammary tissue, liver tissue and blood (Dhamodharan, et al., 2021). The treatment of CAP-CS-NP potentially decreased the expression of these oxidative stress proteins relative to the DMBA-treated control rats. These observations indicate that CAP-CS-NP attenuated oxidative stress in mammary tumors. The expression of cell cycle proteins like cyclin D1 and PCNA was also reduced by CAP-CS-NP (Dhamodharan, et al., 2021). Such data suggest that CAP-CS-NP suppressed the growth of DMBA-induced mammary tumors by inducing cell cycle arrest in G1 phase.

A study by Kunjiappan et al., (2021) investigated the growth-inhibitory activity of capsaicin containing solid lipid nanoparticles (CAP-SLNs) in human liver cancer. These CAP-SLNs are comprised of a lipid core (made of stearic acid) which was stabilized in aqueous media by the presence of Tween-80 (as a surfactant) and sodium deoxycholate (as a co-surfactant). The lipid core (of this capsaicin colloidal nanoparticulate drug) provided a high drug encapsulation efficiency for capsaicin (Kunjiappan, et al., 2021). CAP-SLNs robustly decreased the viability of HepG2 human hepatocellular carcinoma cells *in vitro* at 24 hours. The IC<sub>50</sub> value for CAP-SLN in HepG2 cells was approximately 20 $\mu$ g/ml (Table 7). At a concentration of 400 $\mu$ g/ml, CAP-SLNs decreased the viability of HepG2 cells by 92%. A caveat of these studies that the growth-suppressive activity of CAP-SLNs was not compared with free capsaicin or blank SLNs (Kunjiappan, et al., 2021). An advantage of CAP-SLNs is that they displayed minimal growth-inhibitory activity in normal WI-38 human fibroblast cells (S. P. Huang, et al., 2009). Whereas 20 $\mu$ g/ml CAP-SLN's decrease

the viability of HepG2 cells by 50%, the viability of WI-38 cells is unaffected by CAP-SLNs at concentrations below 200µg/ml. The CAP-SLN's diminished the viability of HepG2 cells by triggering programmed cell death. The pro-apoptotic ability of CAP-SLNs correlated with its ability to elevate the levels of reactive oxygen species (ROS) in HepG2 cells.

Magnetic nanoparticles (also called Nanocomposite) are an important class of nanoparticles used for drug delivery and tumor imaging applications (Ali, et al., 2021; Gul, Khan, Rehman, Khan, & Khan, 2019). Cobalt-based magnetic nanoparticles have proved to be versatile multifaceted probes for drug release, imaging, enhanced thermo/radiation therapy and microrobots (Amiri & Shokrollahi, 2013; Petrarca, et al., 2020). Raibee et al., (2019) synthesized and characterized cobalt-ferric oxide functionalized zeolite hybrid (ZSM-5) nanoparticles (Table 5). These CoFe<sub>2</sub>O<sub>4</sub>-ZSM-5 nanocomposite polymers were coated with egg white (EW) to make them compatible for biological applications (Rabiee & Rabiee, 2019). Finally, capsaicin was loaded on these EW-CoFe<sub>2</sub>O<sub>4</sub>-ZSM-5 nanoparticles by injection methodology and they were tested for their growth-suppressive activity in SK-N-MC human Ewing sarcoma cells. MTT assays showed that these capsaicin-loaded EW-CoFe<sub>2</sub>O<sub>4</sub>-ZSM-5 nanoparticles (CAP-EW-MAGNETIC-NP) displayed concentration-dependent cytotoxic activity in SK-N-MC human neuroblastoma cells at 48 hours (Rabiee & Rabiee, 2019). Specifically, 100µg/ml of CAP-EW-MAGNETIC-NPs decreased the viability of SK-N-MC cells by 33% relative to untreated control cells (Table 7). Notably, the blank EW-MAGNETIC-NP did not have any impact on the growth of SK-N-MC cells. Finally, the authors examined the potential of CAP-EW-MAGNETIC-NPs as a magnetic resonance imaging (MRI) agent (Rabiee & Rabiee, 2019). They evaluated the relaxation curves of CAP-EW-MAGNETIC-NPs at concentrations ranging from 0.78–40µg/ml in a 3-Tesla clinical MRI scanner and found that these capsaicin-loaded magnetic nanoparticles have an excellent potential to be utilized as an MRI contrast agent to image tumors (Rabiee & Rabiee, 2019). It is hoped that future studies from this research group will confirm the imaging properties of CAP-EW-MAGNETIC-NPs in animal models of carcinogenesis.

Osteosarcoma is a cancerous tumor that originates in the mesenchymal spindle-shaped stromal bone tissue. Osteosarcoma is most frequently found in the metaphyseal area of long bones (inside the medullary cavity) and infiltrates the cortex of the bone to involve the surrounding soft tissues (Kuerbitz & Henderson, 2020; Misaghi, Goldin, Awad, & Kulidjian, 2018; Zhao, Wu, Gong, Liu, & Ma, 2021). Surgery is the cornerstone for osteosarcoma therapy with complete surgical excision of the primary tumor being the goal of such surgical treatment. The advent of neoadjuvant induction therapy comprising of high-dose methotrexate, doxorubicin, and cisplatin (MAP) has been found to substantially improve the outcomes of surgery (Misaghi, et al., 2018; Zhao, et al., 2021). Sometimes ifosfamide is also added to the MAP regimen. A major challenge of osteosarcoma therapy is bone injury, bone trauma and bone loss. The reasons for such bone loss include both the direct effects of cancer cells, and the effects of chemotherapeutic drugs used in osteosarcoma treatment (Ahn, et al., 2015; Kuerbitz & Henderson, 2020; Lim, et al., 2013). Therefore, the restoration of bone health has emerged as a vital component of comprehensive osteosarcoma therapy. A new therapeutic strategy for osteosarcoma is to use biopolymers (3D-printed scaffolds, bone-targeting nanomaterials microparticles and hydrogels) to achieve bone regeneration in patients (Ahn, et al., 2015; Rajan, et al., 2017).

Such bone targeting nanomaterials can assimilate into the bone microenvironment to heal diseased bone. Furthermore, the encapsulation of cancer chemotherapy drugs within such matrices can improve the targeting of these anti-cancer drugs to the site of the bone tumor (Ahn, et al., 2015; Rajan, et al., 2017). Rajan et al., (2017) encapsulated capsaicin in a nano-hydroxyapatite-polyxylitol sebacate matrix (CAP-HAP-PXS-NPs) and investigated its growth-suppressive effects on osteosarcoma (Rajan, et al., 2017). As a first step, the authors synthesized hydroxyapatite nanorods by hydrothermal methodology. The xylitol-based polyxylitol sebacate (PXS) matrix was synthesized by the polycondensation method (Rajan, et al., 2017). The PXS polymers were combined with hydroxyapatite nanorods in a microwave oven to generate the HAP-PXS composite. Finally, capsaicin was loaded on this HAP-PXS nanocomposite to generate the CAP-HAP-PXS nanodrug (Table 5).

The growth-inhibitory activity of CAP-HAP-PXS-NPs was investigated in Saos-2 human osteosarcoma cells. MTT assays showed that the treatment of Saos-2 cells with 50-, 75- and 100µg/ml CAP-HAP-PXS-NPs decreased the viability of these cells in a concentration-dependent manner at 24 hours (Rajan, et al., 2017). The growth-suppressive activity of CAP-HAP-PXS-NPs was greater than blank HAP-PXS nanoparticles up to 7 days (Table 7). Unfortunately, the authors did not provide a comparison for the growth-suppressive activity of CAP-HAP-PXS-NPs with free capsaicin (Rajan, et al., 2017). The CAP-HAP-PXS-NPs suppressed the growth of Saos-2 cells by inducing apoptosis. The pro-apoptotic activity of CAP-HAP-PXS-NPs was correlated to generation of ROS and loss of mitochondrial membrane potential of Saos-2 cells. CAP-HAP-PXS-NPs generated a greater amount of ROS than the blank HAP-PXS in Saos-2 cells.

A strength of this study was that the authors examined the impact of CAP-HAP-PXS-NPs on the growth of normal osteoblast-like cells (Rajan, et al., 2017). CAP-HAP-PXS-NPs did not impact the viability of MG63 human osteoblasts. In fact, CAP-HAP-PXS-NPs caused a slight (but significant) increase in the growth of MG63 cells compared to the blank HAP-PXS-NPs. Also, the MG63 cells treated with CAP-HAP-PXS-NPs showed better morphological characteristics (such as cell spreading, adhesion and organization) relative to the blank nanoparticles (Rajan, et al., 2017). This is indeed an unexpected finding since the studies of Bao et al., (2019) show that free capsaicin triggers robust apoptosis in MG63 cells (Bao, Dai, Wang, Tao, & Chai, 2019). The pro-survival effects of CAP-HAP-PXS-NPs may be due to the fact that it displayed potent antioxidant activity in human osteosarcoma cells. Several convergent studies show that bone implant biopolymers become vulnerable to oxidative damage during bone tumor therapy in patients (Ambrosio, et al., 2021; Chindamo, et al., 2020; J. Liao, Han, Wu, & Qian, 2021). Such oxidative damage of bone implants is due to the oxidation by endogenous peroxides produced by the body (Ambrosio, et al., 2021). CAP-HAP-PXS-NPs showed extremely high hydrogen peroxide scavenging capacity in human osteosarcoma cells. The addition of capsaicin to the HAP-PXS nanocomposite not only suppresses the growth of human osteosarcoma cells but it also protects the HAP-PXS nanocomposites from oxidative injury (Rajan, et al., 2017). Based on such observations, capsaicin-based nanomaterials may pave the way for novel oxidation-resistant sustained release therapies in osteosarcoma patients.

A method of improving the delivery and tumor cell-specific targeting of nanoparticle-drugs is to attach cellular ligands on the surface of these nanoparticles. Lv et al. (2017) fabricated a folic acid conjugated lipid nanoparticle drug platform to enhance the delivery of the anti-cancer phytochemical capsaicin to human ovarian cancer cells (Lv, et al., 2017). The overexpression of the folate receptor alpha in epithelial ovarian cancers provides a unique method to design targeted anti-cancer drugs to combat this lethal malignancy (Birrer, et al., 2019; Scaranti, et al., 2020). The levels of folate receptor in ovarian cancers is strongly correlated to response to chemotherapy, survival outcomes and metastatic propensity of ovarian tumors (Birrer, et al., 2019; Fernandez, Javaid, & Chudasama, 2018; Zwicke, et al., 2012). The starting material for these capsaicin-loaded folic acid-conjugated lipid nanoparticles (CFLN) was DSPE-conjugated polyethylene glycol (PEG)-folic acid (DSPE-PEG-FA). The loading of capsaicin on DSPE-PEG-FA nanoparticles was accomplished by using the thin film hydration technique (Lv, et al., 2017). The nanoparticles were lyophilized and characterized by DLS and TEM methodology (Table 5). MTT assays revealed that CFLN potently decreased the viability of SKOV-3 human ovarian carcinoma cells at concentrations ranging from 5–50µg/ml at 24 hours. The growth-suppressive activity of CFLN nanoparticles was greater than blank nanoparticles or free capsaicin in SKOV-3 cells (Lv, et al., 2017). Such results suggested that the presence of the folic acid moiety improved their bioavailability and cancer-suppressing activity of CFLN nanoparticles. An asset of these CFLN was that they did not affect the viability of OSE normal human ovarian epithelial cells (Lv, et al., 2017). This may be explained by the fact that OSE cells lack folate receptors and therefore are not targeted by the CFLN. The growth-inhibitory activity of CFLN was due to its ability to trigger apoptosis in SKOV-3 cells. CFLN triggered a greater magnitude of apoptosis in SKOV-3 cells (~39%) relative to CLN (~15%) or free capsaicin (~6%). The improved pro-apoptotic activity of CFLN (relative to CLN) may be attributed to the ability of folic acid to enhance the uptake, internalization, and intracellular delivery of capsaicin in SKOV-3 cells (Lv, et al., 2017).

A second method of targeted delivery of anti-cancer drugs has been to conjugate them to Vitamin H (also called biotin). Biotin is a vital micronutrient for cellular cell growth and development (Tripodo, Mandracchia, Collina, Rui, & Rossi, 2014). In addition, biotin acts as a co-factor for mitochondrial and cytoplasmic carboxylases (Ren, et al., 2015; Tripodo, et al., 2014; Vinothini, Rajendran, Munusamy, Alarfaj, & Rajan, 2019). Several convergent studies show that human cancer cells take up biotin at a significantly higher rate than normal cells (Tripodo, et al., 2014; Vinothini, et al., 2019). The conjugation of biotin to established anti-cancer drugs like paclitaxel, doxorubicin and gemcitabine has been found to improve their intracellular delivery properties, enhance their anti-cancer effects and minimize their off-target toxicity (Ren, et al., 2015; Tripodo, et al., 2014). Heng et al. (2021) used a biotin-based system to co-deliver biotin and capsaicin to human gastric cancer cells (Heng, 2021). They used the nano-evaporation methodology to co-encapsulate biotin and capsaicin in PEG and polylactide decoglycolide nanoparticles (PNPPs). They characterized the capsaicin-biotin nanoparticles (hereafter called CAP-BT-PNPP) by TEM and DLS measurements (Table 5). The growth-suppressive activity of free capsaicin, capsaicin-nanoparticles (CAP-NP), biotin nanoparticles (BT-NP) and capsaicin-biotin nanoparticles (CAP-BT-PNPP) in gastric carcinoma cells namely cells was evaluated by the MTT assay (Heng, 2021). The

authors determined the impact of all the aforesaid drug formulations on the viability of NCI-N87 and SGC-791 human gastric carcinoma cells. The  $IC_{50}$  values for free-CAP, BT-NPs, CAP-NP ranged from 10–14 $\mu$ M (in NCI-N87 cells), whereas the  $IC_{50}$  value for CAP-BT-PNPP was 2-fold lower ( $\sim 4.97 \pm 1.25 \mu$ M). A similar trend was observed in SGC-791 cells. The  $IC_{50}$  value for CAP-BT-PNPP ( $\sim 6.87 \pm 3.47 \mu$ M) was 2–3-fold lower than free-CAP, BT-NPs, CAP-NP ( $\sim 12$ – $20 \mu$ M) in SGC-791 human gastric cancer cells (Table 7). Flow-cytometry experiments demonstrated that CAP-BT-PNPPs triggered apoptosis in approximately 30% of NCI-N87 and SGC-791 cells (Heng, 2021). The treatment of NCI-N87 and SGC-791 cells with BT-NPs, CAP-NPs induced 10–20% apoptosis in these cells. Most interestingly, the pro-apoptotic activity of BT-NPs and CAP-NPs was not significantly different from CAP-BT-PNPPs in NCI-N87 and SGC-791 cells (Heng, 2021). The fact that the BT-NP and CAP-NP trigger equivalent apoptosis as CAP-BT-PNPPs diminishes the importance of their findings (Heng, 2021). If CAP-NP and BT-NP trigger the same magnitude of cell death (in gastric cancer cells) as CAP-BT-PNPP then the benefits of co-delivery of biotin and capsaicin in PNPPs are not obvious. Another weakness of this paper is that the authors have not determined the apoptotic activity of free capsaicin and blank PNPPs in human gastric cancer cells.

Parasher et al. (2019) used the cluster determinant 44 (CD44) glycoprotein as a drug target to deliver capsaicin nanoparticles in human lung cancers (Poonam Parashar, et al., 2019). CD44s are a family of non-kinase, transmembrane glycoproteins expressed on embryonic stem cells, bone marrow cells and cells arising from connective tissues. CD44 play a key role in cancer development, growth and progression and is overexpressed in several cell types of human cancer cells like prostate cancer, triple-negative breast cancer, pancreatic cancer, and lung cancer (C. Chen, et al., 2018; Sahin & Klostergaard, 2015; H. Xu, Niu, Yuan, Wu, & Liu, 2020). The principal ligand for CD44 is hyaluronic acid (HA), which is an important component of the ECM associated with cancer cells and their microenvironment. HA binds to the ligand binding domain of CD44 activating and recruiting of downstream signaling pathways that induce cell proliferation, increases cell survival, modulates cytoskeletal changes, and enhances metastasis (C. Chen, et al., 2018; Sahin & Klostergaard, 2015; H. Xu, et al., 2020). The authors used nanoprecipitation methods to synthesize capsaicin-loaded poly  $\epsilon$ -caprolactone (PCL) nanoparticles. The capsaicin-PCL nanoparticles were coated with hyaluronic acid to obtain hyaluronic acid-anchored capsaicin-PCLs (HA-PCL-CAP-NPs) (Poonam Parashar, et al., 2019). The physiochemical properties of these HA-PCL-CAP-NPs are summarized in Table 5. Subsequently, the analyzed the growth-inhibitory activity of these capsaicin-loaded hyaluronic acid functionalized nanoparticles in human lung cancers. HA-PCL-CAP-NPs decreased the viability of human A549 non-small cell lung cancer (NSCLC) cells better than CAP-PCL-NPs and free capsaicin over 48 hours (Poonam Parashar, et al., 2019). The  $IC_{50}$  value of HA-PCL-CAP-NPs ( $39.74 \pm 2.11 \mu$ M) was substantially lower than CAP-PCL-NPs ( $46.76 \pm 1.22 \mu$ M) and free capsaicin ( $52.1 \pm 3.17 \mu$ M). An asset of this study was that the anti-tumor activity of HA-PCL-CAP-NPs was examined *in vivo* in the urethane model of lung carcinogenesis (Poonam Parashar, et al., 2019). The administration of 20mg HA-PCL-CAP-NPs/kg body weight (via intravenous route) produced a 3-fold decrease in the volume of lung tumors at the end of 20 weeks (Table 7). The anti-tumor activity of comparative doses of CAP-PCL-NPs (decreasing the tumor

volume by 2-fold) and free capsaicin (decreasing the tumor volume by 1.4-fold) was lower than HA-PCL-CAP-NPs. Kaplan-Meier curves showed that the administration of HA-PCL-CAP-NPs to tumor-bearing rats improved their survival times compared to CAP-PCL-NPs and free capsaicin (Poonam Parashar, et al., 2019). These results correlate well with the finding that majority of the capsaicin released from HA-PCL-CAP-NPs was localized in the lungs of the tumor-bearing mice. Histological examination of the lung revealed that the structural integrity of the lung was almost normal in tumor-bearing rats receiving HA-PCL-CAP-NPs, CAP-PCL-NPs and free capsaicin.

An innovative study by Von Palubtzi et al., (2020) used the structural differences between the glycocalyx in normal cells and tumor cells as a mechanism to target capsaicin-loaded nanoparticles specifically to cancer cells (von Palubitzki, et al., 2020). The glycocalyx refers to the multifunctional layer of glycans that envelops all mammalian cells. This outer glycan layer is the interface between cells and the extracellular space and regulates important cellular functions like cell adhesion, cytoplasmic signaling and endocytosis (H. Kang, et al., 2018; Tarbell & Cancel, 2016). The glycocalyx is made of highly glycosylated membrane-bound proteins which include proteoglycans (such as syndecans) and secreted glycosaminoglycan polymers such as hyaluronic acid. Published data show that proteoglycans bind covalently to glycosaminoglycan chains like heparin sulfate or chondroitin sulfate (H. Kang, et al., 2018; Tarbell & Cancel, 2016). A unique feature about the structure of glycosaminoglycans is that they carry a strong negative charge. Such high negative charge along with polyelectrolyte carbohydrate chains (like heparin sulfate) can induce specific binding of counterions (H. Kang, et al., 2018; Tarbell & Cancel, 2016). The net negative charge of the glycocalyx induces highly specific binding patterns with cationic ligands. Emerging evidence suggest that the composition of the glycocalyx associated with cancer cells is structurally distinct from the glycocalyx of normal cells. The glycocalyx associated with cancer cells recruits specific mitogenic signaling networks involving growth-factors, cytokines and integrins (H. Kang, et al., 2018; Tarbell & Cancel, 2016). Furthermore, the glycocalyx of neoplastic cells promotes the growth and invasion of cancer cells by promoting the interaction of tumor cells with their microenvironment. Von Palubtzi et al. (2020) used whole exome sequencing data (available on public domain internet sites) to characterize the differences between the glycocalyx of bladder cancer and melanoma relative to normal tissues. They observed that the bladder cancer tumors isolated from patients showed greater frequency of mutations and differences in copy number of genes associated with the heparin sulfate and hyaluronic acid pathway than melanoma tissues. Furthermore, the magnitude of surface exposed heparin sulfate (in the glycocalyx of in T24 bladder cancer cells was greater than UROtsa normal urothelial epithelial cells (von Palubitzki, et al., 2020). The net negative charge of the glycocalyx (due to the exposed heparin sulfate moieties) of bladder cancer cells was greater than the glycocalyx of normal urothelial cells. They hypothesized that the negatively charged glycocalyx (of bladder cancer cells) would bind to display greater binding to the positively charged cationic chitosan nanocapsules (Chi-NCAS) relative to normal urothelial epithelial cells. Structured Illumination microscopy experiments confirmed that the negatively charged glycocalyx of bladder cancer cells facilitated the enhanced binding and internalization of Chi-NCAS as compared to the normal UROtsa cells (von Palubitzki, et al., 2020). The

uptake of CAP-Chi-NCAS in T24 human bladder cells was approximately 3-fold higher than UROtsa cells. WST-1 cell viability assays revealed that the CAP-Chi-NCAS (loaded with 250 $\mu$ M capsaicin) decreased the viability of T24 human bladder cells by 40% over 24 hours. In contrast, CAP-Chi-NCAS did not have any impact on the growth of normal UROtsa cells (Table 7). Such data strongly suggest that the CAP-Chi-NCAS were specifically targeting the T24 human bladder cells and spared the normal UROtsa cells (von Palubitzki, et al., 2020). Immunoblotting experiments demonstrated that the treatment of T24 human bladder cells with CAP-Chi-NCAS induced the cleavage of procaspase-3 to generate cleaved caspase-3, whereas no cleavage of procaspase-3 was observed in CAP-Chi-NCAS -treated UROtsa normal urothelial epithelial cells (von Palubitzki, et al., 2020). Taken together, such findings suggest that CAP-Chi-NCAS target the glycocalyx of cancer cells to trigger apoptosis only in human bladder cancer cells while sparing in normal urothelial cells.

The membrane anchored mucin glycoprotein MUC1 (CD227), is overexpressed in greater than 80% of human pancreatic cancers in its glycosylated form (Park, et al., 2015). The glycosylated MUC1 plays a vital role in pancreatic cancer growth, invasion (into the extracellular matrix) metastasis and chemoresistance (Bose & Mukherjee, 2020; Park, et al., 2015). Nigam et al., (2014) fabricated multifunctional fluorescent MUC1 aptamer functionalized nanoparticles. Subsequently, they conjugated these nanoparticles to capsaicin-loaded human serum albumin (HSA) nanoparticles to generate “a nanotheranostic platform” for the therapy of human pancreatic cancer (MUC1-Apt-HSA-CAP-NPs). MTT assays were performed to analyze the growth suppressive activity of these MUC1-Apt-HSA-CAP-NPs in Panc-1 human pancreatic cancer cells (P. Nigam, et al., 2014). The first series of experiments aimed to compare the effect of 25–200 $\mu$ g/ml of MUC1-Apt-HSA-CAP-NPs and free capsaicin on the viability of Panc-1 human pancreatic cancer cells over 24 hours. The authors observed that the IC<sub>50</sub> for MUC1-Apt-HSA-CAP-NPs (~74 $\mu$ g/ml) was lower than the IC<sub>50</sub> for free capsaicin (~97.2 $\mu$ g/ml). It is surprising that the addition of MUC1 aptamer and encapsulation of capsaicin in nanoparticles only caused a modest increase in its growth-inhibitory activity (~1.3-fold), relative to free capsaicin. This trend was further corroborated by MTT assays which compared the effect of MUC1-Apt-HSA-CAP-NPs with HSA-CAP-NPs and free capsaicin at a concentration of 100 $\mu$ g/ml over 24 hours (Table 7). MUC1-Apt-HSA-CAP-NPs decreased the viability of Panc-1 cells by 65% over 24 hours (P. Nigam, et al., 2014). Free capsaicin decreased the viability of Panc-1 cells by approximately 30% and HSA-CAP-NPs reduced the viability of Panc-1 cells by 45% over 24 hours. All these data seem to suggest that the addition of MUC1 aptamer is only having a modest effect in increasing the growth suppressive activity of capsaicin nanoparticles. This may be explained by the fact that the process of immobilization of the MUC1 aptamer (to HSA-CAP-NPs) may produce conformational changes which diminish the binding affinity of these aptamers to MUC1 on the surface of pancreatic cancer cells (P. Nigam, et al., 2014). A caveat of this study is that the authors did not measure the pharmacokinetics and bioavailability of MUC1-Apt-HSA-CAP-NPs. If these MUC1-Apt-HSA-CAP-NPs are unable to release capsaicin over a prolonged period, then they will produce only a modest decrease or no decrease in the viability of Panc-1 cells (P. Nigam, et al., 2014). It is hoped that future studies from the Nigam research group will characterize the drug release kinetics

of these MUC1-Apt-HSA-CAP-NPs and determine their anti-tumor activity in mice models of pancreatic cancer.

A unique study by Wang et al., (2017) explored the anti-neoplastic activity of nanoparticles which released the two anti-cancer drugs irinotecan and capsaicin. The objective of the study was to determine if capsaicin could sensitize human cancer cells to the pro-apoptotic effects of irinotecan. Irinotecan is a topoisomerase 1 inhibitor used in the clinic for the treatment of ovarian, SCLC and colorectal cancer (Fujita, Kubota, Ishida, & Sasaki, 2015; Kciuk, Marciniak, & Kontek, 2020). A major drawback of irinotecan is that it produces severe toxicity in patients. Therefore, identifying supplementary agents that sensitize tumor cells to chemotherapy-induced apoptosis would be valuable for improving patient tolerance and response to chemotherapy. Wang et al., (2017) synthesized of a nanoparticle-based sustained release drug delivery platform which could concomitantly deliver both capsaicin and irinotecan to human cancer cells (referred to as 1-SEDDS) (L. Wang, et al., 2017). They measured the effect of 1-SEDDS on the viability of the human cancer cell lines, HCT-116, SW680 (colon carcinoma), MCF-7, MDA-MB231 (breast carcinoma) and H1299 (lung carcinoma). The growth-inhibitory activity of 1-SEDDS in colon and breast cancer cell lines was 1.5–3.0-fold higher than SN-38 alone (Table 7). Furthermore, 1-SEDDS induced almost 2-fold higher apoptosis than SN-38 alone and 4-fold higher apoptosis than free capsaicin in HCT-116 cells (L. Wang, Chen, et al., 2017). The administration of 1-SEDDS (at a dose 30 mg /kg body weight) potently decreases the growth rate of HCT-116 human colon cancer tumors xenotransplanted in athymic mice. The anti-tumor activity of 1-SEDDS was greater than SN-38 or free capsaicin. 1-SEDDS did not trigger any toxic side effects, like hemolysis or alteration in the body weights of mice (L. Wang, et al., 2017). We hope that future research will foster the development of targeted drug delivery systems capable of releasing an anti-cancer drug and a chemosensitizing agent to the site of the tumor. This would greatly improve the anti-tumor activity of conventional chemotherapeutic drugs and improve health outcomes of cancer patients in the clinic.

Lan et al., (2019) created a polymeric nanomicelle drug delivery system capable of delivering two anti-cancer drugs paclitaxel (PTX) and capsaicin (PTX-CAP-Fmoc-PEG-NM). The initial step of creating the PTX-CAP-Fmoc-PEG micelle was to synthesize the CAP-Fmoc-PEG polymer (Lan, et al., 2019). The CAP-Fmoc-PEG polymer was synthesized by a condensation reaction between capsaicin-succinic anhydride and PEG-Fmoc-Lys-(NH<sub>2</sub>)<sub>2</sub>. Finally, paclitaxel was loaded on this CAP-Fmoc-PEG micelle (by thin film dispersion method) to generate the PTX-CAP-Fmoc-PEG-NM. The PTX-CAP-Fmoc-PEG polymeric micelle was characterized by NMR spectroscopy (Table 5). MTT assays were performed to compare the growth-suppressive activity of PTX-CAP-Fmoc-PEG-NM with CAP-Fmoc-PEG-NM, free capsaicin, and free paclitaxel in A549 (human lung cancer), HepG2 (human hepatocellular cancer) and 4T1 (mouse breast cancer cells) over 24 hours (Lan, et al., 2019). In all three cell lines CAP-Fmoc-PEG-NM displayed very little decrease in cell viability. The growth inhibitory activity of PTX-CAP-Fmoc-PEG-NM was almost identical to free capsaicin and free paclitaxel in A549 and HepG2 cells (Table 7). However, PTX-CAP-Fmoc-PEG-NM showed greater decrease in cell viability (compared to free capsaicin and free paclitaxel) at lower concentrations of 10ng/ml and 100ng/ml. At concentrations higher than 100ng/ml, PTX-CAP-Fmoc-PEG-NM, free capsaicin, and

free paclitaxel showed similar decreases in cell viability (Lan, et al., 2019). This may be explained by the fact that PTX-CAP-Fmoc-PEG-NM released capsaicin slowly into the aqueous environment; only 25% of capsaicin and paclitaxel were released from these micelles in the first 24 hours. It is probable that PTX-CAP-Fmoc-PEG-NM would have displayed greater decrease in the viability of A549, HepG2 and 4T1 cells if the assay had been performed for longer periods of time.

The anti-tumor activity of PTX-CAP-Fmoc-PEG-NM *in vivo* was determined in syngenic mice models. Balb/c mice were injected subcutaneously with the murine breast cancer cell line 4T1. After the reached a threshold volume of 50–100mm<sup>3</sup>, the mice were randomized into five groups of six mice (Lan, et al., 2019). The mice were treated with free paclitaxel (at a dose of 10mg/kg body weight) or CAP-Fmoc-PEG-NMs (10mg/kg body weight) or PTX-CAP-Fmoc-PEG-NMs (10mg/kg body weight). As a control the tumor bearing mice were injected with saline or with 10mg/kg body weight of PTX-Fmoc-PEG-oleic acid micelles. The drugs were injected intravenously once every three days for 18 days (Lan, et al., 2019). The administration of CAP-Fmoc-PEG-NM only decreased the volumes of 4T1 breast tumors by 92% on day 18 of the study (Table 7). The anti-tumor activity of free paclitaxel and PTX-Fmoc-PEG-oleic acid micelles were similar to each other; and both drugs decreased the volume of 4T1 tumors by 88% relative to saline-treated tumor-bearing mice. The intravenous injection of free paclitaxel caused a 43% reduction in tumor volumes whereas CAP-Fmoc-oleic acid decreased the tumor volumes by 58%. All drugs produced no significant changes in the body weight of the tumor-bearing mice throughout the study (Lan, et al., 2019).

Apart from conventional chemotherapy drugs, capsaicin has been found to synergize with targeted anti-cancer drugs like sorafenib and erlotinib (Bort, Spínola, Rodríguez-Henche, & Díaz-Laviada, 2017; J. C. Chen, et al., 2019). Therefore, it is probable that capsaicin nanoparticles may improve the cytotoxic activity of targeted chemotherapeutic drugs. A unique study by Parasher et al., (2018) investigated the combinatorial anti-cancer activity of capsaicin-loaded folic acid functionalized PLGA nanoparticles (CAP-FA-PLGA-NP) with the EGFR inhibitor gefitinib in human NSCLC (P. Parashar, et al., 2019). Overexpression and activating mutations in EGFR have been reported in 10–15% of caucasian non-small cell lung cancer (NSCLC) and in about 50% of Asian NSCLC patients (Bethune, Bethune, Ridgway, & Xu, 2010; Juriši , Obradovic, Pavlovi , & Djordjevic, 2018). The EGFR inhibitors, namely gefitinib and erlotinib, are first line therapies for such NSCLC patients (Hirsh, 2018). The authors synthesized two separate types of nanoparticles; the first one being gefitinib loaded folic acid functionalized nanoparticles (Gnb-FA-PLGA-NP) and the second one being CAP-FA-PLGA –NP. Subsequently, the authors performed an MTT assay to determine the growth-inhibitory activity of a 1:1 combination of Gnb-FA-PLGA-NP and CAP-FA-PLGA-NP in A549 human NSCLC cells over 48 hours (P. Parashar, et al., 2019). As a control the A549 cells were treated with Gnb-FA-PLGA-NP alone or CAP-FA-PLGA-NP alone or free capsaicin or free gefitinib. All the drugs were used in the concentration range of 10nM-100µM. The authors observed that that the IC<sub>50</sub> value for the combination of Gnb-FA-PLGA-NP and CAP-FA-PLGA-NP (IC<sub>50</sub>=23.5±0.76µM) was higher than Gnb-FA-PLGA-NP alone (IC<sub>50</sub>=31.76.5±0.76µM) and CAP-FA-PLGA-NP alone (IC<sub>50</sub>=45.32±0.86µM) in A549 human NSCLC cells. Such findings imply that the

presence of folic acid as a targeting moiety improves the growth suppressive activity of capsaicin and gefitinib nanoparticles (P. Parashar, et al., 2019). The ability of these nanoparticle drugs to decrease the viability of A549 human NSCLC cells followed an order of CAP-FA-PLGA-NPs combined with Gnb-FA-PLGA-NPs > Gnb-PLGA-NPs > CAP-PLGA-NPs > free gefitinib > free capsaicin. Chou-Talalay isobologram analysis revealed that Gnb-FA-PLGA-NP and CAP-FA-PLGA-NP were synergistically suppressing the viability of A549 (Chou, 2008, 2010). The simultaneous intravenous administration of Gnb-FA-PLGA-NP (dose= 20 mg/kg bodyweight) and CAP-FA-PLGA-NP (dose=10 mg/kg bodyweight) robustly suppressed urethane-induced lung carcinogenesis in both male and female albino Wistar rats (P. Parashar, et al., 2019). The anti-tumor activity of the combination of Gnb-FA-PLGA-NP and CAP-FA-PLGA NP was substantially greater than both the drugs administered alone. Kaplan-Meir plots revealed a higher survival of tumor-bearing rats which received the combination therapy (of Gnb-FA-PLGA-NP and CAP-FA-PLGA-NP) relative to all other treatment groups (P. Parashar, et al., 2019). Such findings indicate that the co-administration of the chemotherapeutic drug nanoparticles along with capsaicin nanoparticles as well as the may represent a novel strategy for the treatment and management of human NSCLCs.

Several lines of evidence indicate that the ability of cancers to metastasize to distant organs is the major reason for the lethality of cancer. A crucial step of cancer metastasis is tumor invasion (Meirson, et al., 2020; Wittekind & Neid, 2005). Tumor invasion refers to the process by which cancer cells penetrate the basement membrane into surrounding stroma, neighboring blood vessels and lymph nodes (Meirson, et al., 2020; Wittekind & Neid, 2005). = Amongst the many steps of metastasis, the process of tumor invasion has been targeted by many therapeutic agents to suppress the distant metastasis of human cancers (Meirson, et al., 2020; Wittekind & Neid, 2005). Yu et al. (2019) explored the anti-invasive activity of capsaicin-loaded mesoporous silica-coated gold nanodots in human thyroid cancer. Mesoporous silica nanodots (MSNs) have several advantages (over other types of inorganic nanoparticles) for drug delivery applications. These silica nanodots have large surface area, tailorable pore sizes, controllable molecular shapes (and sizes) and dual functional surfaces (Bharti, Nagaich, Pal, & Gulati, 2015; Vallet-Regí, Colilla, Izquierdo-Barba, & Manzano, 2017). Chemotherapy drugs can be stacked into MSNs eliminating the need for organic solvents which are deleterious to human tissues (Y. Gao, Gao, Shen, & Wang, 2020). These MSNs can be functionalized with a large array of organic sensor compounds which are responsive to stimuli like light, temperature, and heat to create multifaceted drug delivery systems. NIR gold nanorods are light-sensitive nanoparticles which have been explored as photothermal anti-cancer agents in human breast, oral, cervical, and gastric cancer (Sun, et al., 2020; Vines, Yoon, Ryu, Lim, & Park, 2019; Zong, Dong, Yang, Ling, & Zhang, 2021). These NIR gold nanoparticles are activated via NIR laser light, creating the ability to penetrate deep into tumor tissue facilitating the delivery of anti-cancer drugs in a controlled and targeted manner. Yu et a., (2019) used a modification of Stober's method to coat cetyltrimethylammonium bromide (CTAB)-stabilized gold nanorods with mesoporous silica nanoparticles. The resultant nanoparticles were comprised of an outer MSN structure in which gold nanorods were embedded in the interior surface (hereby called Gold-NR-MSNs). Finally, capsaicin was loaded on these gold-NR-MSNs to generate NIR-CAP-Gold-NR-

MSNs (Yu, et al., 2019). The first series of experiments assessed the growth-inhibitory activity of NIR-CAP-Gold-NR-MSNs in FTC-133 and B-CPAP human thyroid cancer lines. As a control, the authors analyzed the cytotoxic activity of capsaicin-coated gold nanorods capped mesoporous silica nanoparticles (CAP-GOLD-MSNs). These CAP-GOLD-MSNs are not triggered by NIR light. MTT assays revealed that CAP-Gold-NR-MSNs decreased the viability of FTC-133 cells by a greater magnitude compared to CAP-GOLD-MSNs (Yu, et al., 2019). The results were verified using a second human thyroid cancer cell line namely B-CPAP and similar results were obtained. The NIR-CAP-Gold-NR-MSNs decreased the viability of B-CPAP cells more robustly than CAP-Gold-MSNs (Table 7). The  $IC_{50}$  for NIR-CAP-Gold-NR-MSNs (approximately  $1.6\mu\text{M}$ ) was 8-fold lower than the  $IC_{50}$  for CAP-Gold-MSNs (approximately  $12.5\mu\text{M}$ ).

Next, the authors compared the anti-migratory activity of NIR-CAP-Gold-NR-MSNs and CAP-Gold-MSNs in B-CPAP cells using the wound healing assay (Yu, et al., 2019). The treatment of  $1\mu\text{M}$  NIR-CAP-Gold-NR-MSNs and CAP-Gold-MSNs decreased the migration of B-CPAP cells by 85% over 24 hours. Encouraged by these findings, the authors performed a Boyden chamber assay to determine the anti-invasive activity of NIR-CAP-Gold-NR-MSNs and CAP-Gold-MSNs in B-CPAP cells over 24 hours. They observed that both NIR-CAP-Gold-NR-MSNs and CAP-Gold-MSNs (at a concentration of  $1\mu\text{M}$ ) reduced the invasion of B-CPAP cells by 3-fold over 24 hours. Most interestingly, the anti-migratory and anti-invasive activity of NIR-CAP-Gold-NR-MSNs was comparable to CAP-Gold-MSNs, at a concentration of  $1\mu\text{M}$  (Yu, et al., 2019). It is unclear why the concentration of  $1\mu\text{M}$  was chosen for the wound healing and Boyden chamber assays. MTT assays reveal that  $1\mu\text{M}$  NIR-CAP-Gold-NR-MSNs decreased the viability of B-CPAP cells by 50% over 24 hours (Yu, et al., 2019). Therefore, it is possible that the results obtained in the migration and invasion assays are merely due to the cytotoxicity of NIR-CAP-Gold-NR-MSNs. To determine if NIR-CAP-Gold-NR-MSNs have an impact on the migration (and invasion) properties of B-CPAP cells, the authors should choose concentrations of NIR-CAP-Gold-NR-MSNs which do not impact the viability of B-CPAP cells. Flow cytometry assays show that the NIR-CAP-Gold-NR-MSNs decreased the viability of B-CPAP cells by triggering both cell cycle arrest and apoptosis (Table 7). The treatment of  $1\mu\text{M}$  NIR-CAP-Gold-NR-MSNs triggered 2-fold greater apoptosis (in B-CPAP cells) relative to CAP-Gold-MSNs over 24 hours (Yu, et al., 2019). Similarly, both NIR-CAP-Gold-NR-MSNs and CAP-Gold-MSNs induced robust cell cycle arrest in S-phase (approximately 60–70% cells in S phase) in B-CPAP cells over 24 hours. The graphs in the paper seem to suggest that the pro-apoptotic and anti-proliferative activity of NIR-CAP-Gold-NR-MSNs is greater than CAP-Gold-MSNs, but no statistical analysis has been performed (Yu, et al., 2019). The lack of statistical analysis in this study makes it impossible to draw any conclusions about the anti-cancer activity of NIR-CAP-Gold-NR-MSNs versus CAP-Gold-MSNs in human thyroid carcinoma cells.

A very important question about capsaicin-loaded nanoparticles is their effect in normal cells and tissues. If these capsaicin containing nanoparticles show toxicity in normal tissues, then they cannot be considered good drug candidates for cancer therapy. Several of the publications suggest that capsaicin nanoparticles are selective for cancer cells versus normal cells. For example, CNDs caused greater decrease in the viability of human cancer

cells (breast cancer and hepatocellular cancer) relative to normal kidney cells (Malar & Bavanilathamuthiah, 2015). Similarly, capsaicin loaded nanoliposomes displayed greater growth inhibitory activity in human cancer cell lines, relative to normal human fibroblasts (A. Al-Samydai, et al., 2021). In the arena of ligand-targeted nanoparticles, CFLN did not affect the viability of OSE normal human ovarian epithelial cells at concentrations ranging from 0.1–50µg/ml (Lv, et al., 2017). Similarly, CAP-Chi-NCAS displayed no growth-suppressive activity in UROtsa normal human urothelial cells (von Palubitzki, et al., 2020). A plethora of published reports show that capsaicin-loaded nanoparticles did not trigger cell death in normal kidney cells, normal human bronchial epithelial cells, dermal fibroblasts, buccal epithelial cells, reconstructed human epidermal epithelial cells at concentrations as high as 500µM (Kaiser, et al., 2015; Kolonko, et al., 2020; von Palubitzki, et al., 2020; X. R. Wang, et al., 2017; Zhu, et al., 2015). Taken together, these findings imply that capsaicin-nanoparticle based anti-cancer drugs are devoid of toxicity towards normal cells and tissues.

The neuroblastoma cell line Neuro-2a is a well-established model for testing the neurotoxicity of drugs (LePage, Dickey, Gerwick, Jester, & Murray, 2005; Viallon, Chinain, & Darius, 2020). Capsaicin nanoparticles did not impact the viability of Neuro-2a cells at concentrations ranging from 12.5ng/ml-10µg/ml. Therefore, it can be concluded that capsaicin nanoparticles are not toxic to neuronal cells at these concentrations (K. Nigam, Gabrani, & Dang, 2019). The intravenous injection of capsaicin nanoparticles in glioma tumor-bearing mice produced no sign of oxidative injury to the BBB, neuronal or neuroglial cells. No damage to the brain parenchyma, encephalopathy (characterized by symmetric vacuolation and microcavitation in selected brain regions) or injury to brain endothelial cells was observed in these mice (Z. Jiang, et al., 2015). Such observations suggest that capsaicin nanoparticles are devoid of off- target neuronal toxicity *in vivo*.

An advantage of capsaicin nanoparticle drugs is that they display reduced skin and gastric irritation in animal models (Anantaworasakul, Chaiyana, Michniak-Kohn, Rungseevijitprapa, & Ampasavate, 2020; Zhu, et al., 2015). Bhagwat et al., (2021) tested the effects of oral administration of capsaicin-biotin-nanoparticles in Swiss albino rats. The morphology of rat mucosa in rats fed with free capsaicin showed disruptions and inflammatory infiltrations. In contrast, the gastric mucosa of rats fed with capsaicin nanoparticles showed relatively normal morphology and structure (Bhagwat, et al., 2021). A similar result was obtained with capsaicin nanomicelles and capsaicin-loaded-PCL nanoparticles (W. Peng, et al., 2015). Experiments in hen's egg test- chorioallantoic membrane (HET-CAM) models demonstrated that capsaicin nanoparticles triggered reduced skin irritation/inflammation than free capsaicin (Anantaworasakul, et al., 2020; W. Peng, et al., 2015). This could be attributed to the entrapment of capsaicin in the nanoparticles which diminished the direct contact of capsaicin with the gastric mucosa (or skin), reducing inflammation (X. R. Wang, et al., 2017). The administration of capsaicin nanoparticles enables the capsaicin to be slowly released in to the skin or gastrointestinal tract (at a lower steady state concentration) thereby decreasing irritation and inflammation of the skin or gastric mucosa.

The anti-tumor activity of capsaicin nanoparticle drugs has been investigated in athymic mouse models or lung carcinogenesis models (Lan, et al., 2019; Poonam Parashar, et al., 2019; L. Wang, et al., 2017). No evidence of organ toxicity or inflammatory events have been reported in these experiments. No signs of distress such as, salivation, vocalization, distress-hunching, tremor, diarrhea, dyspnea, or state of coma was observed in these capsaicin nanoparticle-treated animals. Most importantly, the structural integrity of the lung (in the lung carcinogenesis model) was not affected by the administration of capsaicin nanoparticles.

Several lines of evidence show that intravenous injection is the most common method to administer nanoparticles drugs to cancer patients (Eek, et al., 2016; Johnson, et al., 2019). If these anti-cancer nanoparticle drugs damage blood cells or blood vessels, then they are neither safe nor effective in patients. With this background in mind, several publications have examined the effects of capsaicin nanoparticle drugs on the cells present in the blood. Cell culture studies show that capsaicin-loaded nanoparticles do not induce any damage or disruption of red blood cells in normal human blood. No occurrence of hemolysis, thrombosis and inflammatory events were reported when the animals were administered capsaicin nanoparticle drugs. Furthermore, the capsaicin nanoparticles did not produce any delirious effects on blood rheology (biophysical properties and flow properties of blood) *in vivo*. These observations suggest that capsaicin nanoparticle drugs are safe, effective, and well tolerated in animals.

#### **2.3.4 Signaling Pathways underlying the Anti-Cancer Activity of Capsaicin Nanoparticles**

—A majority of research papers suggest that capsaicin nanoparticles suppress the growth of human cancer cells by inducing programmed cell death in human cancer cells. Capsaicin nanoparticles induce apoptosis in hepatocellular carcinoma, breast carcinoma, lung carcinoma, bladder cancer, ovarian cancer, colorectal cancer and gastric cancer (Table 7). An exception to this trend is the fact that the growth-suppressive activity of CAP-GOLD-MSNs in human thyroid cancer cells was due to a mixture of cell cycle arrest and apoptosis (Yu, et al., 2019). Similarly, both CAP-Gold-MSNs and NIR-CAP-Gold-NR-MSNs induced robust cell cycle (approximately 60–70% cells arrested in S phase) in B-CPAP human thyroid cancer cells over 24 hours. The graphs in the paper seem to suggest that the pro-apoptotic and anti-proliferative activity of NIR-CAP-Gold-NR-MSNs is greater than CAP-Gold-MSNs, but no statistical analysis has been performed to confirm these findings.

The apoptosis pathway in mammalian cells involves mitochondrial swelling, cavitation, and other ultrastructural changes, suggesting that genes involved in mitochondrial function play important roles in the cell death process (Figure 4). Published data show that the pro-apoptotic activity of capsaicin-loaded trimethyl chitosan nanoparticles (CAP-TMC-NP) in HepG2 human hepatocellular carcinoma cells is dependent on the Bax/Bcl2 and caspase-3 pathway (Elkholi, et al., 2014; Hazem, et al., 2021). Real time PCR experiments reveal that the treatment of HepG2 cells with CAP-TMC-NP upregulates the levels of the pro-apoptotic gene Bax with concomitant decrease in the expression of the pro-survival gene Bcl-2. The results of the real-time PCR experiments were verified by immunohistochemistry. The CAP-TMC-NP-treated HepG2 cells showed strong positive staining for Bax and



Based on such results it is tempting to speculate that PTX-CAP-Fmoc-PEG-NMs suppresses the growth of breast cancers by a mixture of apoptosis and necrosis pathways.

Studies by Parasher et al., (2019) revealed that CAP-FA-PLGA-NPs sensitized human NSCLC cells towards the growth suppressive activity of GnB-FA-PLGA-NP. The co-treatment of CAP-FA-PLGA-NPs and GnB-FA-PLGA-NPs decreased the viability of A549 human lung cancer cells to a greater magnitude than each of the drugs administered as a single agent (P. Parashar, et al., 2019). The combination of CAP-FA-PLGA-NPs and GnB-FA-PLGA-NPs triggered both cell cycle arrest and apoptosis in A549 cells. Flow cytometry experiments revealed that the co-administration of CAP-FA-PLGA-NPs and GnB-FA-PLGA-NPs triggered cell cycle arrest in both G0/G1 phase and G2/M phase (P. Parashar, et al., 2019). The pro-apoptotic activity of CAP-FA-PLGA-NPs and GnB-FA-PLGA-NPs was measured using the mitochondrial membrane potential assay. The combination of CAP-FA-PLGA-NPs and GnB-FA-PLGA-NPs triggered a greater magnitude of apoptosis as compared to the individual drugs namely CAP-FA-PLGA-NPs and GnB-FA-PLGA-NPs (P. Parashar, et al., 2019). Similarly, the pro-apoptotic activity of CAP-PLGA-NPs, GnB-PLGA NPs and free gefitinib was lower than the folic acid functionalized nanoparticles. Immunoblotting studies revealed that the combined treatment of CAP-FA-PLGA-NPs and GnB-FA-PLGA-NPs led to an increase in the levels of capsapase-3, caspase-9 and p16 in A549 human NSCLC cells (P. Parashar, et al., 2019). In contrast the expression of MMP-9 was decreased by the co-treatment of CAP-FA-PLGA-NPs and GnB-FA-PLGA-NPs. The matrix metalloprotease family of enzymes plays a vital role in invasion and metastasis of NSCLCs (Blanco-Prieto, et al., 2017; Merchant, et al., 2017). Based on these results the combination of CAP-FA-PLGA-NPs and GnB-FA-PLGA-NPs may regulate display anti-invasive anti-metastatic activities in NSCLCs.

An important mechanism of action underlying the pro-apoptotic activity of capsaicin nanoparticles is their ability to regulate the ROS pathway (Table 7). CNDs triggered increased levels of reduced glutathione and DPPH (2,2-diphenyl-1-picrylhydrazyl) scavenging activity (in breast cancer cells) relative to blank dendrimers and free capsaicin (Malar & Bavanilathamuthiah, 2015). Such findings suggest that the antioxidant activity of capsaicin nanoparticles may play a role in their ability to induce cellular apoptosis. HA-PCL-CAP-NPs potently suppressed the production of ROS in A549 cells. Such inhibition of ROS correlated with the loss of mitochondrial membrane potential (a hallmark of apoptosis) in A549 cells (Poonam Parashar, et al., 2019). HA-PCL-CAP-NP showed robust anti-neoplastic activity in urethane-induced rat lung carcinogenesis model. The authors examined the levels of oxidative stress markers in the lung homogenates obtained from tumor-bearing rats (Poonam Parashar, et al., 2019). The administration of the carcinogen urethane increased the levels of oxidative stress markers TBARS (Thiobarbituric acid reactive substance, a 2.5-fold increase relative to vehicle) and superoxide dismutase (SOD, a 1.5-fold increase relative to vehicle). The levels of protein carbonylation was 3-fold higher in urethane-treated rats, relative to vehicle-treated rats (Poonam Parashar, et al., 2019). Conversely, the enzymatic activity of catalase was decreased by 4-fold in the urethane-treated, as compared to vehicle-treated rats. The administration of HA-PCL-CAP-NPs in lung-tumor-bearing rats restored the levels of TBARS, SOD, catalase activity and protein carbonylation to normal levels, as observed in vehicle-treated rats. A similar observation

was made by Dhamodaran et al., (2021) who explored the signaling pathways underlying the anti-tumor activity of CAP-CS-NPs in human breast cancer. They showed that the intravenous administration of CAP-CS-NPs robustly suppressed DMBA-induced mammary carcinogenesis in rats (Dhamodharan, et al., 2021). They investigated the levels of redox enzymes, detoxification enzymes and cell cycle markers in plasma, liver and the mammary tissue, isolated from these rats (Table 7). The administration of DMBA caused a two-fold elevation of TBARS levels in plasma, liver and mammary tumor tissue. The administration of CAP-CS-NPs abrogated DMBA-induced increase in TBARS levels in all the above-mentioned tissues (Dhamodharan, et al., 2021). The carcinogen DMBA decreased the levels of redox enzymes namely SOD, catalase, GPx, GSH, Vitamin C and E by 2.6-fold in the plasma of rats. The presence of CAP-CS-NPs restored the levels of the above proteins (in the plasma) back to those observed in the control mice (Dhamodharan, et al., 2021). A similar trend was observed in the liver and the mammary tissue of these tumor-bearing rats. The non-enzymatic antioxidants like SOD, catalase, GPx, GSH, Vitamin C and E have excellent free radical scavenging activity and they protect the tissues from oxidative stress (Dhamodharan, et al., 2021). Taken together, such data argue for an antioxidant effect of HA-PCL-CAP-NPs and CAP-CS-NPs and suggest that the anti-tumor activity these nanoparticle drugs may be at least in part mediated by their ability to restore redox balance *in vivo*.

The exposure to carcinogens like urethane and DMBA promote the oncogenic transformation of tissues (Kerdelhué, Forest, & Coumoul, 2016; Schlatter & Lutz, 1990). The liver is the primary site of metabolism for all xenobiotics that enter the body. Phase I enzymes like Cytochrome P450 and Cyt-b5 interact with the xenobiotic compounds to generate reactive species which can directly bind of DNA to trigger mutations and genetic alterations (Hachey, Dawling, Roodi, & Parl, 2003; Michael & Doherty, 2005). The presence of CAP-CS-NPs robustly abrogated DMBA-induced increase of cytochromeP450 and Cyt-b5 in the liver tissue of tumor bearing rats (Dhamodharan, et al., 2021). The phase II enzymes in the liver usually transform the xenobiotic chemicals into aqueous substrates which can be eliminated from the body via the feces/urine (Hachey, et al., 2003; Michael & Doherty, 2005). The presence of DMBA decreased the levels of phase II enzymes like GST, GR and DT-D in the liver of rats. The administration of CAP-CS-NPs restored the levels of these enzymes back to those in control rats (Table 7). These findings support the notion that CAP-CS-NPs neutralized the toxic metabolites arising from DMBA (Dhamodharan, et al., 2021). The presence of DMBA accelerated the proliferation of mammary tumors as evidenced by elevated levels of cyclinD1 and PCNA in these tumors (Dhamodharan, et al., 2021). The administration of CAP-CS-NPs (along with DMBA) ablated the levels of cyclinD1 and PCNA suggesting that the anti-neoplastic activity of CAP-CS-NP is mediated by G1 arrest in these tumor-bearing rats.

### 3. Conclusions and future directions

The phytochemical capsaicin has been formulated in a diverse array of sustained release drug delivery platforms like solid dispersion systems, phospholipid complexes, liposomes, and nanoparticles to improve its solubility, bioavailability, and anti-cancer activity (Chittepu-Reddy, et al., 2018; Rollyson, et al., 2014). Out of all these drug delivery systems, most

published reports have encapsulated capsaicin in nanoparticles. This may be explained by the fact that nanoparticles have several advantages over other forms of sustained release formulations (Anselmo & Mitragotri, 2019; Khan, et al., 2019; Mudshinge, et al., 2011; Zieli ska, et al., 2020). A few advantages of nanoparticle drug delivery systems over other sustained release drugs include long term stability (i.e., long shelf life); high drug loading/encapsulation capacity (i.e., many drug molecules can be incorporated in the nanopolymer matrix); flexibility of loading both hydrophilic and hydrophobic drugs within the nanomatrix; and their compatibility with diverse routes of administration, including oral administration and inhalation. These carriers can be functionalized by biological ligands to ensure the delivery of these drugs to specific tissues/organs (Beltrán-Gracia, et al., 2019). A few of the targeting ligands used in capsaicin nanoparticles include folic acid, biotin, hyaluronic acid, chitosan and MUC1 aptamers. An innovative application of these nanoparticles has been as diagnostic probes for imaging of tumors. For example, the capsaicin-magnetic nanoparticle drug CAP-EW-MAGNETIC-NP was found to have excellent MRI imaging properties (Rabiee & Rabiee, 2019). Several types of human cancers such as breast cancer, pancreatic cancer, squamous cell carcinoma (of the human tongue) and prostate carcinoma overexpress the cognate receptor for capsaicin TRPV1 (L. Li, et al., 2021; Vercelli, Barbero, Cuniberti, Odore, & Re, 2015). The TRPV1 receptor has been also found to be overexpressed in human brain tumors (specifically astrocytomas) where the relative density of TRPV1 has been correlated to the clinical stage and grade of these tumors (Stock, et al., 2012). It may be envisaged that such capsaicin-loaded nanoparticles may have applications for the detection and imaging of such TRPV1-overexpressing tumors. The administration of capsaicin loaded nanoparticles may have a dual therapeutic effect in these tumors. Apart from imaging the tumors, these capsaicin nanoparticles will exert pro-apoptotic and anti-proliferative effects of these cancers and be useful for the therapy of such cancers. It is anticipated that the presence of targeting ligands like folic acid, biotin and chitosan may further improve the imaging properties of such capsaicin-containing nanoparticle drugs. The presence of two ligands (on the nanopolymer drug) will substantially amplify its imaging efficacy and specificity in human cancers.

An exciting development in the field of capsaicin-sustained release drugs has been the discovery of drug delivery platforms which can co-release conventional chemotherapeutic drugs (like irinotecan and paclitaxel) and targeted anti-cancer drugs (like gefitinib) along with capsaicin (Lan, et al., 2019; Qi, et al., 2021; L. Wang, et al., 2017). Several congruent studies have shown that capsaicin sensitizes human cancer cells to the pro-apoptotic effects of chemotherapy. The combination treatment of chemotherapeutic drugs and capsaicin will not only increase the anti-tumor activity of the sustained release drug formulation but will also minimize the adverse side effects of these cytotoxic chemotherapy drugs. Qi et al. (2021) discovered that the dual-drug delivery liposome (capable of delivering curcumin and capsaicin) displayed potent anti-tumor activity in human hepatocellular carcinoma in both cell culture and mouse models (Qi, et al., 2021). In addition to suppressing the growth and metastasis of hepatocellular carcinoma tumors, such dual function liposomes could also combat drug resistance of human hepatocellular carcinoma tumors by decreasing the expression of the multidrug resistance protein P-glycoprotein (Qi, et al., 2021). The standard of care chemotherapy of human liver cancer is the B-Raf inhibitor sorafenib (A. Huang,

Yang, Chung, Dennison, & Zhou, 2020; Ikeda, et al., 2018; Stuart, 2021). Published data show that capsaicin synergizes with sorafenib to trigger increased apoptosis of human hepatocellular carcinoma cells (Bort, et al., 2017). Although, sorafenib improves the overall survival of liver cancer patients, it has toxic side effects on the liver and the gastrointestinal tract. Furthermore, the long-term treatment of liver cancer patients with sorafenib has been shown to promote drug resistance in tumors (A. Huang, et al., 2020; Ikeda, et al., 2018; Stuart, 2021). It is hoped that future studies from the research group of Qi et al. (2021) will involve the creation of sustained release drugs which could administer both sorafenib and capsaicin to human hepatocellular carcinoma cells. Such dual drug delivery liposomes may display higher anti-tumor activity (than the drugs given alone) and circumvent the advent of drug resistance in the liver cancer patients.

The improved bioavailability and anti-neoplastic activity of capsaicin-containing sustained release drugs and related nanoparticle drug delivery systems have the potential to revolutionize cancer therapy in patients by enabling the development of novel treatment regimens in this lethal disease. Future studies will describe novel sustained release formulation which may co-deliver antibody drugs, small interfering RNA, and proteasome inhibitors and, radiosensitizing agents along with capsaicin (Boateng & Ngwa, 2019; Cardoso, Peça, & Roque, 2012; Federico, et al., 2020; K.-W. Huang, et al., 2018; Jhaveri & Torchilin, 2014). Published data reveal that capsaicin improves the therapeutic efficacy of radiation-therapy in human prostate cancer (Venier, et al., 2015). Therefore, the encapsulation of capsaicin in radiation-enhancing nanoparticles may have far reaching impacts on the standard of care for radiation oncology treatments. The development of advanced slow-release capsaicin polymeric drug delivery platforms will pave the way for the discovery of ultrasensitive imaging agents, high-specificity diagnostic signaling probes and improved combination therapies for a wide variety of human cancers.

## Acknowledgements

We acknowledge Dr. S. Chellappan and his laboratory for their continuous support. SDR is a recipient of NSF-SURE and West Virginia-NASA State Grant Consortium undergraduate fellowships respectively. AJC is a recipient of a NASA graduate student fellowship from the West Virginia-NASA State Grant Consortium. PD and MAV are supported by a National Institutes of Health R15 Academic Research Enhancement Award (Grants 1R15CA161491-01A1, 2R15CA161491-02 and 2R15CA161491-03). This work was supported in part by the West Virginia IDeA Network of Biomedical Research Excellence (WV-INBRE) grant (NIH grant P20GM103434; PI: Dr. G. Rankin), the National Institute of General Medical Sciences of the National Institutes of Health under the award number P30GM122733.

## List of abbreviations

<b>1-SEDDS</b>	Self-emulsifying hydrophobic nanoparticle drug delivery system
<b>ASGP-R</b>	Asialoglycoprotein receptor
<b>ATP</b>	Adenosine triphosphate
<b>BIOTIN-NP</b>	Biotin nanoparticles
<b>Bax</b>	BCL2 Associated X, Apoptosis Regulator

<b>Bcl-2</b>	B-cell lymphoma-2
<b>BLANK-CS-NO</b>	Blank Chitosan nanoparticles
<b>BLANK-LIPO</b>	Blank Liposomes
<b>BLANK-TMCS-NP</b>	Blank trimethyl chitosan nanoparticles
<b>BT-NP</b>	Biotin nanoparticles
<b>CAP-BT-PNPP</b>	capsaicin-biotin nanoparticles
<b>CAP-Chi-NCAS</b>	Capsaicin loaded chitosan nanocapsules
<b>CAP-CS-NP</b>	Capsaicin loaded chitosan nanoparticles
<b>CAP-CUR-GAL-LIPO</b>	Capsaicin and curcumin containing galactose functionalized liposomes
<b>CAP-CUR-GLY-LIPO</b>	Capsaicin and curcumin containing glycyrrhetic acid functionalized liposomes
<b>CAP-CUR-GLY-GAL-LIPO</b>	Capsaicin and curcumin containing glycyrrhetic acid and galactose functionalized liposomes
<b>CAP-CUR-LIPO</b>	Capsaicin-curcumin-loaded liposomes
<b>CAP-EW-MAGNETIC-NP</b>	Capsaicin-loaded EW-CoFe <sub>2</sub> O <sub>4</sub> -ZSM-5 nanoparticles
<b>CAP-Fmoc-PEG</b>	Capsaicin fluorenylmethyloxycarbonyl polyeythene glycol
<b>CAP-FA-PLGA-PEG-NP</b>	Capsaicin loaded folic acid functionalized polyethylene glycol-poly lactide decoglycolic acid nanoparticles
<b>CAP-PLGA-NPs</b>	Capsaicin loaded poly lactide decoglycolic acid nanoparticles
<b>CAP-GAL-LIPO</b>	Capsaicin containing galactose functionalized liposomes
<b>CAP-GOLD-MSN</b>	Capsaicin loaded gold nanorods capped mesoporous silica nanoparticles (s
<b>CAP-HAP-PXS-NPs</b>	Capsaicin loaded hydroxyapatite-polyxylitol sebacate nanoparticles
<b>CAP-HSA-NP</b>	Capsaicin loaded human serum albumin nanoparticles
<b>CAP-LIPO</b>	Capsaicin containing non-functionalized liposomes
<b>CAP-PCL-NP</b>	Capsaicin loaded poly- $\epsilon$ -caprolactone
<b>CAP-mPEG-PCL-NP</b>	Capsaicin loaded methoxy polyethylene glycol-poly caprolactone nanoparticle
<b>CAP-NP</b>	Capsaicin nanoparticles

<b>CAP-NANO-LIPO</b>	Capsaicin nanoliposome
<b>CAP-SLN</b>	Capsaicin solid nanoparticles nanoparticles
<b>CAP-SNEDDS</b>	Capsaicin loaded SNEDDS
<b>CAP-SOY-PL</b>	Capsaicin-soyabean phospholipid complex
<b>CAP-TMC-NP</b>	Capsaicin loaded trimethyl chitosan nanoparticles
<b>CFLN</b>	Capsaicin loaded folic acid-functionalized lipid nanoparticles
<b>CMC</b>	Critical micelle concentration
<b>Chi-NCAS</b>	Chitosan nanocapsules
<b>CLN</b>	Capsaicin loaded lipid nanoparticles
<b>CND</b>	Capsaicin nanodendrimers
<b>CNS</b>	Central nervous system
<b>Cyt-P450</b>	Cytochrome P450
<b>Cyt-b5</b>	Cytochrome b5
<b>DEE</b>	Drug entrapment efficiency
<b>DiD</b>	1,1'-dioctadecyl-3,3,3',3'-tetramethylindodicarbocyanine, 4-chlorobenzenesulfonate
<b>DiD-GAL-GLY-LIPO</b>	DiD labeled glycyrrhetic acid and galactose functionalized liposomes
<b>DIR</b>	1,1'-dioctadecyl-3,3,3',3'-tetramethylindotricarbocyanine iodide
<b>DiR-GAL-GLY-LIPO</b>	DiR labeled glycyrrhetic acid and galactose functionalized liposomes
<b>DiR-LIPO</b>	DiR labeled nonfunctionalized PEG liposomes
<b>DLS</b>	Dynamic Light Scattering Technology
<b>DLE</b>	Drug loading efficiency
<b>DMBA</b>	7, 12-Dimethylbenz(a)anthracene
<b>DMEM</b>	Dulbecco's Modified Eagle Medium
<b>DPPC</b>	(1,2-dipamitoyl-sn-glycero-3-phosphocholine)
<b>DPPH</b>	2,2-diphenyl-1-picrylhydrazyl
<b>DSC</b>	Differential Scanning Calorimetry

<b>DSPE</b>	1,2-distearoyl-sn-glycero-3-phosphoethanolamine-N-[methoxy(polyethyleneglycol)-2000]
<b>DSPE-PEG2000</b>	[1,2-distearoyl-sn-glycero-3-phosphoethanolamine-N-{amino (polyethyleneglycol)-2000}]
<b>DT-D</b>	DT-diaphorase
<b>ECM</b>	Extracellular matrix
<b>EMT</b>	Epithelial to mesenchymal transition
<b>EPR</b>	Enhanced permeability and retention
<b>EW</b>	Egg white
<b>FAK</b>	Focal adhesion kinase
<b>FITC</b>	Fluorescein isothiocyanate
<b>FT-IR</b>	Fourier Transform infra-red spectroscopy
<b>GAL</b>	Galactose
<b>GAL-LIPO</b>	Galactose functionalized PEG liposomes
<b>GLY-GAL-LIPO</b>	Glycyrrhetic acid and galactose functionalized PEG liposomes
<b>Gold-NR-MSN</b>	Gold nanorods embedded mesoporous silica nanoparticles
<b>GLY</b>	Glycyrrhetic Acid
<b>GLY- LIPO</b>	Glycyrrhetic acid functionalized PEG liposomes
<b>GnB</b>	Gefitinib
<b>GnB-PLGA-NPs</b>	Gefitinib loaded polylactide decoglycolic acid nanoparticles
<b>GPx</b>	Glutathione Peroxidase
<b>GR</b>	Glutathione Reductase
<b>GSH</b>	Glutathione
<b>GST</b>	Glutathione-S-Transferase
<b>HAP</b>	Hydroxyapatite
<b>HA-PCL-CAP-NPs</b>	Capsaicin-containing hyaluronic acid functionalized poly- $\epsilon$ -caprolactone nanoparticles
<b>HA</b>	Hyaluronic acid
<b>HET-CAM</b>	Hen's egg test- chorioallantoic membrane

<b>HPLC</b>	High performance liquid chromatography
<b>HPLC-MS</b>	HPLC coupled to mass spectrometry
<b>HSA</b>	Human serum albumin
<b>HSC</b>	Hepatic stellate cell
<b>i.p</b>	intraperitoneal
<b>IPM</b>	isopropyl myristate
<b>L/P</b>	Liver plasma ratio
<b>MAP</b>	Methotrexate, doxorubicin and cisplatin
<b>MDR-1</b>	Multidrug resistance protein 1
<b>MMP-9</b>	Matrix metalloprotease 9
<b>mPEG-PCL</b>	Methoxy polyethylene glycol-poly caprolactone
<b>MRI</b>	Magnetic resonance imaging
<b>MRT</b>	Mean residence time
<b>MS</b>	Mass spectrometry
<b>MSN</b>	Mesoporous silica nanoparticles
<b>MTT</b>	(3-(4,5-Dimethylthiazol-2-yl)-2,5-Diphenyltetrazolium Bromide)
<b>MUC1</b>	Mucin1
<b>MUC1-Apt-HSA-CAP-NP</b>	MUC1-aptamer-HSA-Capsaicin-nanoparticles
<b>NIR</b>	Near infrared
<b>NIR-CAP-Gold-NR-MSN</b>	Capsaicin loaded mesoporous silica nanoparticles capped with NIR-sensitive plasmonic gold nanodots
<b>NSCLC</b>	Non-small cell lung cancer cells
<b>PARP</b>	Poly (ADP-ribose) polymerase
<b>PCNA</b>	Proliferating Cell Nuclear Antigen
<b>PBS</b>	Phosphate buffered saline
<b>PEG</b>	Polyethylene glycol
<b>P-gp</b>	P-glycoprotein
<b>PI</b>	Propidium Iodide
<b>PNPP</b>	Poly lactide decoglycolide nanoparticles

<b>PTX-CAP-Fmoc-PEG-NM</b>	Paclitaxel-loaded capsaicin fluorenylmethyloxycarbonyl polyethylene glycol nanomicelle
<b>PXS</b>	Polyxylitol sebacate
<b>Rb</b>	Retinoblastoma tumor suppressor protein
<b>RPMI</b>	Roswell Park Memorial Institute
<b>ROS</b>	Reactive oxygen species
<b>SCLC</b>	Small cell lung cancer
<b>SDDD</b>	Solid Dispersion Drug Delivery
<b>SDDDS</b>	Solid Dispersion Drug Delivery System
<b>SLN</b>	Solid lipid nanoparticle
<b>SOD</b>	Superoxide dismutase
<b>SNEDDS</b>	Self-assembling nanoemulsifying drug delivery systems
<b>TBARS</b>	Thiobarbituric acid reactive substance
<b>TEM</b>	Transmission electron microscopy
<b>TRPV</b>	Transient receptor potential vanilloid
<b>TRPV1</b>	Transient receptor potential vanilloid receptor 1
<b>TRPV6</b>	Transient receptor potential vanilloid receptor 6
<b>SEM</b>	Scanning electron microscopy
<b>XPS</b>	X-ray photoelectron spectroscopy
<b>ZSM-5</b>	Zeolite hybrid nanoparticles

## 7. References

- Aguilar-Pérez KM, Avilés-Castrillo JI, Medina DI, Parra-Saldivar R, & Iqbal HMN (2020). Insight Into Nanoliposomes as Smart Nanocarriers for Greening the Twenty-First Century Biomedical Settings. *Frontiers in Bioengineering and Biotechnology*, 8.
- Ahn JH, Cho WH, Lee JA, Kim DH, Seo J-H, & Lim JS (2015). Bone mineral density change during adjuvant chemotherapy in pediatric osteosarcoma. *Annals of pediatric endocrinology & metabolism*, 20, 150–154. [PubMed: 26512351]
- Al-Samydai A (2019). An Updated Review On Anticancer Activity Of Capsaicin.
- Al-Samydai A, Alshaer W, Al-Dujaili EAS, Azzam H, & Aburjai T (2021). Preparation, Characterization, and Anticancer Effects of Capsaicin-Loaded Nanoliposomes. *Nutrients*, 13.
- Albini A, Pennesi G, Donatelli F, Cammarota R, De Flora S, & Noonan DM (2010). Cardiotoxicity of anticancer drugs: the need for cardio-oncology and cardio-oncological prevention. *Journal of the National Cancer Institute*, 102, 14–25. [PubMed: 20007921]
- Alfarouk KO, Stock C-M, Taylor S, Walsh M, Muddathir AK, Verduzco D, Bashir AHH, Mohammed OY, Elhassan GO, Harguindey S, Reshkin SJ, Ibrahim ME, & Rauch C (2015). Resistance to cancer

chemotherapy: failure in drug response from ADME to P-gp. *Cancer Cell Int*, 15, 71–71. [PubMed: 26180516]

- Ali A, Shah T, Ullah R, Zhou P, Guo M, Ovais M, Tan Z, & Rui Y (2021). Review on Recent Progress in Magnetic Nanoparticles: Synthesis, Characterization, and Diverse Applications. *Front Chem*, 9, 629054. [PubMed: 34327190]
- Alshehri S, Imam SS, Hussain A, Altamimi MA, Alruwaili NK, Alotaibi F, Alanazi A, & Shakeel F (2020). Potential of solid dispersions to enhance solubility, bioavailability, and therapeutic efficacy of poorly water-soluble drugs: newer formulation techniques, current marketed scenario and patents. *Drug Deliv*, 27, 1625–1643. [PubMed: 33207947]
- Ambekar RS, Choudhary M, & Kandasubramanian B (2020). Recent advances in dendrimer-based nanoplatform for cancer treatment: A review. *European Polymer Journal*, 126, 109546.
- Ambrosio L, Raucci MG, Vadalà G, Ambrosio L, Papalia R, & Denaro V (2021). Innovative Biomaterials for the Treatment of Bone Cancer. *International journal of molecular sciences*, 22, 8214. [PubMed: 34360979]
- Amiri S, & Shokrollahi H (2013). The role of cobalt ferrite magnetic nanoparticles in medical science. *Materials Science and Engineering: C*, 33, 1–8.
- Anantaworasakul P, Chaiyana W, Michniak-Kohn BB, Rungseewijitprapa W, & Ampasavate C (2020). Enhanced Transdermal Delivery of Concentrated Capsaicin from Chili Extract-Loaded Lipid Nanoparticles with Reduced Skin Irritation. *Pharmaceutics*, 12.
- Andresen MC (2019). Understanding diverse TRPV1 signaling - an update. *F1000Research*, 8, F1000 Faculty Rev-1978.
- Anselmo AC, & Mitragotri S (2019). Nanoparticles in the clinic: An update. *Bioengineering & translational medicine*, 4, e10143–e10143. [PubMed: 31572799]
- Arbuck SG, Strauss H, Rowinsky E, Christian M, Suffness M, Adams J, Oakes M, McGuire W, Reed E, Gibbs H, & et al. (1993). A reassessment of cardiac toxicity associated with Taxol. *J Natl Cancer Inst Monogr*, 117–130. [PubMed: 7912518]
- Arora V, Campbell JN, & Chung MK (2021). Fight fire with fire: Neurobiology of capsaicin-induced analgesia for chronic pain. *Pharmacol Ther*, 220, 107743. [PubMed: 33181192]
- Arul B, & Ramalingam K (2020). Anticancer Effect of Capsaicin and Its Analogues. In.
- Arvanitis CD, Ferraro GB, & Jain RK (2020). The blood–brain barrier and blood–tumour barrier in brain tumours and metastases. *Nature Reviews Cancer*, 20, 26–41. [PubMed: 31601988]
- Bannerjee S, & McCormack S (2020). Capsaicin for Acute or Chronic Non-Cancer Pain: A : A Review of Clinical Effectiveness, Safety, and Cost-Effectiveness. *CADTH RAPID RESPONSE REPORT: SUMMARY WITH CRITICAL APPRAISAL*.
- Bao Z, Dai X, Wang P, Tao Y, & Chai D (2019). Capsaicin induces cytotoxicity in human osteosarcoma MG63 cells through TRPV1-dependent and -independent pathways. *Cell Cycle*, 18, 1379–1392. [PubMed: 31095448]
- Bárcena C, Stefanovic M, Tutusaus A, Martínez-Nieto GA, Martínez L, García-Ruiz C, de Mingo A, Caballeria J, Fernandez-Checa JC, Marí M, & Morales A (2015). Angiogenin secretion from hepatoma cells activates hepatic stellate cells to amplify a self-sustained cycle promoting liver cancer. *Sci Rep*, 5, 7916. [PubMed: 25604905]
- Barry AE, Baldeosingh R, Lamm R, Patel K, Zhang K, Dominguez DA, Kirton KJ, Shah P, & Dang H (2020). Hepatic Stellate Cells and Hepatocarcinogenesis. *Front Cell Dev Biol*, 8, 709. [PubMed: 32850829]
- Basith S, Cui M, Hong S, & Choi S (2016). Harnessing the Therapeutic Potential of Capsaicin and Its Analogues in Pain and Other Diseases. *Molecules*, 21.
- Beltrán-Gracia E, López-Camacho A, Higuera-Ciapara I, Velázquez-Fernández JB, & Vallejo-Cardona AA (2019). Nanomedicine review: clinical developments in liposomal applications. *Cancer Nanotechnology*, 10, 11.
- Bera S, Maity S, Ghosh B, Ghosh A, & Giri KT (2020). Development and Characterization of Solid Dispersion System for Enhancing the Solubility and Dissolution Rate of Dietary Capsaicin. *Current Drug Therapy*, 15, 143–151.
- Bethune G, Bethune D, Ridgway N, & Xu Z (2010). Epidermal growth factor receptor (EGFR) in lung cancer: an overview and update. *J Thorac Dis*, 2, 48–51. [PubMed: 22263017]

- Bhagwat DA, Swami PA, Nadaf SJ, Choudhari PB, Kumbar VM, More HN, Killedar SG, & Kawtikwar PS (2021). Capsaicin Loaded Solid SNEDDS for Enhanced Bioavailability and Anticancer Activity: In-Vitro, In-Silico, and In-Vivo Characterization. *J Pharm Sci*, 110, 280–291. [PubMed: 33069713]
- Bharti C, Nagaich U, Pal AK, & Gulati N (2015). Mesoporous silica nanoparticles in target drug delivery system: A review. *Int J Pharm Investig*, 5, 124–133.
- Birrer MJ, Betella I, Martin LP, & Moore KN (2019). Is Targeting the Folate Receptor in Ovarian Cancer Coming of Age? *Oncologist*, 24, 425–429. [PubMed: 30635448]
- Blanco-Prieto S, Barcia-Castro L, Páez de la Cadena M, Rodríguez-Berrocal FJ, Vázquez-Iglesias L, Botana-Rial MI, Fernández-Villar A, & De Chiara L (2017). Relevance of matrix metalloproteases in non-small cell lung cancer diagnosis. *BMC Cancer*, 17, 823. [PubMed: 29207990]
- Blanco E, Shen H, & Ferrari M (2015). Principles of nanoparticle design for overcoming biological barriers to drug delivery. *Nat Biotechnol*, 33, 941–951. [PubMed: 26348965]
- Bley K, Boorman G, Mohammad B, McKenzie D, & Babbar S (2012). A comprehensive review of the carcinogenic and anticarcinogenic potential of capsaicin. *Toxicol Pathol*, 40, 847–873. [PubMed: 22563012]
- Boateng F, & Ngwa W (2019). Delivery of Nanoparticle-Based Radiosensitizers for Radiotherapy Applications. *Int J Mol Sci*, 21.
- Bode AM, & Dong Z (2011). The two faces of capsaicin. *Cancer Res*, 71, 2809–2814. [PubMed: 21487045]
- Bort A, Spínola E, Rodríguez-Henche N, & Díaz-Laviada I (2017). Capsaicin exerts synergistic antitumor effect with sorafenib in hepatocellular carcinoma cells through AMPK activation. *Oncotarget*, 8, 87684–87698. [PubMed: 29152112]
- Bose M, & Mukherjee P (2020). Potential of Anti-MUC1 Antibodies as a Targeted Therapy for Gastrointestinal Cancers. *Vaccines (Basel)*, 8.
- Burness CB, & McCormack PL (2016). Capsaicin 8 % Patch: A Review in Peripheral Neuropathic Pain. *Drugs*, 76, 123–134. [PubMed: 26666418]
- Caetano BFR, Tablas MB, Ignotti MG, de Moura NA, Romualdo GR, Barbisan LF, & Rodrigues MAM (2021). Capsaicin lacks tumor-promoting effects during colon carcinogenesis in a rat model induced by 1,2-dimethylhydrazine. *Environ Sci Pollut Res Int*, 28, 2457–2467. [PubMed: 32886307]
- Cardoso MM, Peça IN, & Roque AC (2012). Antibody-conjugated nanoparticles for therapeutic applications. *Curr Med Chem*, 19, 3103–3127. [PubMed: 22612698]
- Cassim S, Chepulis L, Keenan R, Kidd J, Firth M, & Lawrenson R (2019). Patient and carer perceived barriers to early presentation and diagnosis of lung cancer: a systematic review. *BMC Cancer*, 19, 25. [PubMed: 30621616]
- Chakraborty S, Adhikary A, Mazumdar M, Mukherjee S, Bhattacharjee P, Guha D, Choudhuri T, Chattopadhyay S, Sa G, Sen A, & Das T (2014). Capsaicin-induced activation of p53-SMAR1 auto-regulatory loop down-regulates VEGF in non-small cell lung cancer to restrain angiogenesis. *PLoS One*, 9, e99743. [PubMed: 24926985]
- Chan SH, Azlan A, Ismail A, & Shafie NH (2020). Capsaicin: Current Understanding in Therapeutic Effects, Drug Interaction, and Bioavailability. *Mal J Med Health Sci* 16(SUPP6): 216–224.
- Chanda S, Erexson G, Frost D, Babbar S, Burlew JA, & Bley K (2007). 26-Week dermal oncogenicity study evaluating pure trans-capsaicin in Tg.AC hemizygous mice (FBV/N). *Int J Toxicol*, 26, 123–133. [PubMed: 17454252]
- Chang C-F, Islam A, Liu P-F, Zhan J-H, & Chueh PJ (2020). Capsaicin acts through tNOX (ENOX2) to induce autophagic apoptosis in p53-mutated HSC-3 cells but autophagy in p53-functional SAS oral cancer cells. *American journal of cancer research*, 10, 3230–3247. [PubMed: 33163267]
- Chapa-Oliver AM, & Mejía-Teniente L (2016). Capsaicin: From Plants to a Cancer-Suppressing Agent. *Molecules*, 21.
- Chen C, Zhao S, Karnad A, & Freeman JW (2018). The biology and role of CD44 in cancer progression: therapeutic implications. *J Hematol Oncol*, 11, 64. [PubMed: 29747682]
- Chen JC, Ko JC, Yen TC, Chen TY, Lin YC, Ma PF, & Lin YW (2019). Capsaicin enhances erlotinib-induced cytotoxicity via AKT inactivation and excision repair cross-complementary 1

(ERCC1) down-regulation in human lung cancer cells. *Toxicol Res (Camb)*, 8, 459–470. [PubMed: 31160978]

- Chen M, Xiao C, Jiang W, Yang W, Qin Q, Tan Q, Lian B, Liang Z, & Wei C (2021). Capsaicin Inhibits Proliferation and Induces Apoptosis in Breast Cancer by Down-Regulating FBI-1-Mediated NF- $\kappa$ B Pathway. *Drug Des Devel Ther*, 15, 125–140.
- Chenthamara D, Subramaniam S, Ramakrishnan SG, Krishnaswamy S, Essa MM, Lin FH, & Qoronfleh MW (2019). Therapeutic efficacy of nanoparticles and routes of administration. *Biomater Res*, 23, 20. [PubMed: 31832232]
- Cherniakov I, Domb AJ, & Hoffman A (2015). Self-nano-emulsifying drug delivery systems: an update of the biopharmaceutical aspects. *Expert Opin Drug Deliv*, 12, 1121–1133. [PubMed: 25556987]
- Chindamo G, Sapino S, Peira E, Chirio D, Gonzalez MC, & Gallarate M (2020). Bone Diseases: Current Approach and Future Perspectives in Drug Delivery Systems for Bone Targeted Therapeutics. *Nanomaterials (Basel, Switzerland)*, 10, 875.
- Chittepu-Reddy VCS, Kalhotra P, Revilla G, & Gallardo-Velazquez T (2018). Emerging Technologies to Improve Capsaicin Delivery and its Therapeutic Efficacy. In:
- Choi AJ, Kim CJ, Cho YJ, Hwang JK, & Kim C. t. (2009). Effects of Surfactants on the Formation and Stability of Capsaicin-loaded Nanoemulsions. *Food Science and Biotechnology*, 18, 1161–1172.
- Choi CH, Jung YK, & Oh SH (2010). Autophagy induction by capsaicin in malignant human breast cells is modulated by p38 and extracellular signal-regulated mitogen-activated protein kinases and retards cell death by suppressing endoplasmic reticulum stress-mediated apoptosis. *Mol Pharmacol*, 78, 114–125. [PubMed: 20371669]
- Chou TC (2008). Preclinical versus clinical drug combination studies. *Leuk Lymphoma*, 49, 2059–2080. [PubMed: 19021049]
- Chou TC (2010). Drug combination studies and their synergy quantification using the Chou-Talalay method. *Cancer Res*, 70, 440–446. [PubMed: 20068163]
- Clark R, & Lee SH (2016). Anticancer Properties of Capsaicin Against Human Cancer. *Anticancer Res*, 36, 837–843. [PubMed: 26976969]
- Costanzo MT, Yost RA, & Davenport PW (2014). Standardized method for solubility and storage of capsaicin-based solutions for cough induction. *Cough*, 10, 6. [PubMed: 25342957]
- D'Souza S (2014). A Review of In Vitro Drug Release Test Methods for Nano-Sized Dosage Forms. *Advances in Pharmaceutics*, 2014, 304757.
- Danaei M, Dehghankhold M, Ataei S, Hasanzadeh Davarani F, Javanmard R, Dokhani A, Khorasani S, & Mozafari MR (2018). Impact of Particle Size and Polydispersity Index on the Clinical Applications of Lipidic Nanocarrier Systems. *Pharmaceutics*, 10.
- Dapito DH, & Schwabe RF (2015). Chapter 9 - Hepatic Stellate Cells and Liver Cancer. In Gandhi CR & Pinzani M (Eds.), *Stellate Cells in Health and Disease* (pp. 145–162). Boston: Academic Press.
- Dhamodharan K, Vengaimaran M, & Sankaran M (2021). Capsaicin Encapsulated Chitosan Nanoparticles Augments Anticarcinogenic and Antiproliferative Competency Against 7,12 Dimethylbenz(a)anthracene Induced Experimental Rat Mammary Carcinogenesis. *Journal of Pharmaceutical Research International*, 33, 126–144.
- Drescher S, & van Hoogevest P (2020). The Phospholipid Research Center: Current Research in Phospholipids and Their Use in Drug Delivery. *Pharmaceutics*, 12, 1235.
- Drewes AM, Schipper KP, Dimcevski G, Petersen P, Gregersen H, Funch-Jensen P, & Arendt-Nielsen L (2003). Gut pain and hyperalgesia induced by capsaicin: a human experimental model. *Pain*, 104, 333–341. [PubMed: 12855343]
- Eek D, Krohe M, Mazar I, Horsfield A, Pompilus F, Friebe R, & Shields AL (2016). Patient-reported preferences for oral versus intravenous administration for the treatment of cancer: a review of the literature. *Patient Prefer Adherence*, 10, 1609–1621. [PubMed: 27601886]
- Efferth T, & Oesch F (2021). Repurposing of plant alkaloids for cancer therapy: Pharmacology and toxicology. *Semin Cancer Biol*, 68, 143–163. [PubMed: 31883912]
- Elkholi I, Hazem N, El-Kahsef W, Sobh M, Shaalan D, Sobh d. m., & El-Sherbiny I (2014). Evaluation of Anti-Cancer Potential of Capsaicin-Loaded Trimethyl Chitosan-Based Nanoparticles in HepG2 Hepatocarcinoma Cells. *Journal of Nanomedicine & Nanotechnology*, 5, article 240.

- Erin N, Boyer PJ, Bonneau RH, Clawson GA, & Welch DR (2004). Capsaicin-mediated denervation of sensory neurons promotes mammary tumor metastasis to lung and heart. *Anticancer Res*, 24, 1003–1009. [PubMed: 15161056]
- Erin N, Zhao W, Bylander J, Chase G, & Clawson G (2006). Capsaicin-induced inactivation of sensory neurons promotes a more aggressive gene expression phenotype in breast cancer cells. *Breast Cancer Res Treat*, 99, 351–364. [PubMed: 16583263]
- Evangelista S (2015). Novel therapeutics in the field of capsaicin and pain. *Expert Rev Clin Pharmacol*, 8, 373–375. [PubMed: 25959004]
- Fattori V, Hohmann MS, Rossaneis AC, Pinho-Ribeiro FA, & Verri WA (2016). Capsaicin: Current Understanding of Its Mechanisms and Therapy of Pain and Other Pre-Clinical and Clinical Uses. *Molecules*, 21.
- Federico C, Alhallak K, Sun J, Duncan K, Azab F, Sudlow GP, de la Puente P, Muz B, Kapoor V, Zhang L, Yuan F, Markovic M, Kotsybar J, Wasden K, Guenther N, Gurley S, King J, Kohnen D, Salama NN, Thotala D, Hallahan DE, Vij R, DiPersio JF, Achilefu S, Azab AK (2020). Tumor microenvironment-targeted nanoparticles loaded with bortezomib and ROCK inhibitor improve efficacy in multiple myeloma. *Nature Communications*, 11, 6037.
- Fernandez M, Javaid F, & Chudasama V (2018). Advances in targeting the folate receptor in the treatment/imaging of cancers. *Chem Sci*, 9, 790–810. [PubMed: 29675145]
- Friedman JR, Richbart SD, Merritt JC, Brown KC, Denning KL, Tirona MT, Valentovic MA, Miles SL, & Dasgupta P (2019). Capsaicinoids: Multiple effects on angiogenesis, invasion and metastasis in human cancers. *Biomed Pharmacother*, 118, 109317. [PubMed: 31404777]
- Friedman JR, Richbart SD, Merritt JC, Perry HE, Brown KC, Akers AT, Nolan NA, Stevenson CD, Hurley JD, Miles SL, Tirona MT, Valentovic MA, & Dasgupta P (2019). Capsaicinoids enhance chemosensitivity to chemotherapeutic drugs. *Adv Cancer Res*, 144, 263–298. [PubMed: 31349900]
- Fujita K, Kubota Y, Ishida H, & Sasaki Y (2015). Irinotecan, a key chemotherapeutic drug for metastatic colorectal cancer. *World J Gastroenterol*, 21, 12234–12248. [PubMed: 26604633]
- Gala UH, Miller DA, & Williams RO (2020). Harnessing the therapeutic potential of anticancer drugs through amorphous solid dispersions. *Biochimica et Biophysica Acta (BBA) - Reviews on Cancer*, 1873, 188319. [PubMed: 31678141]
- Gangadaran P, Hong CM, & Ahn B-C (2018). An Update on in Vivo Imaging of Extracellular Vesicles as Drug Delivery Vehicles. *Frontiers in pharmacology*, 9.
- Gao A, Hu X. I., Saeed M, Chen B. f., Li Y. p., & Yu H. j. (2019). Overview of recent advances in liposomal nanoparticle-based cancer immunotherapy. *Acta Pharmacol Sin*, 40, 1129–1137. [PubMed: 31371782]
- Gao Y, Gao D, Shen J, & Wang Q (2020). A Review of Mesoporous Silica Nanoparticle Delivery Systems in Chemo-Based Combination Cancer Therapies. *Frontiers in Chemistry*, 8.
- Geng ZM, Li QH, Li WZ, Zheng JB, & Shah V (2014). Activated human hepatic stellate cells promote growth of human hepatocellular carcinoma in a subcutaneous xenograft nude mouse model. *Cell Biochem Biophys*, 70, 337–347. [PubMed: 24676678]
- Gheorghe G, Bungau S, Ilie M, Behl T, Vesa CM, Brisc C, Bacalbasa N, Turi V, Costache RS, & Diaconu CC (2020). Early Diagnosis of Pancreatic Cancer: The Key for Survival. *Diagnostics (Basel)*, 10.
- Ghezzi M, Pescina S, Padula C, Santi P, Del Favero E, Cantù L, & Nicoli S (2021). Polymeric micelles in drug delivery: An insight of the techniques for their characterization and assessment in biorelevant conditions. *J Control Release*, 332, 312–336. [PubMed: 33652113]
- Golombek SK, May JN, Theek B, Appold L, Drude N, Kiessling F, & Lammers T (2018). Tumor targeting via EPR: Strategies to enhance patient responses. *Adv Drug Deliv Rev*, 130, 17–38. [PubMed: 30009886]
- Guerin MV, Finisguerra V, Van den Eynde BJ, Bercovici N, & Trautmann A (2020). Preclinical murine tumor models: a structural and functional perspective. *Elife*, 9.
- Gul S, Khan SB, Rehman IU, Khan MA, & Khan MI (2019). A Comprehensive Review of Magnetic Nanomaterials Modern Day Theranostics. *Frontiers in Materials*, 6.

- Hachey DL, Dawling S, Roodi N, & Parl FF (2003). Sequential action of phase I and II enzymes cytochrome p450 1B1 and glutathione S-transferase P1 in mammary estrogen metabolism. *Cancer Res*, 63, 8492–8499. [PubMed: 14679015]
- Hammer J (2006). Effect of repeated capsaicin ingestion on intestinal chemosensation and mechanosensation. *Aliment Pharmacol Ther*, 24, 679–686. [PubMed: 16907900]
- Harris RL, van den Berg CW, & Bowen DJ (2012). ASGR1 and ASGR2, the Genes that Encode the Asialoglycoprotein Receptor (Ashwell Receptor), Are Expressed in Peripheral Blood Monocytes and Show Interindividual Differences in Transcript Profile. *Mol Biol Int*, 2012, 283974. [PubMed: 22919488]
- Hazem MN, ElKashef FW, El-Sherbiny MI, Emam AA, Shaalan D, & Sobh M (2021). Anticarcinogenic Effects of Capsaicin-Loaded Nanoparticles on In vitro Hepatocellular Carcinoma. *Current Chemical Biology*, 15, 188–201.
- Heng L (2021). A feasible strategy of fabricating hybrid drugs encapsulated polymeric nanoparticles for the treatment of gastric cancer therapy. *Process biochemistry*, v. 109, pp. 19–26-2021 v.2109.
- Hirsh V (2018). Turning EGFR mutation-positive non-small-cell lung cancer into a chronic disease: optimal sequential therapy with EGFR tyrosine kinase inhibitors. *Ther Adv Med Oncol*, 10, 1758834017753338-1758834017753338.
- Huang A, Yang X-R, Chung W-Y, Dennison AR, & Zhou J (2020). Targeted therapy for hepatocellular carcinoma. *Signal Transduction and Targeted Therapy*, 5, 146. [PubMed: 32782275]
- Huang K-W, Lai Y-T, Chern G-J, Huang S-F, Tsai C-L, Sung Y-C, Chiang C-C, Hwang P-B, Ho T-L, Huang R-L, Shiue T-Y, Chen Y, & Wang S-K (2018). Galactose Derivative-Modified Nanoparticles for Efficient siRNA Delivery to Hepatocellular Carcinoma. *Biomacromolecules*, 19.
- Huang SP, Chen JC, Wu CC, Chen CT, Tang NY, Ho YT, Lo C, Lin JP, Chung JG, & Lin JG (2009). Capsaicin-induced apoptosis in human hepatoma HepG2 cells. *Anticancer Res*, 29, 165–174. [PubMed: 19331147]
- Hurley JD, Akers AT, Friedman JR, Nolan NA, Brown KC, & Dasgupta P (2017). Non-pungent long chain capsaicin-analogs arvanil and olvanil display better anti-invasive activity than capsaicin in human small cell lung cancers. *Cell Adh Migr*, 11, 80–97. [PubMed: 27196129]
- Hwang MK, Bode AM, Byun S, Song NR, Lee HJ, Lee KW, & Dong Z (2010). Cocarcinogenic effect of capsaicin involves activation of EGFR signaling but not TRPV1. *Cancer Res*, 70, 6859–6869. [PubMed: 20660715]
- Ikedo M, Morizane C, Ueno M, Okusaka T, Ishii H, & Furuse J (2018). Chemotherapy for hepatocellular carcinoma: current status and future perspectives. *Jpn J Clin Oncol*, 48, 103–114. [PubMed: 29253194]
- Jagięła J, Bartnicki P, & Rysz J (2021). Nephrotoxicity as a Complication of Chemotherapy and Immunotherapy in the Treatment of Colorectal Cancer, Melanoma and Non-Small Cell Lung Cancer. *Int J Mol Sci*, 22.
- Jhaveri AM, & Torchilin VP (2014). Multifunctional polymeric micelles for delivery of drugs and siRNA. *Frontiers in pharmacology*, 5, 77–77. [PubMed: 24795633]
- Jiang L, Zhou S, Zhang X, Wu W, & Jiang X (2018). Dendrimer-based nanoparticles in cancer chemotherapy and gene therapy. *Science China Materials*, 61, 1404–1419.
- Jiang Z, Wang X, Zhang Y, Zhao P, Luo Z, & Li J (2015). Effect of Capsaicin-Loading Nanoparticles on Gliomas. *J Nanosci Nanotechnol*, 15, 9834–9839. [PubMed: 26682421]
- Jin J, Lin G, Huang H, Xu D, Yu H, Ma X, Zhu L, Ma D, & Jiang H (2014). Capsaicin mediates cell cycle arrest and apoptosis in human colon cancer cells via stabilizing and activating p53. *International journal of biological sciences*, 10, 285–295. [PubMed: 24643130]
- Johnson ML, Braiteh F, Grilley-Olson JE, Chou J, Davda J, Forgie A, Li R, Jacobs I, Kazazi F, & Hu-Lieskován S (2019). Assessment of Subcutaneous vs Intravenous Administration of Anti-PD-1 Antibody PF-06801591 in Patients With Advanced Solid Tumors: A Phase 1 Dose-Escalation Trial. *JAMA Oncology*, 5, 999–1007. [PubMed: 31145415]
- Juriši V, Obradovic J, Pavlovi S, & Djordjevic N (2018). Epidermal Growth Factor Receptor Gene in Non-Small-Cell Lung Cancer: The Importance of Promoter Polymorphism Investigation. *Analytical Cellular Pathology*, 2018, 6192187.

- Kaiser M, Kirsch B, Hauser H, Schneider D, Seuss-Baum I, & Goycoolea FM (2015). In Vitro and Sensory Evaluation of Capsaicin-Loaded Nanoformulations. *PLoS One*, 10, e0141017. [PubMed: 26492045]
- Kale VP, Amin SG, & Pandey MK (2015). Targeting ion channels for cancer therapy by repurposing the approved drugs. *Biochim Biophys Acta*, 1848, 2747–2755. [PubMed: 25843679]
- Kang H, Rho S, Stiles WR, Hu S, Baek Y, Hwang DW, Kashiwagi S, Kim MS, & Choi HS (2020). Size-Dependent EPR Effect of Polymeric Nanoparticles on Tumor Targeting. *Advanced Healthcare Materials*, 9, 1901223.
- Kang H, Wu Q, Sun A, Liu X, Fan Y, & Deng X (2018). Cancer Cell Glycocalyx and Its Significance in Cancer Progression. *Int J Mol Sci*, 19.
- Kapse A, Anup N, Patel V, Saraogi GK, Mishra D, & Tekade RK (2020). Polymeric micelles: a ray of hope among new drug delivery systems. In.
- Kawada T, & Iwai K (1985). In Vivo and In Vitro Metabolism of Dihydrocapsaicin, a Pungent Principle of Hot Pepper, in Rats. *Agricultural and Biological Chemistry*, 49, 441–448.
- Kawada T, Suzuki T, Takahashi M, & Iwai K (1984). Gastrointestinal absorption and metabolism of capsaicin and dihydrocapsaicin in rats. *Toxicol Appl Pharmacol*, 72, 449–456. [PubMed: 6710495]
- Kazi M, Al-Swairi M, Ahmad A, Raish M, Alanazi FK, Badran MM, Khan AA, Alanazi AM, & Hussain MD (2019). Evaluation of Self-Nanoemulsifying Drug Delivery Systems (SNEDDS) for Poorly Water-Soluble Talinolol: Preparation, in vitro and in vivo Assessment. *Frontiers in pharmacology*, 10.
- Kciuk M, Marciniak B, & Kontek R (2020). Irinotecan-Still an Important Player in Cancer Chemotherapy: A Comprehensive Overview. *Int J Mol Sci*, 21.
- Kerdelhué B, Forest C, & Coumoul X (2016). Dimethyl-Benz(a)anthracene: A mammary carcinogen and a neuroendocrine disruptor. *Biochimie Open*, 3, 49–55. [PubMed: 29450131]
- Khan I, Saeed K, & Khan I (2019). Nanoparticles: Properties, applications and toxicities. *Arabian Journal of Chemistry*, 12, 908–931.
- Kolonko AK, Efung J, González-Espinosa Y, Bangel-Ruland N, van Driessche W, Goycoolea FM, & Weber WM (2020). Capsaicin-Loaded Chitosan Nanocapsules for wtCFTR-mRNA Delivery to a Cystic Fibrosis Cell Line. *Biomedicines*, 8.
- Kuerbitz SJ, & Henderson MB (2020). Osteosarcoma: A review with emphasis on pathogenesis and chemoresistance. *Medical Research Archives; Vol 8 No 7 (2020): Vol.8 Issue 7, July, 2020*.
- Kunjiappan S, Sankaranarayanan M, Karan Kumar B, Pavadai P, Babkiewicz E, Maszczyk P, Glodkowska-Mrowka E, Arunachalam S, Ram Kumar Pandian S, Ravishankar V, Baskararaj S, Vellaichamy S, Arulmani L, & Panneerselvam T (2021). Capsaicin-loaded solid lipid nanoparticles: design, biodistribution, in silico modeling and in vitro cytotoxicity evaluation. *Nanotechnology*, 32, 095101. [PubMed: 33113518]
- Lan Y, Sun Y, Yang T, Ma X, Cao M, Liu L, Yu S, Cao A, & Liu Y (2019). Co-Delivery of Paclitaxel by a Capsaicin Prodrug Micelle Facilitating for Combination Therapy on Breast Cancer. *Mol Pharm*, 16, 3430–3440. [PubMed: 31199661]
- Laurent S, Forge D, Port M, Roch A, Robic C, Vander Elst L, & Muller RN (2010). Magnetic Iron Oxide Nanoparticles: Synthesis, Stabilization, Vectorization, Physicochemical Characterizations, and Biological Applications. *Chemical Reviews*, 110, 2574–2574.
- Lee S-H, & Clark R (2016). Anti-Tumorigenic Effects of Capsaicin in Colon Cancer. *Journal of Food Chemistry and Nanotechnology*, 2.
- LePage KT, Dickey RW, Gerwick WH, Jester EL, & Murray TF (2005). On the use of neuro-2a neuroblastoma cells versus intact neurons in primary culture for neurotoxicity studies. *Crit Rev Neurobiol*, 17, 27–50. [PubMed: 16307526]
- Li J, Wang X, Zhang T, Wang C, Huang Z, Luo X, & Deng Y (2014). A review on phospholipids and their main applications in drug delivery systems. *Asian Journal of Pharmaceutical Sciences*, 10.
- Li L, Chen C, Chiang C, Xiao T, Chen Y, Zhao Y, & Zheng D (2021). The Impact of TRPV1 on Cancer Pathogenesis and Therapy: A Systematic Review. *International journal of biological sciences*, 17, 2034–2049. [PubMed: 34131404]

- Liao J, Han R, Wu Y, & Qian Z (2021). Review of a new bone tumor therapy strategy based on bifunctional biomaterials. *Bone Res*, 9, 18. [PubMed: 33727543]
- Liao X, Bu Y, Chang F, Jia F, Song G, Xiao X, Zhang M, Ning P, & Jia Q (2019). Remodeling of hepatic stellate cells orchestrated the stroma-derived oxaliplatin-resistance through CCN3 paracrine in hepatocellular carcinoma. *BMC Cancer*, 19, 1192. [PubMed: 31805888]
- Lim JS, Kim DH, Lee JA, Kim DH, Cho J, Cho WH, Lee SY, & Jeon DG (2013). Young age at diagnosis, male sex, and decreased lean mass are risk factors of osteoporosis in long-term survivors of osteosarcoma. *J Pediatr Hematol Oncol*, 35, 54–60. [PubMed: 23128330]
- Lin YT, Wang HC, Hsu YC, Cho CL, Yang MY, & Chien CY (2017). Capsaicin Induces Autophagy and Apoptosis in Human Nasopharyngeal Carcinoma Cells by Downregulating the PI3K/AKT/mTOR Pathway. *Int J Mol Sci*, 18.
- Liu H, & Wu D (2016). In vivo Near-infrared Fluorescence Tumor Imaging Using DiR-loaded Nanocarriers. *Curr Drug Deliv*, 13, 40–48. [PubMed: 26138681]
- Lu Y, Zhang E, Yang J, & Cao Z (2018). Strategies to improve micelle stability for drug delivery. *Nano Res*, 11, 4985–4998. [PubMed: 30370014]
- Luo H, & Shusta EV (2020). Blood-Brain Barrier Modulation to Improve Glioma Drug Delivery. *Pharmaceutics*, 12.
- Lv L, Zhuang YX, Zhang HW, Tian NN, Dang WZ, & Wu SY (2017). Capsaicin-loaded folic acid-conjugated lipid nanoparticles for enhanced therapeutic efficacy in ovarian cancers. *Biomed Pharmacother*, 91, 999–1005. [PubMed: 28525949]
- Ma H, Xie L, Zhang L, Yin X, Jiang H, Xie X, Chen R, Lu H, & Ren Z (2018). Activated hepatic stellate cells promote epithelial-to-mesenchymal transition in hepatocellular carcinoma through transglutaminase 2-induced pseudohypoxia. *Commun Biol*, 1, 168. [PubMed: 30393774]
- Majumder N, N GD, & Das SK (2020). Polymeric micelles for anticancer drug delivery. *Ther Deliv*, 11, 613–635. [PubMed: 32933425]
- Malar C, & Bavanilathamuthiah. (2015). Dendrosomal capsaicin nanoformulation for the invitro anti-cancer effect on HEP 2 and MCF - 7 cell lines. *International journal on applied bioengineering*, 9, 30–35.
- Maruyama K (2011). Intracellular targeting delivery of liposomal drugs to solid tumors based on EPR effects. *Adv Drug Deliv Rev*, 63, 161–169. [PubMed: 20869415]
- Mehanna MM, & Mneimneh AT (2021). Formulation and Applications of Lipid-Based Nanovehicles: Spotlight on Self-emulsifying Systems. *Adv Pharm Bull*, 11, 56–67. [PubMed: 33747852]
- Meirson T, Gil-Henn H, & Samson AO (2020). Invasion and metastasis: the elusive hallmark of cancer. *Oncogene*, 39, 2024–2026. [PubMed: 31745295]
- Merchant N, Nagaraju GP, Rajitha B, Lammata S, Jella KK, Buchwald ZS, Lakka SS, & Ali AN (2017). Matrix metalloproteinases: their functional role in lung cancer. *Carcinogenesis*, 38, 766–780. [PubMed: 28637319]
- Merouani A, Davidson SA, & Schrier RW (1997). Increased nephrotoxicity of combination taxol and cisplatin chemotherapy in gynecologic cancers as compared to cisplatin alone. *Am J Nephrol*, 17, 53–58. [PubMed: 9057954]
- Michael M, & Doherty MM (2005). Tumoral Drug Metabolism: Overview and Its Implications for Cancer Therapy. *Journal of Clinical Oncology*, 23, 205–229. [PubMed: 15625375]
- Midhun DE (2016). Early detection of lung cancer. *F1000Res*, 5.
- Min JK, Han KY, Kim EC, Kim YM, Lee SW, Kim OH, Kim KW, Gho YS, & Kwon YG (2004). Capsaicin inhibits in vitro and in vivo angiogenesis. *Cancer Res*, 64, 644–651. [PubMed: 14744780]
- Mirzavi F, Barati M, Soleimani A, Vakili-Ghartavol R, Jaafari MR, & Soukhtanloo M (2021). A review on liposome-based therapeutic approaches against malignant melanoma. *International Journal of Pharmaceutics*, 599, 120413. [PubMed: 33667562]
- Misaghi A, Goldin A, Awad M, & Kulidjian AA (2018). Osteosarcoma: a comprehensive review. *Sicot j*, 4, 12. [PubMed: 29629690]
- Molinaro AM, Taylor JW, Wiencke JK, & Wrensch MR (2019). Genetic and molecular epidemiology of adult diffuse glioma. *Nature Reviews Neurology*, 15, 405–417. [PubMed: 31227792]

- Mondal R, Bobde Y, Ghosh B, & Giri T (2019). Development and Characterization of a Phospholipid Complex for Effective Delivery of Capsaicin. *Indian Journal of Pharmaceutical Sciences*, 81.
- Mudshinge SR, Deore AB, Patil S, & Bhalgat CM (2011). Nanoparticles: Emerging carriers for drug delivery. *Saudi pharmaceutical journal : SPJ : the official publication of the Saudi Pharmaceutical Society*, 19, 129–141. [PubMed: 23960751]
- Najafi F, Salami-Kalajahi M, & Roghani-Mamaqani H (2021). A review on synthesis and applications of dendrimers. *Journal of the Iranian Chemical Society*, 18, 503–517.
- Nigam K, Gabrani R, & Dang S (2019). Nano-emulsion from Capsaicin: Formulation and Characterization. *Materials Today: Proceedings*, 18, 869–878.
- Nigam P, Waghmode S, Yeware A, Nawale L, Dagde P, Dhudhane A, & Sarkar D (2014). Aptamer Functionalized Multifunctional Fluorescent Nanotheranostic Platform for Pancreatic Cancer. *Journal of Nanopharmaceutics and Drug Delivery*, 2, 280–287.
- Nikzamir M, Hanifehpour Y, Akbarzadeh A, & Panahi Y (2021). Applications of Dendrimers in Nanomedicine and Drug Delivery: A Review. *Journal of Inorganic and Organometallic Polymers and Materials*, 31, 2246–2261.
- Nisini R, Poerio N, Mariotti S, De Santis F, & Fraziano M (2018). The Multirole of Liposomes in Therapy and Prevention of Infectious Diseases. *Frontiers in Immunology*, 9.
- Nomani S, & Govinda J (2016). Nanoliposome: An alternative approach for drug delivery system. *International Journal of Advances in Pharmacy Medicine and Bioallied Sciences*, 2016, 1–10.
- O'Neill J, Brock C, Olesen AE, Andresen T, Nilsson M, & Dickenson AH (2012). Unravelling the mystery of capsaicin: a tool to understand and treat pain. *Pharmacological reviews*, 64, 939–971. [PubMed: 23023032]
- Oliveira V. d. S., de Almeida AS, Albuquerque I. d. S., Duarte FÍC, Queiroz BCSH, Converti A, & Lima Á. A. N. d. (2020). Therapeutic Applications of Solid Dispersions for Drugs and New Molecules: In Vitro and In Vivo Activities. *Pharmaceutics*, 12, 933.
- Ong SG, Ming LC, Lee KS, & Yuen KH (2016). Influence of the Encapsulation Efficiency and Size of Liposome on the Oral Bioavailability of Griseofulvin-Loaded Liposomes. *Pharmaceutics*, 8.
- Pandey H, Rani R, & Aggarwal V (2016). Liposome and their applications in Cancer Therapy. *Brazilian Arch Biol Tech*, 59, 2–9.
- Parashar P, Tripathi CB, Arya M, Kanoujia J, Singh M, Yadav A, Kaithwas G, & Saraf SA (2019). A synergistic approach for management of lung carcinoma through folic acid functionalized co-therapy of capsaicin and gefitinib nanoparticles: Enhanced apoptosis and metalloproteinase-9 down-regulation. *Phytomedicine*, 53, 107–123. [PubMed: 30668390]
- Parashar P, Tripathi CB, Arya M, Kanoujia J, Singh M, Yadav A, & Saraf SA (2019). A facile approach for fabricating CD44-targeted delivery of hyaluronic acid-functionalized PCL nanoparticles in urethane-induced lung cancer: Bcl-2, MMP-9, caspase-9, and BAX as potential markers. *Drug Delivery and Translational Research*, 9, 37–52. [PubMed: 30178279]
- Parikh ND, Mehta AS, Singal AG, Block T, Marrero JA, & Lok AS (2020). Biomarkers for the Early Detection of Hepatocellular Carcinoma. *Cancer Epidemiol Biomarkers Prev*, 29, 2495–2503. [PubMed: 32238405]
- Park JY, Hiroshima Y, Lee JY, Maawy AA, Hoffman RM, & Bouvet M (2015). MUC1 selectively targets human pancreatic cancer in orthotopic nude mouse models. *PLoS One*, 10, e0122100. [PubMed: 25815753]
- Pawar HR, Bhosale SS, & Derle ND (2021). USE OF LIPOSOMES IN CANCER THERAPY: A REVIEW. *Intl Journal Pharm Sci Res*, 3, 3585–3590.
- Peng D, Sun J, Wang Y, Tian J, Zhang Y, Noteborn M, & Qu S (2007). Inhibition of hepatocarcinoma by systemic delivery of Apoptin gene via the hepatic asialoglycoprotein receptor. *Cancer Gene Therapy*, 14, 66–73. [PubMed: 16874360]
- Peng W, Jiang XY, Zhu Y, Omari-Siaw E, Deng WW, Yu JN, Xu XM, & Zhang WM (2015). Oral delivery of capsaicin using MPEG-PCL nanoparticles. *Acta Pharmacol Sin*, 36, 139–148. [PubMed: 25434988]
- Petrarca C, Poma AM, Vecchiotti G, Bernardini G, Niu Q, Cattaneo AG, Gioacchino MD, & Sabbioni E (2020). Cobalt magnetic nanoparticles as theranostics: Conceivable or forgettable? *Nanotechnology Reviews*, 9, 1522–1538.

- Puri A, Loomis K, Smith B, Lee JH, Yavlovich A, Heldman E, & Blumenthal R (2009). Lipid-based nanoparticles as pharmaceutical drug carriers: from concepts to clinic. *Crit Rev Ther Drug Carrier Syst*, 26, 523–580. [PubMed: 20402623]
- Pyun BJ, Choi S, Lee Y, Kim TW, Min JK, Kim Y, Kim BD, Kim JH, Kim TY, Kim YM, & Kwon YG (2008). Capsiate, a nonpungent capsaicin-like compound, inhibits angiogenesis and vascular permeability via a direct inhibition of Src kinase activity. *Cancer Res*, 68, 227–235. [PubMed: 18172315]
- Qi C, Wang D, Gong X, Zhou Q, Yue X, Li C, Li Z, Tian G, Zhang B, Wang Q, Wei X, & Wu J (2021). Co-Delivery of Curcumin and Capsaicin by Dual-Targeting Liposomes for Inhibition of aHSC-Induced Drug Resistance and Metastasis. *ACS Applied Materials & Interfaces*, 13, 16019–16035. [PubMed: 33819006]
- Quintero-Fabián S, Arreola R, Becerril-Villanueva E, Torres-Romero JC, Arana-Argáez V, Lara-Riegos J, Ramírez-Camacho MA, & Alvarez-Sánchez ME (2019). Role of Matrix Metalloproteinases in Angiogenesis and Cancer. *Frontiers in Oncology*, 9.
- Rabah SO (2010). Acute Taxol nephrotoxicity: Histological and ultrastructural studies of mice kidney parenchyma. *Saudi J Biol Sci*, 17, 105–114. [PubMed: 23961065]
- Rabiee N, & Rabiee M (2019). A promising Stimuli-Responsive nanocomposite as a Theranostic agent for Targeted Delivery. *Journal of Bioengineering Research*, 1, 27–36.
- Rajan M, murugan s., Alyahya S, Alharbi N, Km S, & Kumar S (2017). Development of self-repair Nano-rod scaffold materials for Implantation of Osteosarcoma affected Bone Tissue. *New Journal of Chemistry*, 42.
- Ramos-Torres Á, Bort A, Morell C, Rodríguez-Henche N, & Díaz-Laviada I (2016). The pepper's natural ingredient capsaicin induces autophagy blockage in prostate cancer cells. *Oncotarget*, 7, 1569–1583. [PubMed: 26625315]
- Rasmussen MK, Pedersen JN, & Marie R (2020). Size and surface charge characterization of nanoparticles with a salt gradient. *Nature Communications*, 11, 2337.
- Ren WX, Han J, Uhm S, Jang YJ, Kang C, Kim JH, & Kim JS (2015). Recent development of biotin conjugation in biological imaging, sensing, and target delivery. *Chem Commun (Camb)*, 51, 10403–10418. [PubMed: 26021457]
- Reyes-Escogido Mde L, Gonzalez-Mondragon EG, & Vazquez-Tzompantzi E (2011). Chemical and pharmacological aspects of capsaicin. *Molecules*, 16, 1253–1270. [PubMed: 21278678]
- Roggenbuck D, Mytilinaiou MG, Lapin SV, Reinhold D, & Conrad K (2012). Asialoglycoprotein receptor (ASGPR): a peculiar target of liver-specific autoimmunity. *Auto Immun Highlights*, 3, 119–125. [PubMed: 26000135]
- Rollyson WD, Stover CA, Brown KC, Perry HE, Stevenson CD, McNees CA, Ball JG, Valentovic MA, & Dasgupta P (2014). Bioavailability of capsaicin and its implications for drug delivery. *J Control Release*, 196, 96–105. [PubMed: 25307998]
- Sahin IH, & Kloostergaard J (2015). CD44 as a drug delivery target in human cancers: where are we now? *Expert Opin Ther Targets*, 19, 1587–1591. [PubMed: 26374284]
- Scaranti M, Cojocaru E, Banerjee S, & Banerji U (2020). Exploiting the folate receptor alpha in oncology. *Nat Rev Clin Oncol*, 17, 349–359. [PubMed: 32152484]
- Schlatter J, & Lutz WK (1990). The carcinogenic potential of ethyl carbamate (urethane): Risk assessment at human dietary exposure levels. *Food and Chemical Toxicology*, 28, 205–211. [PubMed: 2188890]
- Semalty A (2014). Cyclodextrin and phospholipid complexation in solubility and dissolution enhancement: a critical and meta-analysis. *Expert Opinion on Drug Delivery*, 11, 1255–1272. [PubMed: 24909802]
- Semalty A, Semalty M, Singh D, & Rawat MSM (2010). Preparation and characterization of phospholipid complexes of naringenin for effective drug delivery. *Journal of Inclusion Phenomena and Macrocyclic Chemistry*, 67, 253–260.
- Shi B, Abrams M, & Sepp-Lorenzino L (2013). Expression of asialoglycoprotein receptor 1 in human hepatocellular carcinoma. *J Histochem Cytochem*, 61, 901–909. [PubMed: 23979840]
- Smith MC, Crist RM, Clogston JD, & McNeil SE (2017). Zeta potential: a case study of cationic, anionic, and neutral liposomes. *Anal Bioanal Chem*, 409, 5779–5787. [PubMed: 28762066]

- Song X, Wang S, Zhao C, Zhang W, Wang G, & Jia S (2019). Visual method for evaluating liver function: targeted in vivo fluorescence imaging of the asialoglycoprotein receptor. *Biomedical optics express*, 10, 5015–5024. [PubMed: 31646026]
- Song Y, Kim SH, Kim KM, Choi EK, Kim J, & Seo HR (2016). Activated hepatic stellate cells play pivotal roles in hepatocellular carcinoma cell chemoresistance and migration in multicellular tumor spheroids. *Sci Rep*, 6, 36750. [PubMed: 27853186]
- Srinivasan K (2016). Biological Activities of Red Pepper (*Capsicum annum*) and Its Pungent Principle Capsaicin: A Review. *Crit Rev Food Sci Nutr*, 56, 1488–1500. [PubMed: 25675368]
- Stock K, Kumar J, Synowitz M, Petrosino S, Imperatore R, Smith ES, Wend P, Purfurst B, Nuber UA, Gurok U, Matyash V, Walzlein JH, Chirasani SR, Dittmar G, Cravatt BF, Momma S, Lewin GR, Ligresti A, De Petrocellis L, Cristino L, Di Marzo V, Kettenmann H, & Glass R (2012). Neural precursor cells induce cell death of high-grade astrocytomas through stimulation of TRPV1. *Nat Med*, 18, 1232–1238. [PubMed: 22820645]
- Stuart KE (2021). Systemic treatment for advanced hepatocellular carcinoma. UpToDate.
- Sun Q, Wu J, Jin L, Hong L, Wang F, Mao Z, & Wu M (2020). Cancer cell membrane-coated gold nanorods for photothermal therapy and radiotherapy on oral squamous cancer. *J Mater Chem B*, 8, 7253–7263. [PubMed: 32638824]
- Sutradhar KB, & Amin ML (2013). Nanoemulsions: increasing possibilities in drug delivery. *European Journal of Nanomedicine*, 5, 97–110.
- Tarbell JM, & Cancel LM (2016). The glycocalyx and its significance in human medicine. *J Intern Med*, 280, 97–113. [PubMed: 26749537]
- Tavaluc RT, Hart LS, Dicker DT, & El-Deiry WS (2007). Effects of low confluency, serum starvation and hypoxia on the side population of cancer cell lines. *Cell Cycle*, 6, 2554–2562. [PubMed: 17912032]
- Telange DR, Patil AT, Pethe AM, Fegade H, Anand S, & Dave VS (2017). Formulation and characterization of an apigenin-phospholipid phytosome (APLC) for improved solubility, in vivo bioavailability, and antioxidant potential. *Eur J Pharm Sci*, 108, 36–49. [PubMed: 27939619]
- Toth B, & Gannett P (1992). Carcinogenicity of lifelong administration of capsaicin of hot pepper in mice. *In Vivo*, 6, 59–63. [PubMed: 1627743]
- Toth B, Rogan E, & Walker B (1984). Tumorigenicity and mutagenicity studies with capsaicin of hot peppers. *Anticancer Res*, 4, 117–119. [PubMed: 6380397]
- Tran P, Pyo Y-C, Kim D-H, Lee S-E, Kim J-K, & Park J-S (2019). Overview of the Manufacturing Methods of Solid Dispersion Technology for Improving the Solubility of Poorly Water-Soluble Drugs and Application to Anticancer Drugs. *Pharmaceutics*, 11, 132.
- Tripodo G, Mandracchia D, Collina S, Rui M, & Rossi D (2014). New Perspectives in Cancer Therapy: The Biotin-Antitumor Molecule Conjugates. *Medicinal Chemistry* 2161–0444, S1, 1–8.
- Turgut C, Zhang Newby B. m., & Cutright T (2004). Determination of optimal water solubility of capsaicin for its usage as a non-toxic antifoulant. *Environmental science and pollution research international*, 11, 7–10. [PubMed: 15005134]
- Uceyler N, & Sommer C (2014). High-Dose Capsaicin for the Treatment of Neuropathic Pain: What We Know and What We Need to Know. *Pain Ther*, 3, 73–84. [PubMed: 25069571]
- Ullmann K, Leneweit G, & Nirschl H (2021). How to Achieve High Encapsulation Efficiencies for Macromolecular and Sensitive APIs in Liposomes. *Pharmaceutics*, 13.
- Vallet-Regí M, Colilla M, Izquierdo-Barba I, & Manzano M (2017). Mesoporous Silica Nanoparticles for Drug Delivery: Current Insights. *Molecules*, 23.
- Vasan N, Baselga J, & Hyman DM (2019). A view on drug resistance in cancer. *Nature*, 575, 299–309. [PubMed: 31723286]
- Venier NA, Yamamoto T, Sugar LM, Adomat H, Fleshner NE, Klotz LH, & Venkateswaran V (2015). Capsaicin reduces the metastatic burden in the transgenic adenocarcinoma of the mouse prostate model. *Prostate*, 75, 1300–1311. [PubMed: 26047020]
- Vercelli C, Barbero R, Cuniberti B, Odore R, & Re G (2015). Expression and functionality of TRPV1 receptor in human MCF-7 and canine CF.41 cells. *Vet Comp Oncol*, 13, 133–142. [PubMed: 23510405]

- Verma DD, Verma S, Blume G, & Fahr A (2003). Particle size of liposomes influences dermal delivery of substances into skin. *Int J Pharm*, 258, 141–151. [PubMed: 12753761]
- Viallon J, Chinain M, & Darius HT (2020). Revisiting the Neuroblastoma Cell-Based Assay (CBA-N2a) for the Improved Detection of Marine Toxins Active on Voltage Gated Sodium Channels (VGSCs). *Toxins (Basel)*, 12.
- Vines JB, Yoon JH, Ryu NE, Lim DJ, & Park H (2019). Gold Nanoparticles for Photothermal Cancer Therapy. *Front Chem*, 7, 167. [PubMed: 31024882]
- Vinothini K, Rajendran NK, Munusamy MA, Alarfaj AA, & Rajan M (2019). Development of biotin molecule targeted cancer cell drug delivery of doxorubicin loaded kappa-carrageenan grafted graphene oxide nanocarrier. *Mater Sci Eng C Mater Biol Appl*, 100, 676–687. [PubMed: 30948104]
- von Palubitzki L, Wang Y, Hoffmann S, Vidal YSS, Zobiak B, Failla AV, Schmage P, John A, Osorio-Madrado A, Bauer AT, Schneider SW, Goycoolea FM, & Gorzelanny C (2020). Differences of the tumour cell glycocalyx affect binding of capsaicin-loaded chitosan nanocapsules. *Sci Rep*, 10, 22443. [PubMed: 33384430]
- Waghray D, & Zhang Q (2018). Inhibit or Evade Multidrug Resistance P-Glycoprotein in Cancer Treatment. *Journal of Medicinal Chemistry*, 61, 5108–5121. [PubMed: 29251920]
- Wang L, Chen Q, Wan J, Wu J, Zhou L, Wang H, Zhao L, Yu Z, & Wang H (2017). Self-Emulsifying Hydrophobic Prodrug Conjugate That Enables the Oral Co-Administration and Programmable Release of Dual Antitumor Drugs. *Journal of Biomedical Nanotechnology*, 13, 1260–1271.
- Wang N, Zhu C. r., Zhang X, Zhai X. j., & Lu Y. n. (2018). Food drug interactions involving multiple mechanisms: A case study with effect of Capsaicin on the pharmacokinetics of Irinotecan and its main metabolites in rat. *Journal of Functional Foods*, 40, 292–298.
- Wang XR, Gao SQ, Niu XQ, Li LJ, Ying XY, Hu ZJ, & Gao JQ (2017). Capsaicin-loaded nanolipoidal carriers for topical application: design, characterization, and in vitro/in vivo evaluation. *Int J Nanomedicine*, 12, 3881–3898. [PubMed: 28579775]
- Weller M, Wick W, Aldape K, Brada M, Berger M, Pfister SM, Nishikawa R, Rosenthal M, Wen PY, Stupp R, & Reifenberger G (2015). Glioma. *Nature Reviews Disease Primers*, 1, 15017.
- Weng J, Tong HHY, & Chow SF (2020). In Vitro Release Study of the Polymeric Drug Nanoparticles: Development and Validation of a Novel Method. *Pharmaceutics*, 12.
- Wittekind C, & Neid M (2005). Cancer invasion and metastasis. *Oncology*, 69 Suppl 1, 14–16. [PubMed: 16210871]
- Wu M, Miao H, Fu R, Zhang J, & Zheng W (2020). Hepatic Stellate Cell: A Potential Target for Hepatocellular Carcinoma. *Curr Mol Pharmacol*, 13, 261–272. [PubMed: 32091349]
- Xu H, Niu M, Yuan X, Wu K, & Liu A (2020). CD44 as a tumor biomarker and therapeutic target. *Exp Hematol Oncol*, 9, 36. [PubMed: 33303029]
- Xu Z-C, Shen H-X, Chen C, Ma L, Li W-Z, Wang L, & Geng Z-M (2018). Neupilin-1 promotes primary liver cancer progression by potentiating the activity of hepatic stellate cells. *Oncology letters*, 15, 2245–2251. [PubMed: 29434931]
- Yang J, Li TZ, Xu GH, Luo BB, Chen YX, & Zhang T (2013). Low-concentration capsaicin promotes colorectal cancer metastasis by triggering ROS production and modulating Akt/mTOR and STAT-3 pathways. *Neoplasia*, 60, 364–372. [PubMed: 23581408]
- Yhee JY, Son S, Son S, Joo MK, & Kwon IC (2013). The EPR Effect in Cancer Therapy. In Bae YH, Mersny RJ & Park K (Eds.), *Cancer Targeted Drug Delivery: An Elusive Dream* (pp. 621–632). New York, NY: Springer New York.
- Yu T, Tong L, Ao Y, Zhang G, Liu Y, & Zhang H (2019). Novel design of NIR-triggered plasmonic nanodots capped mesoporous silica nanoparticles loaded with natural capsaicin to inhibition of metastasis of human papillary thyroid carcinoma B-CPAP cells in thyroid cancer chemophotothermal therapy. *J Photochem Photobiol B*, 197, 111534. [PubMed: 31279897]
- Zhang M, Gao S, Yang D, Fang Y, Lin X, Jin X, Liu Y, Liu X, Su K, & Shi K (2021). Influencing factors and strategies of enhancing nanoparticles into tumors in vivo. *Acta Pharmaceutica Sinica B*, 11, 2265–2285. [PubMed: 34522587]
- Zhang S, Wang D, Huang J, Hu Y, & Xu Y (2020). Application of capsaicin as a potential new therapeutic drug in human cancers. *J Clin Pharm Ther*, 45, 16–28. [PubMed: 31545523]

- Zhang YR, Lin R, Li HJ, He WL, Du JZ, & Wang J (2019). Strategies to improve tumor penetration of nanomedicines through nanoparticle design. *Wiley Interdiscip Rev Nanomed Nanobiotechnol*, 11, e1519. [PubMed: 29659166]
- Zhang Z, Wang H, Tan T, Li J, Wang Z, & Li Y (2018). Rational Design of Nanoparticles with Deep Tumor Penetration for Effective Treatment of Tumor Metastasis. *Advanced Functional Materials*, 28, 1801840.
- Zhao X, Wu Q, Gong X, Liu J, & Ma Y (2021). Osteosarcoma: a review of current and future therapeutic approaches. *BioMedical Engineering OnLine*, 20, 24. [PubMed: 33653371]
- Zhu Y, Zhang J, Zheng Q, Wang M, Deng W, Li Q, Firempong CK, Wang S, Tong S, Xu X, & Yu J (2015). In vitro and in vivo evaluation of capsaicin-loaded microemulsion for enhanced oral bioavailability. *J Sci Food Agric*, 95, 2678–2685. [PubMed: 25400282]
- Zieli ska A, Carreiró F, Oliveira AM, Neves A, Pires B, Venkatesh DN, Durazzo A, Lucarini M, Eder P, Silva AM, Santini A, & Souto EB (2020). Polymeric Nanoparticles: Production, Characterization, Toxicology and Ecotoxicology. *Molecules*, 25.
- Zong Q, Dong N, Yang X, Ling G, & Zhang P (2021). Development of gold nanorods for cancer treatment. *J Inorg Biochem*, 220, 111458. [PubMed: 33857697]
- Zwicke GL, Mansoori GA, & Jeffery CJ (2012). Utilizing the folate receptor for active targeting of cancer nanotherapeutics. *Nano Rev*, 3.

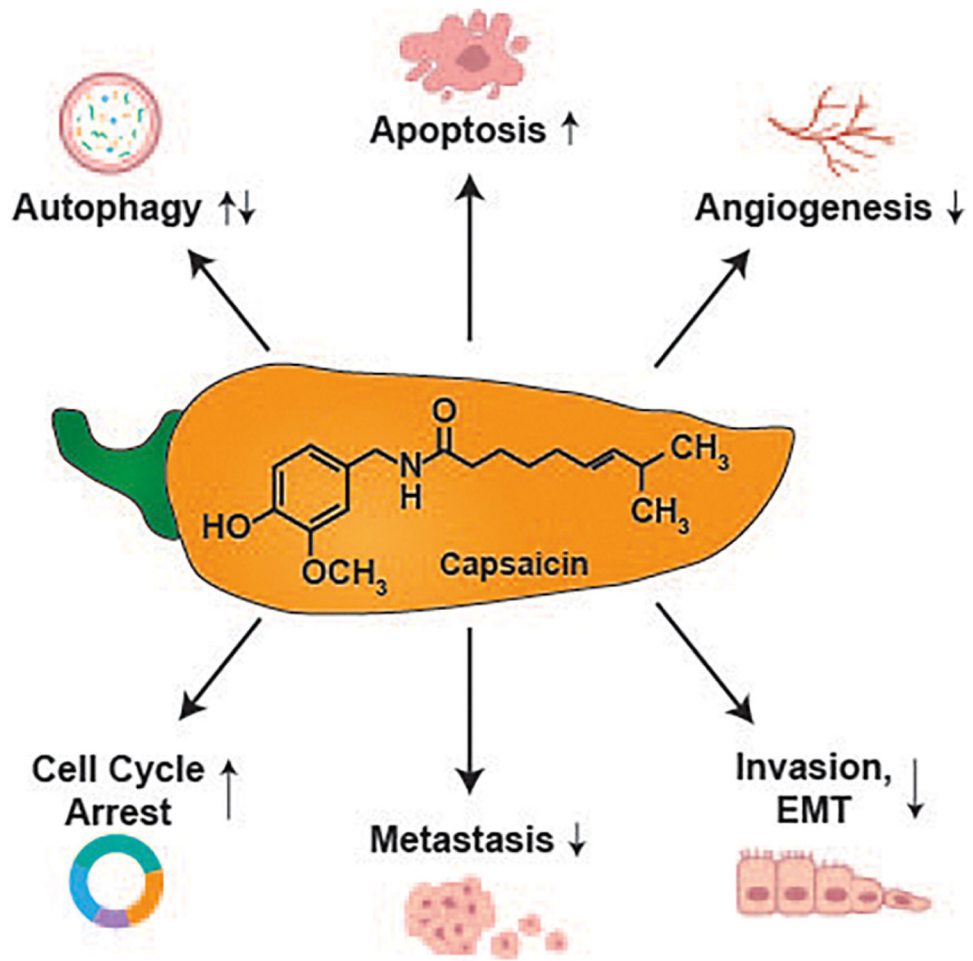


**Figure 1.**  
Molecular mechanisms underlying the anti-cancer activity of capsaicin

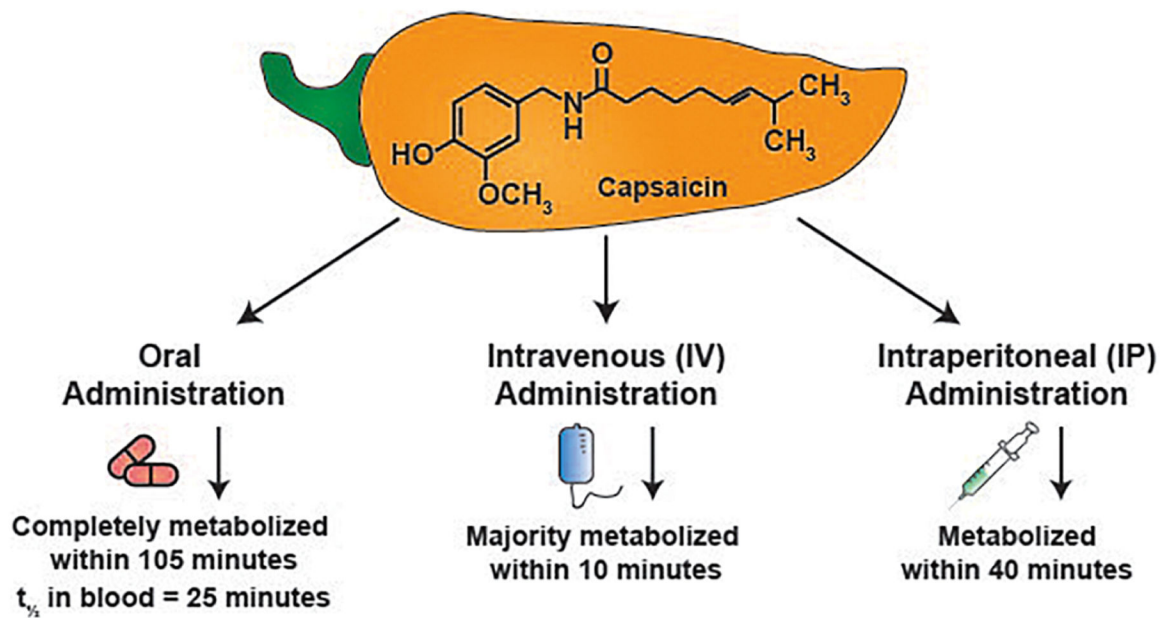


**Figure 2.**  
The biological half-life of capsaicin upon oral, intravenous and intraperitoneal administration in rodents and humans

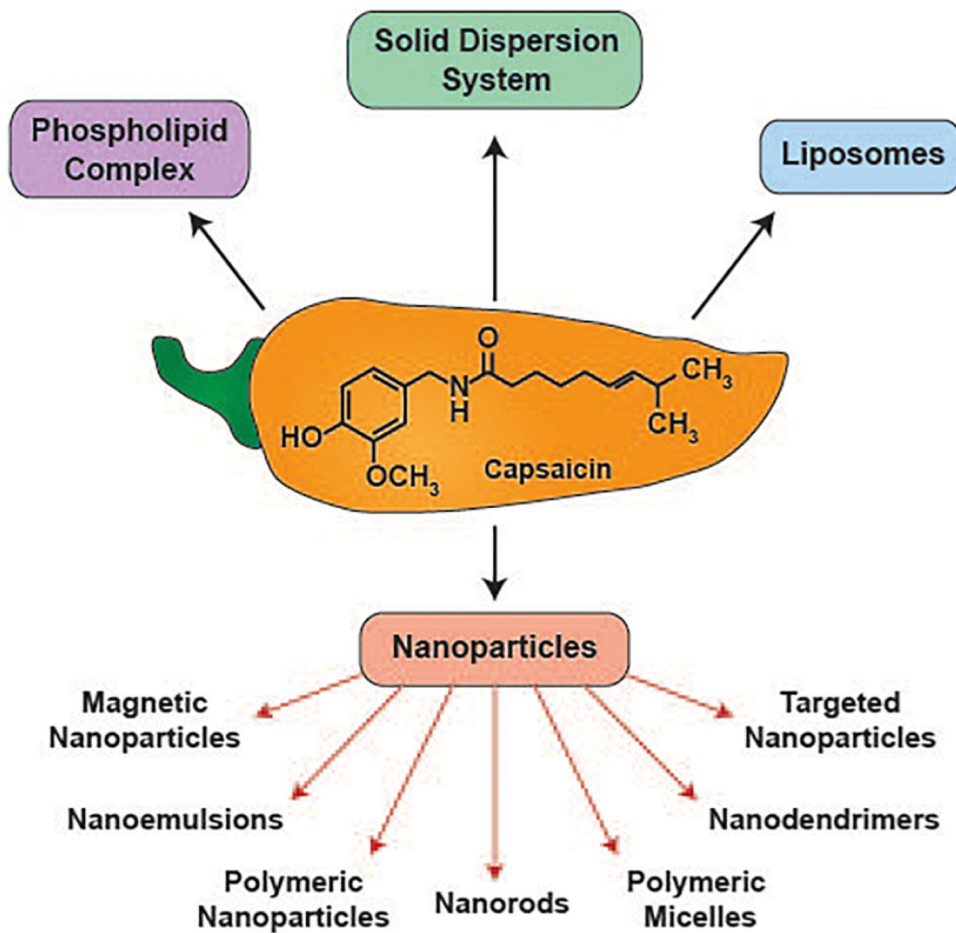


**Figure 3.** Sustained release formulations of capsaicin explored for their growth-suppressive activity in human cancers

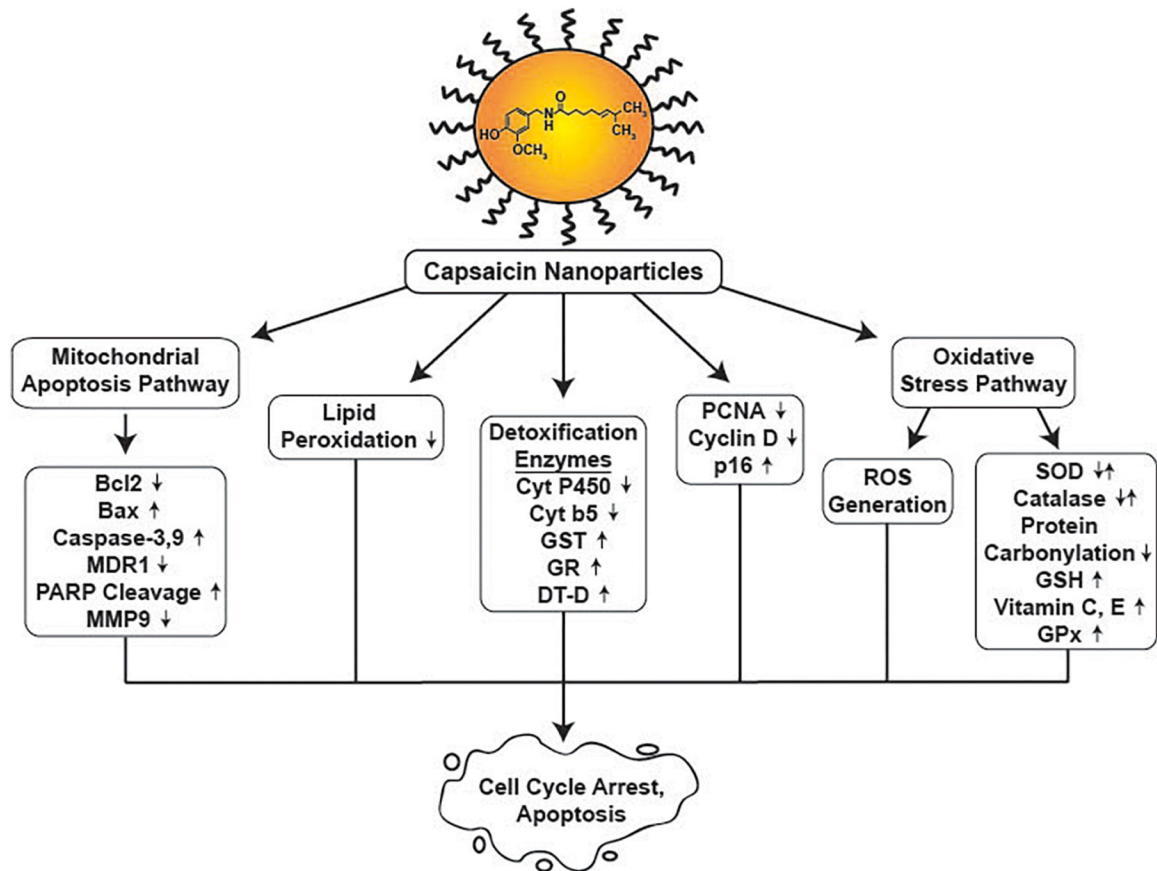


**Figure 4.** Signaling pathways underlying the growth-inhibitory activity of capsaicin nanoparticles

**Table 1:**

Physicochemical properties of capsaicin sustained release drugs

Name of drug	Type of sustained release formulation	Composition of sustained release formulation	Method of synthesis	Nature of the sustained release drug particles	Size (nm)	Poly dispersity index	Zeta potential (mV)	Drug loading efficiency (%)	Drug entrapment efficiency (%)	Stability
CAP-UREA-SDDDS	Solid State dispersion system	Urea scaffold	Solvent evaporation method	Amorphous paper	ND	ND	ND	ND	ND	Up to 8 days
CAP-SOY-PL	Phospholipid complexes	Soyabean phospholipids	Solvent evaporation method	Amorphous droplets	ND	ND	ND	ND	ND	Up to 30 hours
CAP-CUR-GLY-GAL-LIPO	Liposome	DSPE-PEG	Thin film evaporation method	Spherical droplets	138.9 ± 2.9	0.17±0.01	-38.8±6.3	2.0±0.05	89.9 ± 0.1	Up to 13 days
CAP-CUR-GLY- LIPO	Liposome	DSPE-PEG	Thin film evaporation method	Spherical droplets	143.5 ± 3.25	0.15±0.01	-47.3±3.2	2.1±0.02	93.5 ± 1.4	Up to 13 days
CAP-CUR-GAL-LIPO	Liposome	DSPE-PEG	Thin film evaporation method	Spherical droplets	140.9 ± 3.8	0.18±0.02	-43.9±2.3	2.2±0.03	95.8 ± 1.6	Up to 13 days
CAP-CUR-LIPO	Liposome	DSPE-PEG	Thin film evaporation method	Spherical droplets	148.7± 3.4	0.16±0.03	-55.9±3.2	2.1±0.07	90.3 ± 3.8	Up to 13 days

Table 2:

Drug release and biodistribution properties of capsaicin sustained release drugs

Name of drug	Type of sustained release formulation	Composition of sustained release formulation	In Vitro drug release			In vivo biodistribution studies		
			Drug release pattern	Cellular uptake of drug	Comparison of drug release pattern with free capsaicin/blank formulation	Models	Organ biodistribution	Comparison of drug release pattern with free capsaicin/blank formulation
CAP-UREA-SDDDS	Solid State dispersion system	Urea scaffold	<ul style="list-style-type: none"> <li>Approximately 38% of the drug cargo (capsaicin) was released within the first hour</li> <li>Approximately 100% of the capsaicin was released within 8 days</li> </ul>	ND	CAP-UREA-SDDDS released capsaicin more slowly than free capsaicin	ND	ND	ND
CAP-SOY-PL	Phospholipid complexes	Soyabean phospholipids	<ul style="list-style-type: none"> <li>Approximately 60% of the capsaicin was released within 10 hours</li> <li>Approximately 100% of the drug was released at 30 hours</li> </ul>	ND	CAP-SOY-PL released capsaicin more slowly than free capsaicin	ND	ND	ND
CAP-CUR-GLY-GAL-LIPO	Liposome	DSPE-PEG	<ul style="list-style-type: none"> <li>Approximately 60% of the drug cargo (capsaicin) was released within 15 hours</li> <li>Approximately 60% of the drug</li> <li>95% of the drug was</li> </ul>	<ul style="list-style-type: none"> <li>Maximal uptake of liposomal drugs is at 4 hours in HepG2 cells</li> <li>At 4 hours the uptake of GLY-GAL-LIPO &gt; GLY-LIPO = GAL-LIPO &gt; blank-LIPO</li> </ul>	<ul style="list-style-type: none"> <li>Drug retention of GLY-, GAL- functionalized liposomes was greater than free capsaicin</li> </ul>	B16/H22 tumor-bearing Balb/c mice	<ul style="list-style-type: none"> <li>Most of the GLY-, GAL- functionalized liposomes were found in the liver.</li> <li>GLY-, GAL- functionalized liposomes were only localized to the H22 liver tumor. No liposomes</li> </ul>	ND

Name of drug	Type of sustained release formulation	Composition of sustained release formulation	In Vitro drug release			In vivo biodistribution studies		
			Drug release pattern	Cellular uptake of drug	Comparison of drug release pattern with free capsaicin/blank formulation	Models	Organ biodistribution	Comparison of drug release pattern with free capsaicin/blank formulation
			released at 48 hours	<ul style="list-style-type: none"> <li>Maximal retention of liposomal drugs is at 12 hours in HepG2 /LX2 co-cultured cells</li> <li>At 12 hours and 24 hours the retention of GLY- GAL- LIPO &gt; GLY- LIPO = GAL- LIPO &gt; blank- LIPO</li> </ul>			<ul style="list-style-type: none"> <li>were detected in the B16 melanoma tumor</li> <li>GLY-, GAL- functionalized liposomes showed deep penetration inside the solid H22 liver tumor</li> </ul>	

Table 3:

Anti-cancer activity of capsaicin sustained release drugs

Name of drug	Type of sustained release formulation	Targeting ligand	Drug cargo	Growth inhibitory activity <i>in vitro</i>	Is the <i>in vitro</i> growth inhibitory activity greater than free capsaicin	Anti-tumor activity <i>in vivo</i>	Is the <i>in vivo</i> growth inhibitory activity greater than free capsaicin	Mechanism of growth-inhibitory activity	Signaling mechanisms
CAP-UREA-SDDDS	Solid State dispersion system	None	Capsaicin	MCF-7 MDA-MB-231	Yes, in MCF-7 cells	ND	ND	ND	ND
CAP-SOY-PL	Phospholipid complexes	None	Capsaicin	MCF-7 MDA-MB-231	Yes, in MDA-MB231 cells	ND	ND	ND	ND
CAP-CUR-GLY-GAL-LIPO	Liposome	GLY, GAL	Capsaicin, Curcumin	HepG2, HepG2/LX2 co-cultured cells	Yes	<ul style="list-style-type: none"> <li>H22 tumor bearing Balb/c mice</li> <li>H22/LX2 tumor bearing Balb/c mice</li> <li>H22 orthotopic Balb/c mice</li> <li>Lung colonization mice model</li> </ul>	Yes	<ul style="list-style-type: none"> <li>Increase of apoptosis</li> <li>Inhibition of angiogenesis</li> <li>Inhibition of HSC activation</li> <li>Inhibition of EMT, migration and metastasis</li> </ul>	<ul style="list-style-type: none"> <li>Decrease of P-gp in HepG2/LX2 cells</li> <li>Decrease of ECM deposition and remodeling.</li> <li>Downregulation of alpha-smooth muscle actin, CD31</li> <li>Increase in E-cadherin levels, decrease in Vimentin expression</li> </ul>

**Table 4:** Comparative analyses of the anti-cancer activity of all types of curcumin-capsaicin liposomes

Type of experiment	HepG2 cells	HepG2/LX2 co-cultured cells	H22 cells	H22/LX2 co-cultured cells
Decrease in cell viability (as measured by MTT assay)	CAP-CUR-GAL-GLY-LIPO > CAP-CUR-GLY-LIPO = CAP-CUR-GAL-LIPO > CAP-CUR-LIPO > mixture of curcumin and capsaicin > free curcumin > free capsaicin	ND	ND	ND
Cytotoxic activity (as measured by Calcein AM/PI Live dead assay)	CAP-CUR-GAL-GLY-LIPO > CAP-CUR-GLY-LIPO = CAP-CUR-GAL-LIPO > CAP-CUR-LIPO > mixture of curcumin and capsaicin > free curcumin > free capsaicin	CAP-CUR-GAL-GLY-LIPO > CAP-CUR-GLY-LIPO = CAP-CUR-GAL-LIPO > CAP-CUR-LIPO > mixture of curcumin and capsaicin > free curcumin = free capsaicin	ND	ND
Decrease in levels of P-glycoprotein	ND	CAP-CUR-GAL-GLY-LIPO > CAP-CUR-LIPO > mixture of curcumin and capsaicin > free curcumin	ND	ND
Inhibition of EMT	ND	CAP-CUR-GAL-GLY-LIPO > CAP-CUR-LIPO > mixture of curcumin and capsaicin > free curcumin	ND	ND
Wound healing migration assay	CAP-CUR-GAL-GLY-LIPO > CAP-CUR-GLY-LIPO = CAP-CUR-GAL-LIPO > CAP-CUR-LIPO > mixture of curcumin and capsaicin > free curcumin > free capsaicin	CAP-CUR-GAL-GLY-LIPO = CAP-CUR-GLY-LIPO = CAP-CUR-GAL-LIPO > CAP-CUR-LIPO > mixture of curcumin and capsaicin > free curcumin > free capsaicin	ND	ND
Anti-cancer activity in tumor-bearing Balb/c mice	ND	ND	CAP-CUR-GAL-GLY-LIPO > CAP-CUR-LIPO > CAP-CUR-LIPO > mixture of curcumin and capsaicin > free curcumin	CAP-CUR-GAL-GLY-LIPO > CAP-CUR-GAL-LIPO > CAP-CUR-LIPO > mixture of curcumin and capsaicin > free curcumin > free capsaicin
Decrease in alpha-smooth-muscle actin in tumors xenografted in Balb/c mice	ND	ND	ND	CAP-CUR-GAL-GLY-LIPO > CAP-CUR-GAL-LIPO > CAP-CUR-LIPO > mixture of curcumin and capsaicin > free curcumin > free capsaicin
Decrease in ECM deposition/remodeling in tumors xenografted in Balb/c mice	ND	ND	ND	CAP-CUR-GAL-GLY-LIPO > CAP-CUR-GAL-LIPO > CAP-CUR-LIPO = mixture of curcumin and capsaicin > free curcumin > free capsaicin
Decrease in CD31 staining in tumors xenografted in Balb/c mice	ND	ND	ND	CAP-CUR-GAL-GLY-LIPO > CAP-CUR-GAL-LIPO > CAP-CUR-LIPO > mixture of curcumin and capsaicin > free curcumin > free capsaicin

Type of experiment	HepG2 cells	HepG2/LX2 co-cultured cells	H22 cells	H22/LX2 co-cultured cells
Ability to inhibit the formation of metastatic nodules in the lungs of mice in Lung colonization assay	ND	ND	CAP-CUR-GAL-GLY-LIPO > CAP-CUR-GAL-LIPO > CAP-CUR-LIPO > mixture of curcumin and capsaicin > free curcumin > free capsaicin	ND
Anti-metastatic activity in orthotopic model of liver cancer metastasis	ND	ND	CAP-CUR-GAL-GLY-LIPO > CAP-CUR-LIPO > mixture of curcumin and capsaicin > free curcumin	ND
Decrease in alpha-smooth-muscle actin in orthotopic model of liver cancer metastasis	ND	ND	CAP-CUR-GAL-GLY-LIPO > CAP-CUR-LIPO > mixture of curcumin and capsaicin = free curcumin	
Decrease in ECM deposition/remodeling in orthotopic model of liver cancer metastasis	ND	ND	CAP-CUR-GAL-GLY-LIPO > CAP-CUR-LIPO > mixture of curcumin and capsaicin = free curcumin	ND
Decrease in CD31 staining in orthotopic model of liver cancer metastasis	ND	ND	CAP-CUR-GAL-GLY-LIPO > CAP-CUR-LIPO > mixture of curcumin and capsaicin = free curcumin	ND

Table 5:

Physicochemical properties of capsaicin nanoparticle drugs

Name of nanoparticle drug	Type of nanoparticle	Composition Of nanoparticle	Method of synthesis	Nano particle shape	Size (nm)	Poly dispersity index	Zeta potential (mV)	Drug loading efficiency (%)	Drug entrapment efficiency (%)	Stability
CND	Dendrimers	Oleoyl chloride bound to PEG 400	Esterification reaction	Aggregates	143.1	ND	ND	ND	ND	ND
CAP-HAP-PXS-NPs	Nanocomposite polymers	PXS polymers wrapped around HAP nanorods	Hydrothermal-poly condensation reaction	Aggregate clusters	ND	ND	ND	ND	ND	Up to 10 days
CAP-SNEEDS	Self-assembling nanoemulsifying drug delivery systems	Isopropyl myristate, Tween-80 and ethanol	Dispersion and agitation	Spherical droplets	60–80	0.24–0.43	37	ND	94–98	Up to 90 days
CAP-TMC-NP	Polymeric nanoparticles	Trimethyl chitosan	Ionotropic gelation	Spherical	294±53.3	ND	-32.2	ND	ND	ND
CAP-EW-MAGNETIC-NP	Magnetic nanocomposite polymers	Egg white coated cobalt-ferric oxide functionalized zeolite hybrid	Dispersion and agitation	Spherical without aggregation	24	ND	-19.2	28	ND	ND
NIR-CAP-Gold-NR-MSN-NP	Nanodots	Gold nanorods embedded in mesoporous silica nanoparticles	Modified Stober reaction	Spherical	110	ND	ND	ND	ND	ND
CAP-mPEG-PCL	Polymeric nanoparticles	mPEG-PCL block copolymer	Ring opening polymerization method	Spherical shape with hollow inner structure	118±1.7	ND	-8.3±1.9	9.4±2.3	76±5.1	Up to one week
CAP-SLN	Solid lipid nanoparticle	Stearic acid Nanoemulsion with Tween-80 as the surfactant and sodium deoxycholate as co-surfactant	Solvent evaporation-emulsification technique	Spherical	60±6	0.7±0.02	-2	32.1±0.1	86.1±4.1	Up to 45 hours
CAP-NANO-LIPO	Nanoliposome	Ratio of DPPC: Cholesterol: DSPE/PEG2000 =75:20:5	Thin film hydration technique	Spherical	118.5	0.13	-13.9	0.75±0.2	32.1	Up to 4 months
CFLN	Polymeric nanoparticles	DSPE-PEG	Thin film hydration technique	Spherical	62.5	Described as good, no values mentioned in the paper	ND	9.5±1.4	95.5±2.4	Up to 25 hours

Name of nanoparticle drug	Type of nanoparticle	Composition Of nanoparticle	Method of synthesis	Nano particle shape	Size (nm)	Poly dispersity index	Zeta potential (mV)	Drug loading efficiency (%)	Drug entrapment efficiency (%)	Stability
CAP-FA-PLGA-PEG-NP	Polymeric nanoparticles	PEG and Polylactide decoglycolic acid	Oil-in-water emulsion Technique	Spherical	213±5.2	Less than 0.3	14.5±0.9	21.8±1.3	46±2.3	Up to 90 days
CAP-BT-PNPP	Polymeric nanoparticles	PEG and Polylactide decoglycolide	Evaporation technique	Spherical	83.4±0.5	0.152±0.03	-7.1±0.3	ND	ND	Up to 8 days
HA-PCL-CAP-NP	Polymeric nanoparticles	Poly $\epsilon$ -caprolactone	Nano precipitation	Spherical	194±2.9	0.2±0.03	-27.9±3.2	13±0.4	52.9±1.1	Up to 3 months
CAP-Chi-NCAS	Polymeric nanoparticles	Chitosan	Solvent displacement technique	Spherical	157±53	0.2±0.03	-49.5±8.1	ND	~90	ND
CAP-CS-NP	Polymeric nanoparticles	Chitosan	Iontropic gelation	Spherical	ND	ND	ND	ND	ND	ND
MUC1-Apt-HSA-CAP-NP	Polymeric nanoparticles	Human serum albumin	Desolvation technique	Spherical	52–120	ND	-34.7	ND	ND	ND
1-SEDDS	Self-emulsifying hydrophobic nanoparticle drug delivery system	Tween-80	Dispersion and agitation	Spherical without aggregation	23±3.5	0.184	ND	ND	80–82	ND
PTX-CAP-Fmoc-PEG-NM	Polymeric micelles	Polyethylene glycol	Thin Film dispersion method	Spherical without aggregation	199.2–237.4	ND	-0.51	12.06	94.2	Up to 5 days

Table 6:

Drug Release and biodistribution Properties of capsaicin nanoparticle drugs

Name of nanoparticle drug	Type of nanoparticle	Composition of nanoparticle	In Vitro drug release		In vivo biodistribution studies		
			Drug release pattern	Comparison of drug release pattern with free capsaicin/blank nanoparticles	Models	Organ biodistribution	Comparison of drug release pattern with free capsaicin/blank nanoparticles
CND	Dendrimers	Oleoyl chloride bound to PEG 400	ND	ND	ND	ND	ND
CAP-HAP-PXS-NPs	Nanocomposite polymers	PXS polymers wrapped around HAP nanorods	<ul style="list-style-type: none"> <li>Less than 10% of the drug cargo (capsaicin) was released within 24hours</li> <li>Approximately 60% of the drug was released at 10 days</li> </ul>	ND	ND	ND	ND
CAP-SNEEDDS	Self-assembling nanoemulsifying drug delivery systems	Isopropyl myristate, Tween-80 and ethanol	<ul style="list-style-type: none"> <li>Approximately 80% of the drug cargo (capsaicin) was released within 15 minutes</li> <li>Approximately 100% of the drug was released at 45 minutes and maintained at 100% till 90 minutes</li> </ul>	<ul style="list-style-type: none"> <li>CAP-SNEEDDS released capsaicin more slowly than free capsaicin</li> </ul>	Wistar Albino rats	ND	<ul style="list-style-type: none"> <li>CAP-SNEEDDS released capsaicin (in the plasma) more slowly than free capsaicin</li> <li>Approximately 50% of total capsaicin released from CAP-SNEEDDS was detected at 24 hours. The amounts of free capsaicin in the plasma after 24 hours were negligible</li> <li>Bioavailability, elimination half-life, MRT</li> </ul>

Name of nanoparticle drug	Type of nanoparticle	Composition of nanoparticle	In Vitro drug release		In vivo biodistribution studies			
			Drug release pattern	Comparison of drug release pattern with free capsaicin/blank nanoparticles	Models	Organ biodistribution	Comparison of drug release pattern with free capsaicin/blank nanoparticles	
CAP-TMC-NP	Polymetric nanoparticles	Trimethyl chitosan	ND	ND	ND	ND	ND	of CAP-SNEDDS > free capsaicin
CAP-EW-MAGNETIC-NP	Magnetic nanocomposite polymers	Egg white coated cobalt-ferric oxide functionalized zeolite hybrid	<ul style="list-style-type: none"> <li>Approximately 65% of the drug cargo (capsaicin) was released within 24 hours</li> <li>Greater than 70% of the drug was released between 1–5 days</li> <li>The rate of capsaicin released from CAP-EW-MAGNETIC-NP was greater at pH=5.5 (pH of duodenum) than at pH =7.4 (pH of small intestine)</li> </ul>	ND	ND	ND	ND	ND
NIR-CAP-Gold-NR-MSN-NP	Nanodots	Gold nanorods embedded in mesoporous silica nanoparticles	ND	ND	ND	ND	ND	ND
CAP-mPEG-PCL	Polymetric nanoparticles	mPEG-PCL block copolymer	<ul style="list-style-type: none"> <li>Greater than 80% of the drug cargo (capsaicin) was released</li> </ul>	ND	C57BL6 syngeneic models of glioma	<ul style="list-style-type: none"> <li>Capsaicin was detected in the brain</li> <li>Peak levels of capsaicin in the brain was observed</li> </ul>	ND	ND

Name of nanoparticle drug	Type of nanoparticle	Composition of nanoparticle	In Vitro drug release		In vivo biodistribution studies		
			Drug release pattern	Comparison of drug release pattern with free capsaicin/blank nanoparticles	Models	Organ biodistribution	Comparison of drug release pattern with free capsaicin/blank nanoparticles
CAP-SLN	Solid lipid nanoparticle	Stearic acid nano-emulsion with Tween-80 as the surfactant and sodium deoxycholate as co-surfactant	<ul style="list-style-type: none"> <li>within 24 hours</li> <li>Release of capsaicin from CAP-SLNs was maximal at pH=5.4 (pH of duodenum).</li> <li>Maximal release of capsaicin (from CAP-SLNs) occurred at 31 hours</li> <li>Approximately 77% of the capsaicin was released from CAP-SLNs at a pH=5.4; and 52% of the drug was released at pH=7.2 (pH of small intestine)</li> </ul>	ND	<i>Rattus norvegicus</i> rats	<ul style="list-style-type: none"> <li>from 3 hours to 24hours</li> <li>Maximal bioavailability of capsaicin (released from CAP-SLNs) was observed at 24 hours</li> <li>Amount of capsaicin detected in the liver&gt;kidney&gt;heart&gt;spleen&gt;lungs</li> </ul>	ND
CAP-NLIPO	Nanoliposome	Ratio of DPPC: Cholesterol: DSPE/PEG2000 =75:20:5	<ul style="list-style-type: none"> <li>Capsaicin was released from the nanoliposomes in a biphasic pattern at pH=7.4.</li> <li>Initially the drug was released at a fast pace; about 12% of the capsaicin was released within the first hour</li> </ul>	<ul style="list-style-type: none"> <li>Below 40 hours, the release of the drug (capsaicin) cargo from CAP-NLIPO was slower than free capsaicin</li> <li>After 40 hours, the rate of drug</li> </ul>	ND	ND	ND

Name of nanoparticle drug	Type of nanoparticle	Composition of nanoparticle	In Vitro drug release		Models	In vivo biodistribution studies	
			Drug release pattern	Comparison of drug release pattern with free capsaicin/blank nanoparticles		Organ biodistribution	Comparison of drug release pattern with free capsaicin/blank nanoparticles
			<ul style="list-style-type: none"> <li>After 5 hours, the rate of drug release becomes slower and prolonged. About 24% of the capsaicin was released at 48 hours</li> </ul>	<ul style="list-style-type: none"> <li>release from CAP-NLIPO becomes slower than free capsaicin</li> </ul>			
CFLN	Polymeric nanoparticles	DSPE-PEG	<ul style="list-style-type: none"> <li>Approximately 30% of the drug cargo (capsaicin) was released within 24 hours</li> <li>The presence of FA did not have any effect on the <i>in vitro</i> drug release pattern</li> </ul>	<ul style="list-style-type: none"> <li>Both CLFN and CLN had similar <i>in vitro</i> drug release pattern</li> </ul>	Sprague Dawley Rats	ND	<ul style="list-style-type: none"> <li>Bioavailability, elimination half-life, of CFLN (in plasma) &gt; free capsaicin</li> </ul>
CAP-FA-PLGA-PEG-NP	Polymeric nanoparticles	PEG and Poly(lactide decoglycolic acid)	<ul style="list-style-type: none"> <li>Capsaicin was released in a biphasic pattern.</li> <li>Initially the drug was released at a fast pace; about 35% of the capsaicin was released within the first 4 hours</li> <li>After 4 hours, the rate of drug release becomes slower and prolonged. About 60% of the capsaicin</li> </ul>	<ul style="list-style-type: none"> <li>The uptake of CAP-FA-PLGA-PEG-NP &gt; free Capsaicin in human A549 cells.</li> </ul>	Wistar Albino rats bearing lung tumors	<ul style="list-style-type: none"> <li>CAP-FA-PLGA-PEG-NP</li> <li>Amount of capsaicin detected in the lung &gt; liver &gt; heart &gt; spleen &gt; kidney</li> <li>Free Capsaicin</li> <li>Amount of capsaicin detected in the liver &gt; spleen &gt; kidney &gt; heart &gt; lung</li> </ul>	ND

Name of nanoparticle drug	Type of nanoparticle	Composition of nanoparticle	In Vitro drug release		Models	In vivo biodistribution studies	
			Drug release pattern	Comparison of drug release pattern with free capsaicin/blank nanoparticles		Organ biodistribution	Comparison of drug release pattern with free capsaicin/blank nanoparticles
CAP-BT-PNPP	Polymeric nanoparticles	PEG and polylactide decoglycolide	<ul style="list-style-type: none"> <li>was released at 24 hours</li> <li>The drug cargo was released steadily within the first 5 hours, followed by a period of sluggish release, attaining the maximal levels at the end of 1 week</li> <li>Approximately 20% of the drug cargo was released within 24 hours</li> <li>Approximately 45–55% of the drug cargo was released at the end of 1 week</li> <li>The presence of biotin increased the magnitude of drug released <i>in vitro</i></li> </ul>	<ul style="list-style-type: none"> <li>The <i>in vitro</i> drug release efficacy of CAP-BT-PNPP &gt; BT-NP &gt; CAP-NP &gt; free capsaicin</li> </ul>	ND	ND	ND
HA-PCL-CAP-NP	Polymeric nanoparticles	Poly $\epsilon$ -caprolactone	<ul style="list-style-type: none"> <li>Biphasic release pattern</li> <li>The presence of HA did not have any effect on the <i>in vitro</i> drug release pattern</li> </ul>	<ul style="list-style-type: none"> <li>The <i>in vitro</i> drug release efficacy of HA-PCL-CAP-NP &gt; CAP-NP &gt; PCL-NP</li> </ul>	Wistar Albino rats bearing lung tumors	<p><u>HA-PCL-CAP-NP</u>:</p> <ul style="list-style-type: none"> <li>Amount of capsaicin was detected in the lung &gt; liver &gt; heart &gt; spleen &gt; kidney</li> </ul> <p><u>CAP-PCL-NP</u>:</p>	<p>Bioavailability, elimination half-life, of HA-PCL-CAP-NP (in plasma) &gt; CAP-PCL-NP &gt; free capsaicin</p>

Name of nanoparticle drug	Type of nanoparticle	Composition of nanoparticle	In Vitro drug release		In vivo biodistribution studies		
			Drug release pattern	Comparison of drug release pattern with free capsaicin/blank nanoparticles	Models	Organ biodistribution	Comparison of drug release pattern with free capsaicin/blank nanoparticles
CAP-Chi-NCAS	Polymeric nanoparticles	Chitosan	<ul style="list-style-type: none"> <li>CAP-Chi-NC release 3-fold higher amounts of capsaicin in T24 bladder cancer cells relative to UROtsa normal urothelial cells</li> </ul>	ND	ND	<ul style="list-style-type: none"> <li>Amount of capsaicin was detected in the liver &gt; lung &gt; spleen &gt; heart &gt; kidney</li> <li>Free Capsaicin</li> <li>Amount of capsaicin was detected in the liver &gt; spleen &gt; heart &gt; kidney &gt; lung</li> </ul>	ND
CAP-CS-NP	Polymeric nanoparticles	Chitosan	ND	ND	ND	ND	ND
MUC1-Apt-HSA-CAP-NP	Polymeric nanoparticles	Human serum albumin	ND	ND	ND	ND	ND
1-SEDDS	Self-emulsifying hydrophobic nanoparticle drug delivery system	Tween-80	<ul style="list-style-type: none"> <li>About 80% of the drugs from 1-SEDDS is released at 6 hours at a pH=7.4 (pH of small intestine)</li> <li>No drug release was observed at acidic pH, specifically at pH=1.2 (pH of the stomach) or at pH=4.5,</li> </ul>	ND	ND	ND	1-SEDDS does not induce hemolysis

Name of nanoparticle drug	Type of nanoparticle	Composition of nanoparticle	In Vitro drug release		Models	In vivo biodistribution studies	
			Drug release pattern	Comparison of drug release pattern with free capsaicin/blank nanoparticles		Organ biodistribution	Comparison of drug release pattern with free capsaicin/blank nanoparticles
PTX-CAP-Fmoc-PEG-NM	Polymeric micelles	Polyethylene glycol	<ul style="list-style-type: none"> <li>5.4 (pH of the duodenum)</li> <li>About 30% of the drug cargo (paclitaxel) was released within 24 hours</li> <li>About 20% of the capsaicin was released at 24 hours</li> </ul>	<ul style="list-style-type: none"> <li>The <i>in vitro</i> drug release efficacy of PTX-CAP-Fmoc-PEG-NM &gt; free paclitaxel</li> <li>The <i>in vitro</i> drug release efficacy of PTX-CAP-Fmoc-PEG-NM &gt; free capsaicin</li> </ul>	<p>Balb/c mice implanted with subcutaneous 4T1 murine breast cancer tumors</p>	<ul style="list-style-type: none"> <li>Amount of paclitaxel present in the tumors of PTX-CAP-Fmoc-PEG-NM-treated mice &gt; amount of paclitaxel present in the tumors of mice administered with free paclitaxel</li> <li>Amount of paclitaxel present in the heart, kidney of PTX-CAP-Fmoc-PEG-NM-treated tumor-bearing mice &gt; amount of paclitaxel present in the heart, kidney of tumor-bearing mice administered with free paclitaxel</li> </ul>	<ul style="list-style-type: none"> <li>PTX-CAP-Fmoc-PEG-NM released paclitaxel (in the plasma) more slowly than free paclitaxel</li> <li>Bioavailability, biological half-life of PTX-CAP-Fmoc-PEG-NM &gt; Free paclitaxel</li> <li>Clearance time of free paclitaxel &gt; PTX-CAP-Fmoc-PEG-NM</li> </ul>

Table 7:

Anti-cancer activity of capsaicin nanoparticle drugs

Name of nanoparticle drug	Type of nanoparticle	Composition of nanoparticle	Targeting ligand	Drug cargo	Growth inhibitory activity <i>in vitro</i>	Anti-tumor activity <i>in vivo</i>	Growth-inhibitory Activity on normal cells/tissues	Mechanism of Growth-inhibitory activity	Signaling mechanism	Other uses
CND	Dendrimers	Oleoyl chloride bound to PEG 400	None	Capsaicin	MCF-7 HepG2	ND	2-fold less active on normal monkey kidney cells	ND	Antioxidant pathway	ND
CAP-HAP-PXS-NPs	Nanocomposite polymers	PXS polymers wrapped around HAP nanorods	None	Capsaicin	Saos-2, MG63	ND	No impact on osteoblasts	Apoptosis	Generation of ROS, loss of mitochondrial membrane potential	ND
CAP-SNEDDS	Self-assembling nanoemulsifying drug delivery systems	Isopropyl myristate, Tween-80 and ethanol	None	Capsaicin	HT-29	ND	ND	Apoptosis, Necrosis	ND	ND
CAP-TMC-NP	Polymeric nanoparticles	Trimethyl chitosan	None	Capsaicin	HepG2	ND	ND	Apoptosis	Increase in Bax, decrease in Bcl2, MDR1	ND
CAP-EW-MAGNETIC-NP	Magnetic nanocomposite polymers	Egg white coated cobalt-ferric oxide functionalized zeolite hybrid	None	Capsaicin	SK-N-MC	ND	ND	ND	ND	Tumor Imaging
NIR-CAP-Gold-NR-MSN-NP	Nanodots	Gold nanorods embedded in mesoporous silica nanoparticles	Near infrared light sensitivity of gold nanorods	Capsaicin	FTC-133 B-CPAP	ND	ND	Apoptosis, S-phase arrest	ND	Anti-migratory drug, Anti-invasive drug
CAP-mPEG-PCL	Polymeric nanoparticles	mPEG-PCL block copolymer	None	Capsaicin	U251	ND	ND	Apoptosis	ND	ND
CFLN	Polymeric nanoparticles	DSPE-PEG	Folic acid	Capsaicin	SKOV-3	ND	No impact on OSE normal ovarian epithelial cells; no toxicity in rats	Apoptosis	ND	ND
CAP-FA-PLGA-PEG-NP	Polymeric nanoparticles	PEG and Polylactide decoglycolic acid	Folic acid	Capsaicin	A549	Urethane-induced lung cancer model in rats	No toxicity in rats	Apoptosis	Increase in p16, caspase-3, caspase-9; decrease in MMP-9, ROS,	ND

Name of nanoparticle drug	Type of nanoparticle	Composition of nanoparticle	Targeting ligand	Drug cargo	Growth inhibitory activity <i>in vitro</i>	Anti-tumor activity <i>in vivo</i>	Growth-inhibitory Activity on normal cells/tissues	Mechanism of Growth-inhibitory activity	Signaling mechanism	Other uses
CAP-SLN	Solid lipid nanoparticle	Stearic acid nano-emulsion with Tween-80 as the surfactant and sodium deoxycholate as co-surfactant	None	Capsaicin	HepG2	ND	No impact on WST-1 normal human fibroblast cells	Apoptosis	loss of mitochondrial membrane potential, regulation of oxidative stress biomarkers	ND
CAP-NANO-LIPO	Nanoliposome	Ratio of DPPC: Cholesterol: DSPE/PEG2000 =75:20:5	None	Capsaicin	MCF-7, MDA-MB-231, K562, Panc1, A375	ND	No impact on normal human fibroblast cells	ND	ND	ND
CAP-BT-PNPP	Polymeric nanoparticles	PEG and polylactide decoglycolide	Biotin	Capsaicin	NCI-N87, SGC-791	No toxicity in rat models; no gastric irritation in rats	ND	Apoptosis	ND	ND
HA-PCL-CAP-NP	Polymeric nanoparticles	Poly $\epsilon$ -caprolactone	Hyaluronic acid	Capsaicin	A549	Urethane-induced lung cancer model in rats	No toxicity in rats	Apoptosis	Increase in Bax, caspase-9; decrease in MMP-9; regulation of oxidative stress biomarkers: TBARS, SOD, catalase activity and protein carbonylation	ND
CAP-Chi-NCAS	Polymeric nanoparticles	Chitosan	Chitosan	Capsaicin	T24	ND	No impact on UROtsa normal urothelial epithelial cells	Apoptosis		ND
CAP-CS-NP	Polymeric nanoparticles	Chitosan	None	Capsaicin	ND	DMBA-induced lung cancer model in rats	ND	Cell cycle arrest	Decrease in PCNA, cyclin D1; Decrease in oxidative stress biomarkers: TBARS, GPx,	ND

Name of nanoparticle drug	Type of nanoparticle	Composition of nanoparticle	Targeting ligand	Drug cargo	Growth inhibitory activity <i>in vitro</i>	Anti-tumor activity <i>in vivo</i>	Growth-inhibitory Activity on normal cells/ tissues	Mechanism of Growth-inhibitory activity	Signaling mechanism	Other uses
MUC1-Apt-HSA-CAP-NP	Polymeric nanoparticles	Human serum albumin	MUC1 aptamer	Capsaicin	Panc-1	ND	ND	ND	GSH, Vitamin C and E, SOD and catalase activity; Increase in the expression of detoxification markers: Cyt P450, Cyt-b5, GST, GR, DT-D	Tumor Imaging
1-SEDDS	Self-emulsifying hydrophobic nanoparticle drug delivery system	Tween-80	None	Capsaicin, SN38	HCT116, SW480, MDA-MB-231, MCF-7, H1299	Athymic mice tumor xenograft model	No hemolysis in blood	Apoptosis	Cleavage of PARP, caspase-3	ND
PTX-CAP-Fmoc-PEG-NM	Polymeric micelles	Polyethylene glycol	None	Capsaicin, paclitaxel	A549, HepG2, 4T1	Syngeneic mice tumor xenograft model	ND	Apoptosis	ND	ND